

DEVELOPMENT OF AN AGENT-BASED MODEL TO RECAPITULATE
MURINE PATELLAR TENDON HEALING AS A FUNCTION OF AGE

AN ABSTRACT

SUBMITTED ON THE TWENTY-SECOND DAY OF APRIL,
2021 TO THE DEPARTMENT OF BIOMEDICAL
ENGINEERING IN PARTIAL FULLFILLMENT OF
REQUIREMENTS OF TULANE UNIVERSITY FOR THE
DEGREE OF BACHELOR OF SCIENCE IN ENGINEERING
AND MASTERS OF SCIENCE IN ENGINEERING

BY:

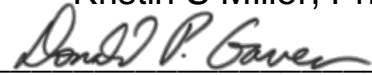


JORDAN ROBINSON

APPROVED BY:



Kristin S Miller, PhD



Donald P Gaver, PhD



Mary Mulcahey, MD

Abstract

The patellar tendon transmits loads from the quadriceps to the tibia promoting locomotion. The main etiological factor behind patellar tendinopathies is thought to be excessive loading and unloading during athletic activity (Pearson & Hussain, 2014). The extracellular matrix (ECM) composition and fibroblast-like tenocytes dictate tendon's uniaxial mechanical properties (Kannus, 2000). Following injury, a flood of inflammatory cells and spike in certain gene expressions work together to remove damaged tissue, trigger fibroblast proliferation, and deposit a provisional collagen matrix (Thomopoulos et al., 2015). Despite these processes, healed tendons demonstrate significant functional deficits (Mienaltowski et al., 2016). Moreover decrease in cell migration and fiber alignment with age further hampers healing outcomes (Dunkman et al., 2013). Efforts to restore tendon function are impeded by a lack of understanding of the early healing process, which may be age- and sex-dependent (Fryhofer et al., 2016; Mienaltowski et al., 2016). The tendon healing process can be further understood using an agent-based model (ABM). ABMs simulate individual agents and the interactions between them and their environment. This approach has the advantage of building complexity from the ground up, mimicking the underlying tendon physiology (Conte & Paolucci, 2014). Therefore, the objectives of this study were to 1) formulate a literature based ABM of murine patellar tendon healing with varying initial conditions to recapitulate changes observed with aging, and 2) Conduct simulations to determine whether ABM recapitulated salient features of healing, and to make predictions about healing outcomes.

DEVELOPMENT OF AN AGENT-BASED MODEL TO RECAPITULATE
MURINE PATELLAR TENDON HEALING AS A FUNCTION OF AGE

A THESIS

SUBMITTED ON THE TWENTY-SECOND DAY OF APRIL,
2021 TO THE DEPARTMENT OF BIOMEDICAL
ENGINEERING IN PARTIAL FULLFILLMENT OF
REQUIREMENTS OF TULANE UNIVERSITY FOR THE
DEGREE OF BACHELOR OF SCIENCE IN ENGINEERING
AND MASTERS OF SCIENCE IN ENGINEERING

BY:



JORDAN ROBINSON

APPROVED BY:



Kristin S Miller, PhD



Donald P Gaver, PhD



Mary Mulcahey, MD

Acknowledgements

First and foremost, I would like to acknowledge Dr. Kristin Miller for her guidance, mentorship, and support during my time in the Biomechanics of Growth and Remodeling lab. She has always given me detailed and useful feedback, and she pushed me to do the highest quality work, and to push beyond my limitations and learn new skills. I would also like to thank Dr. Mary Mulcahey. While she was not directly involved in the Agent-based modelling project, her collaboration is instrumental to collecting data that will inform future versions of tendon healing models from our lab. I would also like to acknowledge the members of the Biomechanics of Growth and Remodeling lab. I remember being very lost and intimidated as a sophomore joining the lab, but they cultivated a very open and welcoming atmosphere that really made me feel at home every time I stepped into the lab. Lastly, I would like to thank the Biomedical Engineering department, not only for educating me on the principals of biomedical engineering, but also for providing the resources necessary for me to become an effective researcher.

Contents

Abstract	2
Acknowledgements	4
List of Figures, Tables, and Equations	7
I. Introduction	10
Specific Aims	12
II. Background	13
1. Anatomy of the Knee	13
2. Anatomy of Tendons	14
3. Tendinopathy	18
4. Tendon homeostasis and healing	20
5. Current state of tendon computational modeling	24
III. ABM Formulation	26
1. Introduction	26
2. Literature Searches	28
ECM Ground Substance	29
Healing Mechanisms	32
Alignment	33
Macrophages	34
Rule scoring	35
Computational techniques	37
Coding in NetLogo	38
Rule Generation	39
3. ABM Framework	42
IV. ABM Simulations	48
1. Introduction	48
2. Methods	50
Parameterization of TGF- β	50
Parametrization of IGF-I	52
Parametrization of PDGF	53
Healing at Different ages	53
3. Results	54
Parameterization of TGF- β	54

Parametrization of IGF-I	59
Parametrization of PDGF	60
Healing at different ages	63
4. Discussion	67
V. Conclusions	70
Future Work	70
Bibliography	73
Biography	79
Appendix	80
ABM NetLogo code	80

List of Figures, Tables, and Equations

FIGURE 1: ANATOMY OF THE KNEE FROM AN ANTERIOR ASPECT. IMAGE COURTESY OF ST. LUKE’S HEALTH SYSTEM 13

FIGURE 2: TENDONS ARE COMPOSED OF A HIERARCHY OF COLLAGEN FIBERS WHICH ENDOW TENDONS WITH MANY OF THEIR PROPERTIES (KANNUS, 2000)..... 14

FIGURE 3: A TYPICAL STRESS-STRAIN CURVE FOR A TENDON FEATURING TOE REGION AND LINEAR REGION. HERE THE TRANSITION STRAIN IS ABOUT 2% STRAIN, THE LINEAR REGION EXISTS BETWEEN 2% AND 6% STRAIN, AND FAILURE BEGINS ABOVE 6% STRAIN..... 17

FIGURE 4: THE STAGES OF TENDON HEALING, (FROM LEFT TO RIGHT) INFLAMMATION , REPARATION, AND REMODELING. INFLAMMATION IS CHARACTERIZED BY AN INCREASE IN PLATELETS, VARIOUS IMMUNE CELLS, AND STEM CELLS. THIS STAGE SEES INCREASES IN SEVERAL INTERLEUKINS AND GROWTH FACTORS OCCUR. PROLIFERATION IS CHARACTERIZED BY INCREASE IN CELLULARITY AND COLLAGEN PRODUCTION, AND CONTINUED MOLECULAR CHANGE. THE REMODELING STAGES ARE CHARACTERIZED BY NEW COLLAGEN FIBERS ORGANIZING THEMSELVES, AND THE SLOWING OF MOLECULAR CHANGE.(SCHNEIDER ET AL., 2018) 23

FIGURE 5: FLOWCHART ILLUSTRATING THE BROAD FUNCTIONS OF THE HEALING/AGING ABM. NEWLY ADDED PROCESSES AND THEIR DIRECT AFFECTS ARE HIGHLIGHTED IN BLUE. USER CAN INPUT WHETHER AN INJURY OCCURS, AS WELL AS THE AGE OF THE MOUSE AT THE TIME OF INJURY. THESE CHOICES AFFECT INFLAMMATION, MOLECULAR ACTIVITY, AND CAN TRIGGER INFLAMMATION. THE CHANGES IN GROWTH FACTORS CAUSE CHEMOTAXIS. THESE PROCESSES LEAD TO THE FINAL STEP OF THIS FRAMEWORK: THE OUTPUT OF COLLAGEN ALIGNMENT..... 44

FIGURE 6: FLOWCHART SHOWING THE INTERACTIONS BETWEEN PROVISIONAL MATRIX PROTEINS (FIBRINOGEN & FIBRIN) AND THE VARIOUS GROWTH FACTORS AND CYTOKINES RELEASED BY MACROPHAGES AND FIBROBLASTS FOLLOWING AN INJURY. FOLLOWING THE INJURY, AND THE DIRECT CONSEQUENCES IT HAS ON THE COMPOSITION OF TENDON ECM, THE EFFECTS OF FIBRINOGEN, IGF, AND FIBRIN..... 45

FIGURE 7: THE GRAPHICAL DISPLAY OF THE ABM SHOWS A NUMBER OF FIBROBLAST-LIKE TENOCYTES ON A MULTICOLORED BACKGROUND REPRESENTING THE ECM SET TO A COLORIMETRIC SCALE. IN THIS IMAGE, THE BACKGROUND REPRESENTS COLLAGEN CONTENT WHERE BLUE REPRESENTS A RELATIVE VALUE OF 1, THE AMOUNT OF COLLAGEN PRESENT IN A 120 DAY-OLD TENDON, AND RED IS A RELATIVE VALUE OF 0. THE GRAPHS ON THE LEFT SIDE OF THE IMAGE PLOT THE RELATIVE VALUES OF MATRIX COMPONENTS THAT ARE EXPRESSED BY AND INTERACT WITH TENOCYTES. THE GRAPHS ON THE RIGHT PLOT THE VALUES OF MATRIX PROPERTIES DETERMINED BY INTERACTIONS BETWEEN CELLS AND THE MATRIX, NAMELY THE KEY OUTPUTS OF COLLAGEN AMOUNT, COLLAGEN ORGANIZATION (R-BAR) AND FIBROBLAST COUNT. IN THIS IMAGE, AN INJURY OCCURS AT THE AGE OF 270 DAYS OLD AND HAS UNDERGONE 140 DAYS OF HEALING. 47

FIGURE 8: AVERAGE AND CONFIDENCE INTERVAL OF MAXIMUM RELATIVE TGF-B PLOTTED AGAINST EVENLY SPACED $K_{(1,TGF-B)}$ VALUES BETWEEN 5 AND 15 FOR 30 RUNS AT EACH VALUE (BLACK). THE FITTED EQUATION, DETERMINED BY MATLAB’S “FIT” FUNCTION (RED), AND THE INTERPOLATED VALUE CORRESPONDING TO LITERATURE (BLUE). THIS EXPERIMENT ESTABLISHES THE LINEAR RELATIONSHIP BETWEEN THE $K_{(1,TGF-B)}$ SPIKE CONSTANT AND THE MAXIMUM RELATIVE AMOUNT OF TGF-B. THE EXPERIMENTAL DATA IS THEN FIT TO A LINEAR CURVE AND THE VALUE OF $K_{(1,TGF-B)}$ IS DETERMINED USING THIS LINEAR EQUATION. 54

FIGURE 9: PLOT OF RELATIVE TGF-B CONTENT VS DAYS SINCE INJURY AFTER APPLYING ONLY THE FIRST CONSTANT, $K_{(1,TGF-B)}$ USING A VALUE OF 11 FOR 30 RUNS. AVERAGE RELATIVE TGF-B (DARK GREEN), STANDARD DEVIATION (LIGHT BLUE), AND MAXIMUM/MINIMUM (BLACK). THE SHADED AREA REPRESENTS THE DIFFERENCE BETWEEN THE STANDARD DEVIATION AND THE MAXIMUM/MINIMUM VALUES. THIS GRAPH MAKES IT CLEAR THAT FURTHER PARAMETRIZATION IS NEEDED TO DEFINE THE DECAY IN TGF- B VALUES..... 55

FIGURE 10: PLOT OF AVERAGE AND CONFIDENCE INTERVAL OF RELATIVE TGF-B AMOUNT 15 DAYS AFTER INJURY PLOTTED AGAINST EVENLY SPACED $K_{(2,TGF-B)}$ VALUES BETWEEN 5 AND 15 FOR 30 RUNS AT EACH VALUE (BLACK). THE FITTED EQUATION, DETERMINED BY MATLAB’S “FIT” FUNCTION (RED), AND THE INTERPOLATED VALUE CORRESPONDING TO LITERATURE (BLUE). THIS EXPERIMENT ESTABLISHES THE EXPONENTIAL RELATIONSHIP BETWEEN THE $K_{(2,TGF-B)}$ SPIKE CONSTANT AND THE RELATIVE AMOUNTS OF TGF-B 15 DAYS AFTER INJURY. THE EXPONENTIAL CURVE IS USED TO DETERMINE THE VALUE OF OF $K_{(2,TGF-B)}$ 56

FIGURE 11: PLOT OF RELATIVE TGF-B CONTENT VS DAYS SINCE INJURY AFTER APPLYING BOTH CONSTANTS, $K_{(1,TGF-B)}$ AND $K_{(2,TGF-B)}$ USING A VALUES OF 8.33 AND 1.89 RESPECTIVELY FOR 50 RUNS. AVERAGE RELATIVE TGF-B (OLIVE GREEN), STANDARD DEVIATION (LIGHT BLUE), AND MAXIMUM/MINIMUM (BLACK). THE SHADED AREA REPRESENTS THE DIFFERENCE BETWEEN THE STANDARD DEVIATION AND THE MAXIMUM/MINIMUM VALUES. THIS GRAPH DEMONSTRATES THE SPIKE IN TGF-B CONTENT OCCURRING DURING THE INFLAMMATORY PHASE OF HEALING, AND THE DECAY OF THIS GROWTH FACTOR’S CONTENT TO NORMAL VECTORS SOON AFTER. 57

FIGURE 12: VIEW OF THE ABM 3-DAYS AFTER AN INJURY WITH THE BACKGROUND SET TO REPRESENT THE TOTAL TGF-B CONTENT. BLUE REPRESENTS HIGH AMOUNT OF TGF- B, AND RED IS A LOW AMOUNT OF COLLAGEN. THIS IMAGE ILLUSTRATES THE LOCALIZATION OF THE INCREASED TGF-B VALUES AS REPORTED IN NATSU-UME ET AL. 58

FIGURE 13: PLOT OF RELATIVE IGF CONTENT VS DAYS SINCE INJURY AFTER APPLYING THE CONSTANT, $K_{(IGF)}$ USING A VALUE OF 5 FOR 30 RUNS. AVERAGE RELATIVE IGF (OLIVE GREEN), STANDARD DEVIATION (LIGHT BLUE), AND MAXIMUM/MINIMUM (BLACK). THE SHADED AREA REPRESENTS THE DIFFERENCE BETWEEN THE STANDARD DEVIATION AND THE MAXIMUM/MINIMUM VALUES. THESE DATA ILLUSTRATE THE SPIKE IN IGF CONTENT, WHICH REACHES A PEAK 21 DAYS AFTER INJURY AS WELL AS THE SLOW DECAY OF IGF CONTENT BACK TO BASELINE LEVELS AS HEALING PROGRESSES BEYOND THIS PEAK..... 59

FIGURE 14: PLOT OF AVERAGE AND CONFIDENCE INTERVAL OF FIBROBLAST PERCENTAGE 9 DAYS AFTER INJURY PLOTTED AGAINST EVENLY SPACED PDGF PRODUCTION VALUES BETWEEN FIVE AND FIFTY FOR 100 RUNS AT EACH VALUE (BLACK). THE FITTED EQUATION, DETERMINED BY MATLAB'S "FIT" FUNCTION (RED), AND THE INTERPOLATED VALUE CORRESPONDING TO LITERATURE (BLUE). THE RESULTS OF THIS GRAPH SHOW THAT WHILE THERE IS A CLEAR TREND IN THE RELATIONSHIP BETWEEN FIBROBLAST PERCENTAGE AND PDGF PRODUCTION, THE HIGH AMOUNT OF STOCHASTIC VARIABILITY FOR THIS OUTPUT MEANS THAT THE MODEL IS NOT VERY SENSITIVE TO PDGF PRODUCTION..... 61

FIGURE 15: AVERAGE FIBROBLAST PERCENTAGE AND CONFIDENCE INTERVAL AT ONE, THREE, AND NINE DAYS AFTER INJURY FOR 100 SIMULATION RUNS, USING THE VALUE OF PDGF DETERMINED PREVIOUSLY. THIS GRAPH SHOWS THAT FIBROBLAST PERCENTAGE REMAINS LOW IN THE FIRST FEW DAYS FOLLOWING INJURY, BUT TENDS TO DOMINATE THE WOUND AREA AFTER ABOUT NINE DAYS OF HEALING..... 62

FIGURE 16: (A) COMPARISON OF TOTAL RELATIVE COLLAGEN OF (BLUE) HEALTHY AND (ORANGE) HEALING 120-DAY OLD TENDON SIMULATIONS. (B) COMPARISON OF TOTAL RELATIVE COLLAGEN OF (BLUE) HEALTHY AND (ORANGE) HEALING 270-DAY OLD TENDON SIMULATIONS. (C) COMPARISON OF TOTAL RELATIVE COLLAGEN OF (BLUE) HEALTHY AND (ORANGE) HEALING 540-DAY OLD TENDON SIMULATIONS. ABM PREDICTS THAT THE HEALING TENDON WILL NOT REACH THE LEVEL OF COLLAGEN OF ITS HEALTHY COUNTER PART BY SIX WEEKS POST-INJURY FOR 120-DAY OLD OR 270-DAY OLD MICE, BUT IT DOES PREDICT RECAPITULATION OF HEALTHY COLLAGEN LEVELS FOR A 540 DAY-OLD MOUSE. 63

FIGURE 17: PREDICTION OF THE DIFFERENCE IN RELATIVE COLLAGEN OF BETWEEN THE ENTIRE TENDON AND THE WOUND SITE. COMPARED BETWEEN MICE INJURED AT 120- 270- AND 540-DAYS OLD. THIS GRAPH SHOWS THAT THE DIFFERENCE BETWEEN THE WOUND SITE AND FULL TENDON DECREASES OVER TIME, AND THAT THIS DIFFERENCE IS VERY COMPARABLE FOR ALL AGE GROUPS AFTER SIX WEEKS OF HEALING. 64

FIGURE 18: (A) COMPARISON OF COLLAGEN ALIGNMENT BETWEEN (BLUE) HEALTHY AND (ORANGE) HEALING 120-DAY OLD TENDON SIMULATIONS. (B) COMPARISON OF COLLAGEN ALIGNMENT BETWEEN (BLUE) HEALTHY AND (ORANGE) HEALING 270-DAY OLD TENDON SIMULATIONS. (C) COMPARISON OF COLLAGEN ALIGNMENT BETWEEN (BLUE) HEALTHY AND (ORANGE) HEALING 540-DAY OLD TENDON SIMULATIONS. ABM PREDICTS THAT THERE IS A DIFFERENCE IN THE COLLAGEN ALIGNMENT BETWEEN THE HEALING AND HEALTHY TENDONS FOR MICE INJURED AT 120 DAYS, BUT NOT FOR MICE INJURED AT 270 OR 540 DAYS..... 65

FIGURE 19: PREDICTED COLLAGEN ALIGNMENT AFTER SIX WEEKS OF HEALING IN THE INJURY SITE OF (A) A TENDON INJURED AT 120-DAYS OLD (B) A TENDON INJURED AT 270-DAYS OLD AND (C) A TENDON INJURED AT 540-DAYS OLD. THE DECREASE IN COLLAGEN ALIGNMENT IS MUCH MORE NOTICEABLE IN THE YOUNGER TWO TENDONS, WHILE THE TENDON INJURED AT 540 DAYS OLD APPEARS TO HAVE A MUCH MORE CONSTANT AMOUNT OF ALIGNMENT ACROSS ALL COORDINATES. 65

FIGURE 20: PREDICTED FIBROBLAST PERCENTAGE AT KEY POST-INJURY TIMEPOINTS FOR (BLUE) MICE INJURED AT 120-DAYS-PLD, (ORANGE) MICE INJURED AT 270 DAYS-OLD, AND (YELLOW) MICE INJURED AT 540 DAYS-OLD. ABM PREDICTS A MUCH LONGER TIME FOR OLDER MICE TO REACH FIBROBLAST DOMINANCE AT THE WOUND SITE..... 66

FIGURE 21: PREDICTED INJURY-SITE FIBROBLAST COUNT AT KEY POST-INJURY TIMEPOINTS FOR (BLUE) MICE INJURED AT 120-DAYS-PLD, (ORANGE) MICE INJURED AT 270 DAYS-OLD, AND (YELLOW) MICE INJURED AT 540 DAYS-OLD. ABM PREDICTS FEWER FIBROBLASTS REACH THE SITE OF INJURY WITH INCREASING AGE. 67

TABLE 1: SCORING SYSTEM USED TO EVALUATE THE RELEVANCE OF ARTICLES INVESTIGATED FOR INCORPORATION IN THE ABM. 37

TABLE 2: LIST OF BEHAVIORS, RULES, SOURCES, AND SCORES FOR THE RULES DEFINED IN THE AGING/HEALING ABM 42

EQUATION 1 38

EQUATION 2 40

EQUATION 3 40

EQUATION 4 40

EQUATION 5 40

EQUATION 6 46

EQUATION 7 46

EQUATION 8 50

EQUATION 9	51
EQUATION 10	52
EQUATION 11	52
EQUATION 12	54
EQUATION 13	60

I. Introduction

Tendons, ligaments, and cartilage are orthopedic tissues found in and around joints that are responsible for facilitating articulation by transmitting loads and maintaining joint health and stability. In 2012, 126 million Americans reported musculoskeletal conditions. This represents half of the US adult population. These conditions are reported in 70% of the elderly (above 65) population (US Bone and Joint Initiative, 2014). Furthermore, 30% of musculoskeletal conditions were described as a tendinopathy (J. F. Kaux et al., 2011). Tendon injury can occur as an acute, catastrophic rupture, or as a long-term injury, characterized by chronic inflammation. Tendon injuries are often accompanied by a build-up of microtears over a long period of time, compromising tissue mechanics and leading to a more serious injury (Sharma et al., 2006). tendon injuries are problematic not only because of their debilitating effects on the people who experience them, but also because healing often results in suboptimal mechanical outcomes, regardless of treatment method (Schneider et al., 2018). The long-term effects of a tendon injury limit joint function when it comes to transmitting loads and lead to a decrease in overall quality of life.

Tendon's ability to transfer tensile loads is a result of its microstructure, which confers mechanical properties like elastic strength and stiffness. Tendons are composed of fibroblast-like tenocytes surrounded by an extracellular matrix (ECM) primarily consisting of type I collagen fibers aligned in the direction of loading, and organized in hierarchically into fibrils, and bundles (Kannus, 2000). Damage caused by injury and aging disrupts the highly organized nature of tendon ECM, therefore compromising its mechanical properties and reducing functionality. Tendon

microstructure is optimal for transferring loads, but this comes at the cost of low vascularity and cellularity. So, even though injured tendons are capable of repairing themselves, they are never able to regain their pre-injury functionality (Schneider et al., 2018).

There are several studies that have used mouse models to investigate the mechanical and structural effects of the healing process on the patellar tendon. These studies tend to focus on long-term healing outcomes and do not include data for mice within the first week of healing, corresponding to the inflammatory response to injury. (Dunkman et al., 2013, 2014; Mienaltowski et al., 2016). Biochemical studies quantifying the distribution of growth factors following an injury form the basis of the computer model developed as part of this research (Molloy et al., 2003; Sciore et al., 1998; Sugg et al., 2014). While it is known that age and sex effect the healing process, the specifics of how these factors dictate the biochemistry of healing, and deposition of collagen are not well known. This lack of knowledge motivated one of the objectives of this research, which was to conduct a pilot study to determine whether sex and age play a crucial role in dictating the mechanisms of the inflammatory healing, thereby providing a more complete picture of tendon healing mechanisms.

Because of the known functional deficit following tendon injury, there is a need to find therapeutics that will lead to improved healing. One method to investigate possible therapeutics is the use of computer modelling, specifically using cells-as-agents methodology to investigate the interaction between different types of cells and their environments. Agent-based models (ABM) have been used to study how mechanical loading affects Achilles tendon healing (Chen et al., 2018), arterial adaptation to

hypertension (Thorne et al., 2011a), and in prior research in this lab it has been used to recapitulate the properties of patellar tendon aging (Vanosdoll, 2017). To our knowledge, no such model has been developed to investigate healing in the patellar tendon. Hence, our second objective is to develop a literature-derived ABM to expand on previous work by recapitulating patellar tendon healing.

Specific Aims

The first aim was to conduct an in-depth literature search focusing on the salient growth factors, cytokines, and cell types involved in healing, specifically during the understudied inflammatory phase encompassing the first seven to ten days of healing. The results of this literature search were evaluated based on their methods and given a numerical score. The most relevant of these rules were used to build upon previous work to formulate a literature-based ABM of murine patellar tendon healing with varying initial conditions to recapitulate changes observed with aging.

The second aim was to evaluate the model's predictive capabilities. This will be accomplished by running the model at varying injury conditions and comparing the results both to the results published literature and between injury groups.

The ABM represents an injury model of the murine patellar tendon, whose output depends upon age at the time of injury. The molecular parameters of the ABM are adjustable allowing for healing outcomes to be evaluated using a wide range of initial conditions. It is hypothesized that this ABM will recapitulate the changes in ECM composition, and cellularity inherent to the inflammatory phase of healing. It is also hypothesized that the suboptimal healing outcomes observed as a function of

increasing age will be reflected by combining the novel patellar tendon healing framework with the established aging model.

II. Background

1. Anatomy of the Knee

The knee joint is critical for locomotion and general mobility in humans. The joint connects the femur to the tibia and incorporates the patella, commonly known as the kneecap. The femur and tibia are both capped by cartilage, providing a shock absorbing cushion between the two bones. The femur and tibia are attached via four ligaments. The

anterior cruciate ligament (ACL) and posterior cruciate ligament (PCL) are located in the central part of the knee and stabilize the joint in the sagittal plane. The medial collateral ligament (MCL) and lateral collateral ligament (LCL) are located on either side of the joint and stabilize the knee in the coronal plane. Three hamstring muscles: the biceps femoris, semitendinosis, and semimembranosis located posterior to the femur cause knee flexion through tendons attaching to the tibia and fibula. Meanwhile, the vastus lateralis, vastus medialis, vastus intermedius, and rectus femoris are located anterior to the femur and cause extension by attaching to the patella through the quadriceps tendon. The patella is then connected to the tibia by the patellar tendon (Flandry & Hommel, 2011).

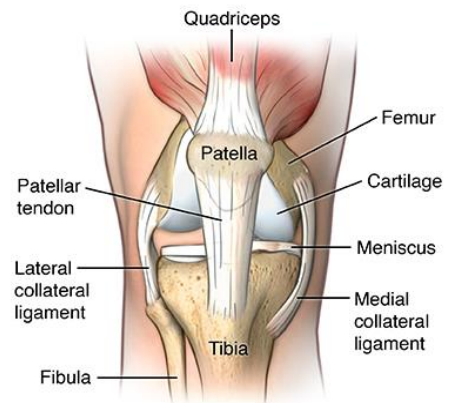


Figure 1: Anatomy of the knee from an anterior aspect. Image courtesy of St. Luke's health system

The patellar tendon is the focus of this research. It is the primary structure mediating knee extension. Therefore, it is responsible for transmitting force to the tibia during locomotion. As a result, the patellar tendon undergoes constant cycles of loading and unloading. The use of the patellar tendon in this manner leaves it susceptible to injuries. From chronic pain and inflammation to sudden catastrophic ruptures, the consequences for overworking tendons are severe.

2. Anatomy of Tendons

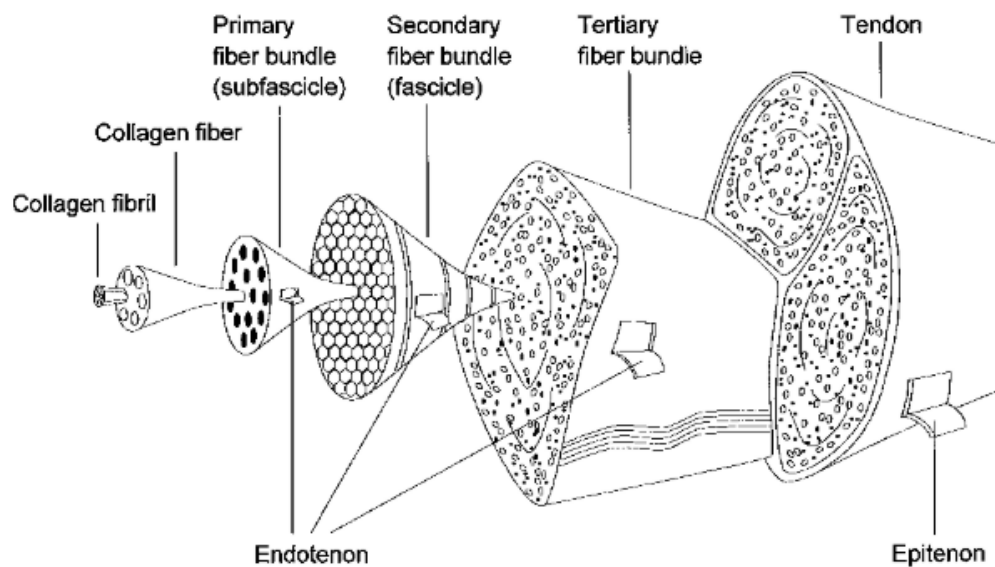


Figure 2: Tendons are composed of a hierarchy of collagen fibers which endow tendons with many of their properties (Kannus, 2000)

Tendons are a type of connective tissue that connects muscle to bone and are critical in facilitating bodily movement. The primary structural component of tendon is the collagen fibril, a triple helix of collagen. These fibrils are organized into fibers and bundles of fibers (figure 2) in a hierarchical manner to create a rope-like structure with high tensile strength. The presence of this collagen dominated extracellular matrix (ECM) is one of the main characteristics of tendon. While there are many types of

collagen, tendons are mainly composed of type I collagen. The ECM is kept alive by fibroblast-like tenocytes. Collagen molecules are organized into microfibrils, fibrils, fibers, and different levels of fiber bundles (Kannus, 2000).

Elastic fiber complexes add an elastic quality to tendons and are composed of elastin surrounded by molecules like fibrillin 1, fibrillin 2, decorin, and biglycan. Elastin present in tendons is located between fascicles at a concentration of between 1% and 10% depending on the type of tendon. It can stretch up to 100% and is thought to work in conjunction with lubricin to promote adjacent fascicles sliding over each other (Thorpe et al., 2013). This structural organization causes mechanical properties to arise that allow tendons to store energy and transmit a force uniaxially from muscle to bone, thus facilitating bodily movements.

Surrounding the collagen fibers, is a ground substance composed of a variety of molecules. One class of molecules that make up the ground matrix is the proteoglycans, and more specifically small leucine-rich proteoglycans (SLRPs) like decorin, biglycan, fibromodulin, and lumican. The exact role of these proteoglycans is largely yet to be elucidated. However, differences in concentration based on tendon regions have been found (Thorpe et al., 2013). Glycosaminoglycans (GAGs), and glycoproteins also contribute to the ground substance. These molecules give the ECM a hydrophilic character, increasing elasticity under compressive and shear loads (Kannus, 2000). Research has been done to elucidate the function of decorin and biglycan in tendon development and healing. Changes in decorin and biglycan concentration have been detected with age, and injury. These changes have also been correlated with changes in tendon architecture. The last class of molecule present in the ground substance are

the growth factors, whose abundance depends on the tendon's current stage of development or healing. These molecules are crucial for maintaining homeostasis, as their signals tell tendon cells to proliferate, produce collagen, or migrate to the site of an injury (Molloy et al., 2003).

Tendon ECM also contains cross-links between collagen molecules. These cross-links impart certain mechanical properties as well. Enzymatic cross-links stabilize fibril structures and are, therefore, a key part of tendon formation. Enzymatic cross-linking affects the mechanical properties of collagen-rich tissues. Trivalent crosslinking between collagen triple helices prevents damage and confers stiffness to the tendon leading to the development of less compliant tissue. Breakage of these crosslinks is believed to be an important mode of fiber damage. The relationship between crosslink density and mechanical properties has been studied in multiple animal models with varying results (Eekhoff et al., 2018) . Meanwhile, advanced glycation end-products (AGEs), like pentosidine, accumulate with age when lysine in collagen triple helices come into contact with glucose. These types of cross-links are thought to impair fibril function, ultimately leading to stiffening, and a loss of viscoelastic properties (Depalle et al., 2015).

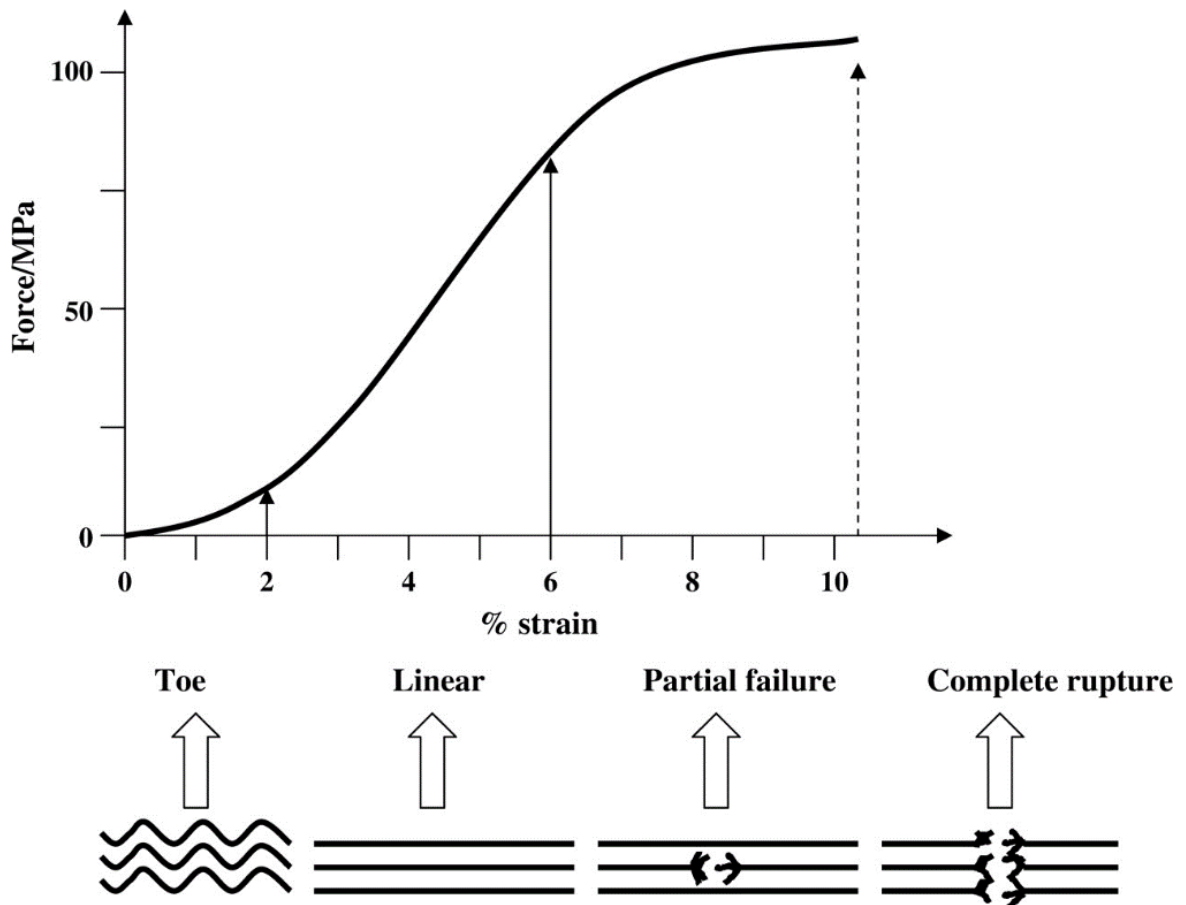


Figure 3: A typical stress-strain curve for a tendon featuring toe region and linear region. Here the transition strain is about 2% strain, the linear region exists between 2% and 6% strain, and failure begins above 6% strain

With no load, the tendon's matrix has a wavelike structure. As load is applied, the naturally crimped collagen fibers straighten out. This process is captured in the toe region of the stress-strain curve. When the tendon is stretched passed the toe region, it has a linear stress-strain relationship. The transition between the toe region and this linear region occurs after only a small amount of force, and has a typical strain value of 2% (Rees et al., 2006). Tendons vary in the amount of load that they experience, and Tendons that experience higher loads tend to be more elastic out of the necessity to stretch more (Alexander, 2002).

3. Tendinopathy

Tendinopathy is an umbrella term that describes any degenerative condition of a tendon, and in 2011 accounted for 30% of musculoskeletal conditions, with prevalence correlated to increasing age (J.-F. Kaux et al., 2011). more thorough examination is required to diagnose tendinosis or tendinitis, which are more specific conditions (Sharma et al., 2006). Overuse is a leading cause of tendon injuries, making up 30-50% of tendon injuries in athletes (J.-F. Kaux et al., 2011). However, a multitude of other factors including ischemia and biochemical imbalances are hypothesized to contribute to tendinopathy (Sharma et al., 2006). The repeated loading and unloading that occurs during physical activity is thought to cause damage in the form of microtears and to accumulate over time. This idea is supported by a couple of observations. Firstly, that 75% of Achilles tendon injuries occur in men ages 30-49, a demographic which is generally still somewhat active, but susceptible to injuries due to age. Secondly, it was observed that biopsies from tendon surgeries showed a tendency towards confirmed signs of degradation like increased collagen disorganization and apoptosis in tendons with tendinopathy (Bell et al., 2018a). One study even found major degeneration of tendon tissue in 97% of ruptured tendons compared to only in 34% of control tendons (Sharma et al., 2006).

In the case of patellar tendons, damage appears to accumulate as a result of excessive jumping activities, leading to the common name: jumper's knee, which is especially prevalent in volleyball and basketball players, reported at rates of 44.6% and 31.9% respectively for elite players (Pearson & Hussain, 2014). The repetitive explosive high magnitude load on the knee is thought to increase the risk of patellar tendinopathy.

As a result of damage, structural and mechanical properties tend to fade over time, eventually leading to a rupture. A decrease in inflammatory cell prevalence is characteristic of tendinopathy, impairing healing and promoting collagen fiber disorganization (Pearson & Hussain, 2014).

Damage to tendon tissues is prevalent among the adult population, especially in athletes and people whose occupations require repeated heavy lifting. Understanding injury mechanisms and injury-related changes in mechanical properties such as ultimate stress, tensile strength, elasticity, and the ECM structure which dictates these properties is paramount for improving public health. Many of these properties exhibit age-dependent behavior, thereby making their understanding a critical part of caring for and preserving quality of life for an aging population. Cross-linking is also affected by aging. Specifically, AGE cross-links build up over time due to the reaction between collagen molecules and glucose, a process known as glycation. The build-up of these cross-links makes the collagen molecules less soluble and less active to enzymes. Mechanically, this leads to less flexibility of collagen molecules. On a larger scale, it leads to the stiffening of tendons, increased failure load, and decreased viscoelasticity (Bailey et al., 1998; Gautieri et al., 2014)

Sex is another important factor to consider in relation to tendon injuries. It has been shown that collagen production increases in males more than in females following bouts of exercise (Magnusson et al., n.d.) and that the presence of estrogen attenuates collagen production and fibroblast proliferation (Yu et al., 2001). Following injuries, females are known to have greater functional deficit from tendon healing than males. Additionally, a greater incidence of disability following tendon injuries is observed in

female patients(Sarver et al., 2017). In a review of patient records concerning tendon injuries, 61% of females and only 34% of males had a comorbidity known to be a tendinopathy risk factor (Garner et al., 2015).

Despite the clear existence of a sex-based disparity in both prevalence and healing outcomes related to sex, both the research and medical fields tend to ignore this factor. Sex is not normally considered in studies of Tendon properties outside of clinical research. Sex is also not considered in guidelines for tendon injury treatment and rehabilitation, possibly stemming from the limited understanding of biological difference between male and female tendons. In one study, a mouse model showed slight differences in cell composition, proteomes, and transcriptomes, but very few differences in structure-function relationships(Sarver et al., 2017). This trend followed an earlier study which investigated Achilles tendon mechanical properties in male and female rats and found no difference in failure stress or stiffness but did identify a greater linear modulus in females compared to males. This same study concluded that larger muscle fiber size combined with inferior tendon mechanics led to the higher clinical rate of Achilles tendon injuries in men (A. M. Pardes et al., n.d.) and implied that the distinction between male and female tendon properties is not as simple as one sex being superior to the other.

4. Tendon homeostasis and healing

Fibroblast-like tenocytes are responsible for producing and regulating the tendon ECM, including producing and secreting collagen, elastin, proteoglycans, GAGs, and regulatory molecules and growth factors. One of the most important classes of regulatory molecules is the matrix metalloproteinases (MMPs). This class of 24

molecules enzymatically degrades ECM and requires zinc to function. MMP function is inhibited by tissue inhibitors of metalloproteinases (TIMPs) (Del Buono et al., 2013). These two classes of molecules work together to regulate the degree of net synthesis and degradation of ECM. Specifically, MMPs-1, 2, 8, 13, 14, and 18 all play a role in binding to and degrading all types of collagen (Del Buono et al., 2013).

Circulating growth factors play a role in collagen synthesis as well. A wide variety of molecules are positively correlated with collagen synthesis. Transforming growth factor β (TGF- β) and mechanical tension both stimulate collagen formation (Kjær, 2004). Along with TGF- β , platelet-derived growth factor (PDGF) also stimulates collagen production. Insulin-like growth factor (IGF) expression is stimulated by PDGF and has been shown to increase fibroblast recruitment.

TGF- β , IGF-I, and PDGF along with vascular endothelial growth factor (VEGF) and basic fibroblast growth factor (bFGF) are all significantly upregulated during various stages of tendon healing as part of the inflammatory, and post-inflammatory response (Molloy et al., 2003). One study found that injecting IGF-I directly into a rat Achilles tendon transection caused a reduction in inflammation and a decrease in functional deficit post-healing. IGF-I is most prevalent in the early inflammatory phase. The research concluded that IGF-I limits the amount of inflammation that occurs during healing and accelerates the healing process (Kurtz et al., 1999). Other growth factors associated with collagen formation include interleukins: IL-1, -6, -8, Nitrous Oxide, and prostaglandins (Kjær, 2004).

A study using mice with knockout genes for the proteoglycans decorin and biglycan showed that these molecules exhibit an age-dependent influence on tendon

healing. Specifically, they found that decorin expression was detrimental to the aging process. While decorin is vital in regulating the process of tendon development, it promotes larger fibril diameters in aging tendons, which pack poorly and decrease fiber alignment as well as the formation of cross-links. The absence of decorin was also associated with the formation of calcification areas within the tendon. Biglycan null mice have shown many of the same deficiencies as decorin null mice to a lesser degree, and expression of biglycan appeared to increase in decorin null mice, most likely to compensate for the deficit in decorin (Dunkman et al., 2013; Thorpe et al., 2013). A study in which SLRP concentration was measured in murine patellar tendons both before and after injury concluded that tendon's mechanical properties decrease with age; while their ability to heal remains ineffective at all ages (Mienaltowski et al., 2016).

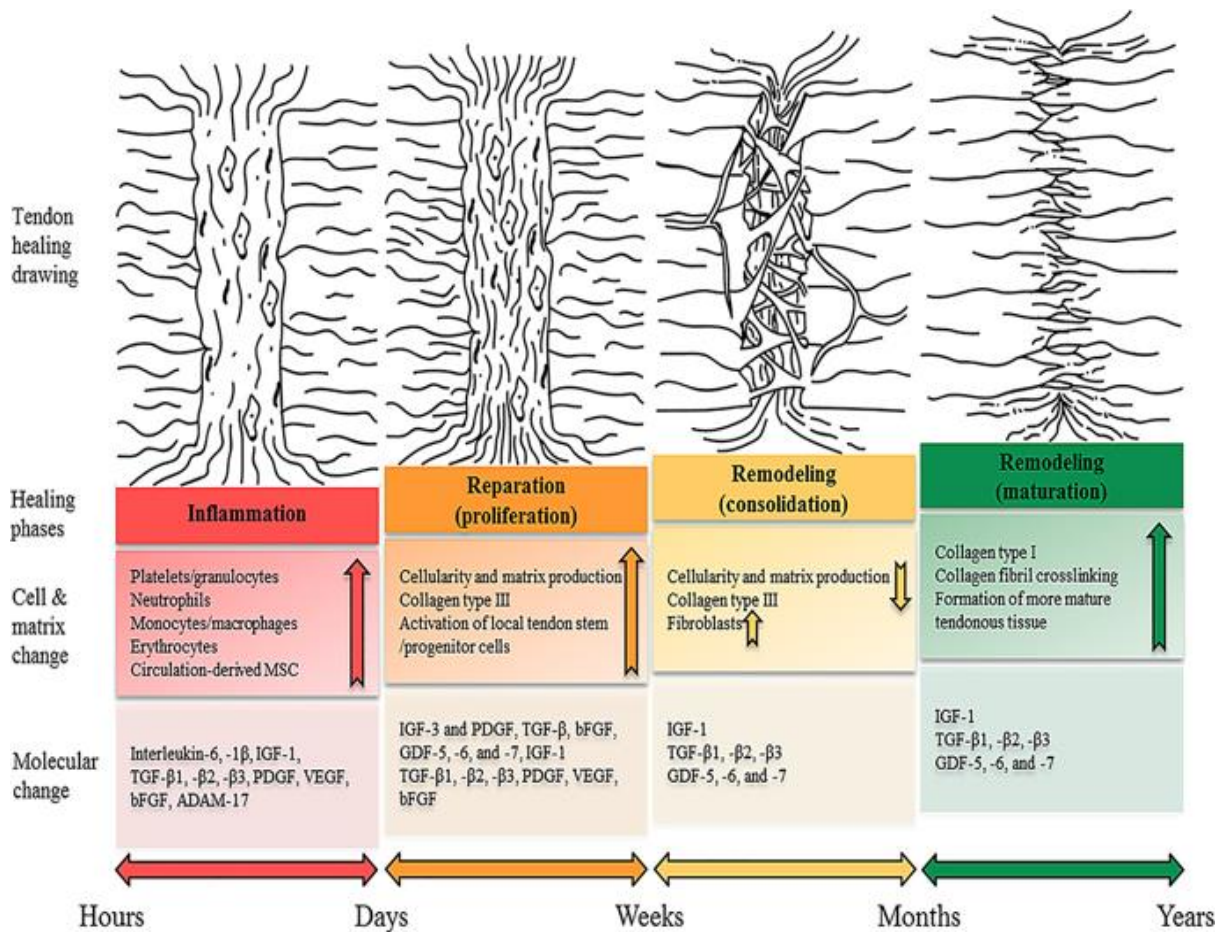


Figure 4: the stages of tendon healing, (from left to right) inflammation, repair, and remodeling. Inflammation is characterized by an increase in platelets, various immune cells, and stem cells. This stage sees increases in several interleukins and growth factors occur. Proliferation is characterized by increase in cellularity and collagen production, and continued molecular change. The Remodeling stages are characterized by new collagen fibers organizing themselves, and the slowing of molecular change. (Schneider et al., 2018)

As a result of their relative lack of cells and vasculature, tendons are deficient in healing and no therapeutics have provided a long-term healing outcome (Schneider et al., 2018). Following an acute injury like a tendon tear, healing occurs in three steps. The first is the inflammatory phase. The inflammatory phase is characterized by an abundance of cells entering the site of the injury. These cells, including neutrophils, monocytes, and macrophages, are responsible for initiating phagocytosis and digesting necrotic material (Sharma et al., 2006). Inflammation is also characterized by an

upregulation of IGF-I, TGF- β , PDGF, VEGF, and bFGF, stimulating tenocyte proliferation, angiogenesis, and collagen production (Molloy et al., 2003).

The next phase of healing is the proliferative phase, which begins between a few days and a week after the injury. During this phase, fibroblast concentration and, subsequently, collagen production peaks. After inflammation, the proliferation phase is triggered and generally lasts for a few weeks. During this time tenocytes follow collagen fibers through a process called contact guidance to reach the site of injury. Once they arrive, they begin to reproduce. The increase in number of fibroblast cells allows for maximum collagen production (Thomopoulos et al., 2015).

Following the proliferative stage is the remodeling phase, during which the cellularity and vascularity in the newly formed tissue decreases. New collagen tissue becomes organized and forms cross-links during this stage as well. The repaired tissue begins to resemble normal, healthy tissue. However, the diameter of the remodeled collagen fibers and the amount of enzymatic crosslinks will both be inferior to that of the pre-injury tendon. (Molloy et al., 2003; Sharma et al., 2006).

5. Current state of tendon computational modeling

Computer models are a key tool for analyzing tendon mechanics and the mechanisms of tendon healing and aging. These models can elucidate certain properties that are hard or impossible to study using physical experiments. For example, finite element modelling can provide data on stress distribution, allowing researchers to quantify and visualize stress concentrations following tendon injuries (Theodossiou & Schiele, 2019). Microstructurally motivated strain energy functions

(SEFs) are useful to study age-dependent healing at a mechanistic level. This lab's past research sought to evaluate the descriptive abilities of SEFs and to identify one for use in a growth and remodeling (G&R) model. The three SEFs investigated were: Gasser–Ogden–Holzapfel (GOH), Shearer (SHR), and Freed-Rajagopol (FR) models. To evaluate these models, experimental data was used to inform the bounds of the models' parameters and the models underwent sensitivity testing. It was concluded that each model has its own set of pros and cons, and that at the time of the experiment, the GOH model was the best for implementation in a G&R model (Akintunde & Miller, 2018).

Several research groups have used various modeling techniques to study tendon healing and development. One example of which is a study that used literature to develop Elementary cell responses (or ECRs) in a computational model to investigate the inflammatory secretion of TGFB, IL1B, and MMP 1 in the healing Achilles tendon under differing strain conditions (Mehdizadeh et al., 2017). In an attempt to elucidate the properties of tendon development for use during healing applications, researchers at the University of Pennsylvania developed a model to analyze the quantitative relationship between tendon composition during development and tendon's mechanical properties (Ansorge et al., 2012).

Agent-based models, or ABMs are a type of computational model in which individual actors, known as agents, are individually simulated. Agent types can each have their own unique variables and behaviors assigned to them. Agents can also interact with their environment. This method allows emergent properties to arise from smaller scale interactions, making it ideal to model biological tissues. One such example is a model created at the University of Virginia used to study arteries in

hypertension, using endothelial cells and smooth muscle cells as agents (Thorne et al., 2011a). ABMs have also been used in the context of tendons. In research also conducted at the University of Virginia Chen, et al. used an ABM to investigate the effects of mechanical loading on Achilles tendon healing in rats. The model's input was an OpenSim model of a rat Achilles tendon and used fibroblasts as agents to provide outputs of collagen content and collagen alignment. They used the model to investigate cyclic loading in both unrepaired and surgically repaired tendons and predicted that this loading would type lead to increased collagen synthesis, but that it does not cause a change in collagen alignment .They also performed experiments with intermittent loading and found that this type of loading had wide ranging effects on cell alignment, which explained some of the variance within published animal model research (Chen et al., 2018).

The research discussed here is based upon previous work in this lab, in which an ABM of murine patellar tendon aging was developed. In this model, fibroblasts were used as agents, and interacted with a collagen dominated ECM, that also contained the growth factors: TGF- β , IGF, and PDGF. It also simulated the presence of the inflammatory cytokine, IL-1 β , and the matrix degrading protein, MMP1 and its inhibitor, TIMP. This model was able to successfully recapitulate the decrease in cellularity and collagen content, and increase in AGE crosslinking that is observed with respect to aging (Vanosdoll, 2017).

III. ABM Formulation

1. Introduction

The first step in generating a computer model of any living system is to conduct a literature search to define the model's framework. Since this ABM's aging parameters were already defined during prior research, they were used as a starting point. What remained to be seen, however was how these same parameters would be affected by injury. Therefore, the bulk of the literature reviewed related to the mechanisms of tendon inflammation and healing. However, it was also necessary to conduct research on techniques for evaluating computational models.

The parameters included in the ABM of tendon aging were the growth factors: TGF- β , PDGF, and IGF as well as an inflammatory cytokine, IL-1 β . MMP-1 and TIMP were also included for their properties regulating collagen amount. Lastly, AGE crosslinks were also included because their increase with respect to age is thought to contribute to the decrease in mechanical properties observed with respect to aging (Vanosdoll, 2017). Among its many effects, TGF- β is known to regulate MMP-1 expression and stimulate collagen production, both of which are important functions during the healing process necessitating its increase in expression following injury (Molloy et al., 2003). IGF is also known to stimulate collagen production and works with PDGF to stimulate cell proliferation (Molloy et al., 2003). While it has been observed that PDGF concentration increases during healing, no known study has quantified the spike in PDGF expression, leaving its role in the healing process somewhat unclear (Molloy et al., 2003). IL-1 β is known to be a regulator of MMP-1 during aging (Vanosdoll, 2017). during healing, it is an inflammatory cytokine that is induced by the beginning of provisional matrix formation (Perez et al., 1999). MMP-1 belongs to the proteinase class of enzymes and functions to degrade collagen fibers, maintaining

homeostasis (Berglund et al., 2007; Fu et al., 2002; Jones et al., 2006; Manning et al., 2014). Its presence is increased during healing as well, likely for the purpose of degrading portions of the ECM that have become disorganized as a result of injury (Del Buono et al., 2013). Conversely, TIMP is an inhibitor of MMP-1 activity, making its inclusion important for maintaining the model's homeostasis (Del Buono et al., 2013).

While the Aging ABM laid a solid foundation for the homeostatic mechanisms of the murine patellar tendon, there is no consideration given to the alignment of collagen fibers, which is a key determinant of the tendon's mechanical properties (Kannus, 2000). There was also no fibroblast migration or macrophage recruitment included in the model, both of which are key considerations for modeling injury response. Because of these gaps in knowledge, it became necessary to target those areas for an in-depth literature search, as well as to look for studies in which the spikes in growth factors, cytokines, and homeostatic regulators were quantified.

2. Literature Searches

The in-depth literature search to determine a ruleset governing the ABM was made up of five distinct miniature literature searches. The first literature search identified how molecules that are a part of the existing aging ABM change during healing. The second focused more on the big picture of tendon healing and was necessary to determine the direction of this research. The third literature search focused on collagen alignment since this would be an output necessary to evaluate healing outcomes. The fourth literature search identified the key aspects of macrophage function in the context of wound healing and was necessary for integrating the healing

framework with the existing aging framework. Lastly, A literature search was conducted with the aim of understanding techniques of computational modeling, specifically agent-based models. The information gathered in this literature search was also useful in deciding the mathematical techniques necessary to translate published research results into a mathematical context usable for programming.

ECM Ground Substance

The relative amount of key ground substance components like growth factors, cytokines, and collagen regulating proteins was a key parameter of the previous aging ABM. Therefore, it was necessary to learn how the relative concentrations of these molecules, changed in response to injuries. To this end, the search terms: Tendon with PDGF, TGF- β , IGF, IL-1B, MMP1, and TIMP were used as search terms to find articles that investigate the ground substance molecules involved in the tendon aging ABM in a healing context. The growth factors, PDGF, TGF- β , and IGF were all covered in a review article about growth factors in tendon and ligament healing (Molloy et al., 2003). This review article led to an abundance of studies covering not only the growth factors, but cytokines, and regulatory proteins as well.

The findings of the first literature search were used to adapt the parameters of the old ABM that would need to be changed with respect to time since injury. In a review article, Molloy et al. showed that multiple growth factors key to tendon healing and remodeling spiked soon after injury in mice and rabbits (Molloy et al., 2003). Another key finding was that quantified spikes in IGF-I, TGF β , and IL-1B production following tendon injury are caused by inflammatory cells entering the injury (Mienaltowski et al., 2016) (Dunkman et al., 2013)(Molloy et al., 2003). According to literature reviewed, the

relative amount of IGF Reaches its peak three weeks after the time of injury. The results of semiquantitative reverse transcription polymerase chain reaction show a five-fold increase in IGF mRNA content three weeks after injury was induced in the medial collateral ligament of New Zealand white rabbits (Sciore et al., 1998). The amount of IGF slowly decreases back to normal in the subsequent weeks. The same study found that the relative amount of TGF- β mRNA followed a similar pattern of increasing initially, and slowly decreasing (Sciore et al., 1998). Guerra et al used an ELISA assay to directly quantify the amount of TGF-B in the injured Achilles tendons of Winstar/Uni Rats. Crucially, this research included a timepoint 8 days after injury, within the critical inflammatory period this research is investigating. In an older study, Natsu-ume et al. excised full patellar tendons from rats, incubated them in an anti- TGF- β antibody, and used immunofluorescent staining to quantify TGF- β presence in three zones of the patellar tendon (Natsu-ume et al., 1997). Since this article did not directly quantify the number of TGF- β molecules, it is not an ideal candidate for use in constructing a mathematical rule defining the change in quantity of this molecule. Nevertheless, the key finding that TGF- β spikes both earlier, and in higher amounts near the injury in comparison to the origin and insertion reinforces the idea that TGF- β is crucial to regulating repair mechanisms at the site of injury.

While multiple articles reviewed agreed that there is a spike in PDGF localized to the site of injury, There is a paucity of articles in which this growth factor spike is quantified (enoch David John Leaper, 2008). Because of this lack of information and the role PDGF plays as both a chemoattractant, and a promotor of fibroblast proliferation, quantification of changes in PDGF content following injury became a key step in ABM

formulation. While the exact response of PDGF to injury is unknown, experiments investigating interactions between PDGF and human dermal fibroblasts in culture sheds some light upon the decay rate of PDGF content (Heldin, H E Westeson & Westermark8, 1982).

The expression of the inflammatory cytokine, IL-1B, spikes very quickly following tendon injuries. In studies quantifying IL-1 β content using ELISA assay, an IL-1 β concentration of 5 times the normal amount was found 1 day after injury, much like the growth factors discussed earlier, this quantity slowly decreased in the following weeks after an injury (Da Ré Guerra et al., 2016; Koshima et al., 2007). Another study quantifying relative mRNA with respect to time reported a spike of up to 15 times the normal amount, and showed that mRNA expression for IL-1 β returned to normal 6 to 12 days after injury (Berglund et al., 2007).

Increases in MMP-1 and its inhibitor, TIMP, are also known to occur following Tendon injury (Berglund et al., 2007; Fu et al., 2002; Jones et al., 2006; Karousou et al., 2008; Manning et al., 2014). However, since the function of the increase in MMP-1 is to remove damaged collagen fibers, this increase was not chosen for use in this ABM. Because the injury mode used in the ABM simply deletes all collagen within the defined injury area, this function has already been carried out. As such, it would be redundant to include changes in MMP-1 and TIMP in the model.

The results of this literature search revealed how the functions of the ECM ground substance during homeostasis are translated to the context of healing. Each of these molecules plays a crucial role in the essential functions of inflammation, proliferation, and remodeling (Da Ré Guerra et al., 2016; Jones et al., 2006; Molloy et

al., 2003). Critically, it is widely observed that changes in growth factor is localized to the injured area (Natsu-ume et al., 1997). While this literature yielded the most quantitative results out of all the literature reviewed, challenges arose because of a lack of consistency in the methods used in the reviewed literature. Multiple animal models, tissue types, and quantification methods present difficulties in determining which results are most applicable to the murine patellar tendon. One source in particular investigated multiple ECM components, but consistently reported results that differed by orders of magnitude from its counterparts (Da Ré Guerra et al., 2016; Jones et al., 2006; Manning et al., 2014).

Healing Mechanisms

After Identifying injury related changes in ground substance molecules, it was necessary to gather for information detailing known healing mechanisms to determine what features should be added to the ABM. For this search, review articles covering the stages of tendon healing (Thomopoulos et al., 2015) were used as a starting point and its citations were used to find the review article's most relevant sources that ultimately led to the generation of rules concerning the roles of the provisional matrix (J. Y. Hsieh et al., 2017), fibroblast migration (Mcdougall et al., 2006) (P. Hsieh & Chen, 1983), and the pathways that lead to the spikes in growth factor secretion mentioned above (enoch David John Leaper, 2008). The most important of these mechanisms are known as contact guidance and chemotaxis. Contact guidance is the phenomenon that determines how cells move in a fibrous matrix. Fibroblasts and fibroblast-like cells adhere to the fibers of the matrix which surrounds them and consequently move in the direction of these fibers (Guido & Tranquillo, 1993). In the highly aligned collagen matrix

found in tendons, this results in tenocyte motion to bias towards movement along the tendon's axial direction. Chemotaxis is a type of cell signaling in which cells are attracted by a gradient of a molecular ECM component (Guido & Tranquillo, 1993). For the purposes of this ABM, TGF- β and PDGF are the two chemotactic signals.

Alignment

While conducting the initial literature searches, it was observed that collagen alignment is key to determining healing outcomes and would therefore need to be an output for this ABM. Not only does collagen alignment decrease with aging, but it is also decreases in healed tendons compared to its healthy counterparts of the same age (Dunkman et al., 2013)(Dunkman et al., 2014). Collagen's rope-like microstructure is responsible for tendon's unique ability to transfer large uniaxial loads (Kannus, 2000). If this structure is disrupted, the tendon's mechanical properties are compromised, leaving the tendon susceptible to chronic injury.

To reflect the importance of collagen alignment to healing outcomes, it was necessary to gather information about what factors lead to these changes. Articles by dunkman et al. quantifying the decrease in collagen organization with both age and injury were used as a starting place to investigate collagen alignment (Dunkman et al., 2013, 2014). While the factors affecting collagen alignment mostly remain a mystery, these studies conclude that decorin and, to a lesser extent, biglycan are related to these observed changes in alignment. Decorin and biglycan were also used as search terms in conjunction with "tendon" to look for a relationship between relative amounts of these molecules and both age and time since acute injury in small animal models.

Other studies conclude that the changes in collagen alignment are not molecular in nature, but rather that they are a result of tenocyte migration. Tenocytes produce collagen as they move, meaning that the fibers they produce often have the same direction as the migrating tenocytes (Guido & Tranquillo, 1993). Consequently, if tenocytes move in a direction other than the axial direction while performing healing functions, it is hypothesized that they may also be contributing to the loss of collagen organization observed in healed tendons. A dermal wound healing model was used to form the backbone of the ABM's tenocyte migration and ECM realignment logic (Mcdougall et al., 2006). In this model, fibroblast motion is defined using the relative amounts of chemotactic molecules and the direction of existing collagen fibers. Change in alignment is based on both the direction of fibroblast motion and the predominant direction of existing fibers. While this model does not deal with tendon tissue, it is reasonable to conclude that it is applicable to the tendon healing ABM because it simulates the interaction between fibroblasts and a collagen dominated matrix.

Macrophages

The function of macrophages and their intimate involvement in regulating the spikes in growth factors and other molecules that characterize the inflammatory phase is a key consideration in the generation of a healing model. "Macrophage" was used as a search term along with "tendon" to find relevant articles. This resulted in several articles detailing numerous aspects of macrophage functions during the inflammatory phase of healing.

Macrophage activity is key to the tendon's healing mechanisms. These cells are responsible for removing necrotic tissue (Marsolais et al., 2001), secreting cytokines

and growth factors (J. Y. Hsieh et al., 2017; Marsolais et al., 2001), and removing the provisional matrix at the end of the inflammatory phase (Marsolais et al., 2001). The activity of macrophages is also modulated by the composition of the provisional matrix. In the presence of fibrinogen, macrophages display anti-inflammatory behavior, but in the presence of fibrinogen's precursor, fibrin, they display inflammatory behavior (P. Hsieh & Chen, 1983; Perez et al., 1999; Smiley et al., 2001). Macrophages have also been observed transitioning to a fibroblast-like phenotype under the right conditions (Marsolais et al., 2001).

Rule scoring

An ABM of arterial adaption to hypertension developed by Thorne inspired the method used herein to evaluate the reliability of the literature derived rules (Thorne et al., 2011a). This scoring system required a few minor modifications to make it relevant for this study's purposes. The scoring system awards 1-10 points in four categories, and averages these four scores, resulting in a final score out of ten. The four categories scored are: article agreement, similarity, physiological methods, and quantification methods. For article agreement, points were awarded for the number of articles that agreed with the source in question and were subtracted for articles disagreeing with the source in question. The similarity score is based on whether the cell types used in the study matched the ones used in the ABM, and the degree of similarity of the organ investigated to the murine patellar tendon. Points are also awarded if the study used a murine model, and less points are awarded for other small animals. other animals received zero points. Next, the physiological methods were evaluated. In vivo methods were scored the highest, ex vivo methods received less points, and in vitro methods

received the fewest points. Lastly, quantification methods were scored. For this score, quantitative data was preferred over qualitative data, direct measurement methods were preferred over indirect methods.

<i>ABM Rule Scoring</i>
1. Article Agreement
0=0
1/2=5
3/4=7
5/6=9
7+=10
(-1 for every conflicting article)
2. Similarity
<i>a. Tendon Type</i>
Patellar=10
Other Energy Storing (Achilles/SDFT/Supraspinatus)=7
Other =3
Non-Tendon Data=0
<i>b. Species</i>
Mouse=10
Other Small animals (Rats/rabbits etc.)=5
Others=0
<i>c. Cell Type</i>
Fibroblast/Macrophage=10
Other=0
3. Quantification Methods
In vivo, non-linear, residual, anisotropy, heterogeneity accounted for = 10
Ex vivo, pre-conditioned, acute testing, comp. sound = 8
Ex vivo, cultured, pre-conditioned, comp. sound = 6
In vitro, acute testing, environment sound = 4
In vitro, culture = 2
4. Data Type
<i>a. Numerical</i>
Numerical=10
Theoretical=6 (inferred)
Descriptive=2
<i>b. Measured Indirectly</i>
Measured Directly=10
Measured Indirectly=6
Extrapolated=4

Table 1: Scoring system used to evaluate the relevance of articles investigated for incorporation in the ABM.

Computational techniques

Knowledge of modelling techniques was required to determine the best way to construct the ABM and perform experiments using it. Articles leveraging ABMs to investigate Achilles tendon and arterial healing showed possible ways that cells could be programmed to interact with their ECM (Id et al., 2018) (Thorne et al., 2011b). Furthermore, it was necessary to find a statistical method to determine the number of experimental runs needed to obtain significant results. Lastly, it was necessary to determine a method of scoring all of the literature-derived rules to evaluate confidence in each individual facet of the model.

An element of stochastic variation is introduced into the model because the initial placement, proliferation, and apoptosis of modeled cells are randomized. Therefore, it is necessary to run the ABM multiple times to obtain significant results, accounting for the varying initial conditions at the time of injury. Since the model is run both before and after injury, experiments with injuries occurring at aged and geriatric timepoints require more simulations to reach a significant conclusion, accounting for the variation in conditions at the time of injury. To evaluate whether the appropriate number of runs are conducted, many researchers use a confidence interval, which is a range of values in which researchers can be reasonably confident that the true value of a parameter exists. (Byrne, 2013). The confidence interval is described by the following equation:

$$C = m \pm \frac{S}{\sqrt{n}} * z^*$$

Equation 1

Where S is the standard deviation of the data, n is number of runs, m is the mean, and $z^* = 1.96$. This value of z^* is used when a 95% confidence interval is desired. When a higher level of confidence is desired, a larger value is used. For example, when a 99% confidence interval is desired, $z^* = 2.576$ (Byrne, 2013).

Coding in NetLogo

NetLogo is an open-source software developed specifically for the generation of ABMs. ABMs in NetLogo consist of 3 main agent types: turtles, patches, and links. Turtles are individual actors that can move about the model and interact with other agents. Patches are stationary and form the background of the simulation. Links represent connections between turtles, and they are represented as a line connecting the two agents.

NetLogo also comes with a built in GUI that includes a view of the agents and can be customized with codable buttons; inputs can be customized using sliders, switches, choosers, or typed inputs; and outputs can be shown using plots and monitors. NetLogo also comes with an extensive library of models covering a wide range of topics. It also comes with a number of tools, most notably of which is BehaviorSpace, which can be used to run experiments with a desired output and range of parameter values.

Rule Generation

The key step linking published experimental results with the NetLogo ABM is the formulation of a set of specific, salient rules backed by a reasonable level of confidence. While there is no direct translation from the activity within living tissues to an in-silico simulation, this set of rules forms the backbone of the ABM by approximating these activities and assigning instructions to the various agents present in the model.

The representation of the biopsy punch injury and the ECM changes that result directly from this injury followed relatively directly from the reviewed literature. The dimensions of the tendon were determined by data collected during the lab's pilot study investigating sex-based differences in tendon healing and the size of the simulated biopsy punch matched the dimensions of a previously validated biopsy punch procedure (Lin et al., 2004).

Changes in IGF, TGF- β , IL-1 β , and decorin in the days and weeks following an injury were quantified in several papers, using a variety of animal models, modes of injury, and quantification techniques. These methods were analyzed using the method described in Table 1. For each of these molecules, a piecewise function was defined connecting the data points collected by researchers. While this method may fail to capture minute variations in the relative concentration of certain growth factors, it is useful for evaluating the overall shape of these curves. These rules would require further experimentation to define an appropriate weight for the piecewise function at each interval.

The phenomenon of fibroblast migration by contact guidance is strongly linked to the healing process (Guido & Tranquillo, 1993). The transportation of fibroblasts to the

site of injury allows for new collagen production to occur, rebuilding the tendon and restoring its functionality. As such formulating rules for this kind of migration was necessary for ensuring the model's ability to predict healing outcomes. Unfortunately, there is very little research from which to determine the details of fibroblast migration. One commonly agreed upon characteristic of contact guidance is that cells tend to move in the primary fiber direction, and deposit new collagen fibers in the direction of movement. A computational model of dermal healing was used to formulate the rules for contact guidance within a tendon (Mcdougall et al., 2006). This model's interaction between fibroblasts and a collagen dominated ECM were the key deciding factors in deciding to use it for the purposes of the ABM. A set of vector equations, taking multiple ECM components into account are used to calculate the direction of fibroblast movement:

$$\frac{d\vec{f}}{dt} = \dot{f}(t) = s * \frac{\vec{v}}{\|\vec{v}\|}$$

Equation 2

$$\vec{v}(t) = (1 - \rho) * \frac{\vec{u}(t)}{\|\vec{u}(t)\|} + \rho \frac{\dot{f}(t - \tau)}{\|\dot{f}(t - \tau)\|}$$

Equation 3

$$\vec{u}(t) = (1 - \alpha) * \vec{c} + \alpha * \vec{b}$$

Equation 4

$$\frac{d\theta}{dt} = \|\vec{f}\| * k * \sin(\theta - \phi)$$

Equation 5

In these equations, the vector \vec{f} represents the path of a fibroblast, it is the critical output of this set of equations. α and ρ are positive constants, while \vec{c} and \vec{b} are the vectors describing the quantity and direction of collagen and fibrin fibers most closely matching the direction of the chemotactic gradient. τ is a time delay, s represents cell speed, and k represents the ability of the collagen matrix to change directions.

ABM Rules Table		
Behavior	ABM Rule	References and Confidence Score
Biopsy punch injury	All patches within the radius of the biopsy punch set collagen amount to zero	(Lin et al., 2004) Score: 10
IGF spike following injury	5 * <i>normal</i> 3 weeks after injury 2.75 * <i>normal</i> 6 weeks after injury 2 * <i>normal</i> 14 weeks after injury	(Dunaiski & Belford, n.d.; Sciore et al., 1998). Score: 7.25
TGF- β spike following injury	4 * <i>normal</i> 8 days after injury 2 * <i>normal</i> 15 days after injury 1.25 * <i>normal</i> 6 weeks after injury 1 * <i>normal</i> 14 weeks after injury	(Da Ré Guerra et al., 2016; Natsu-ume et al., 1997; Sciore et al., 1998). Score: 7.625
Decorin changes following injury	Decorin content decreases following injury and recovers as healing progresses Associated with decreased collagen organization following healing	(Karousou et al., 2008; Manning et al., 2014; Mienaltowski et al., 2016; Sugg et al., 2014) Score: 7.75
Decorin changes with age	Decorin content is increased in geriatric mice compared to adult mice	(Dunkman et al., 2013) Score: 7
IL-1 β spike following injury	5 * <i>normal</i> 1 day after injury 4 * <i>normal</i> 3 days after injury	(Berglund et al., 2007; Da Ré Guerra et al., 2016; Koshima et al., 2007; Sugg et al., 2014)

	3 * <i>normal</i> 7 days after injury 2 * <i>normal</i> 21 days after injury 1 * <i>normal</i> 42 days after injury	Score: 6.5
Contact guidance	Fibroblasts migration is based on the gradient of PDGF and TGF- β .	(Guido & Tranquillo, 1993; Mcdougall et al., 2006) Score:7.91
Collagen matrix realignment	$\frac{d\theta}{dt} = k\ f\ \sin(\phi - \theta)$	(Mcdougall et al., 2006) Score: 6.67
Provisional matrix formation	Fibrinogen enters injury site quickly after injury.	(Doolittle, 2017) Score: 7
Fibrinogen to fibrin transition	IGF plays a role in catalyzing transition to fibrin	(Gligorijević et al., 2017) Score: 4
Macrophage behavior in presence of fibrinogen	Suppression of TGF- β production, Stimulation of IL-1 β production	(J. Y. Hsieh et al., 2017; Perez et al., 1999; Smiley et al., 2001) Score:6.42
Macrophage behavior in presence of fibrin	Stimulation of TGF- β production	(J. Y. Hsieh et al., 2017) Score: 4.67
Fibroblast behavior at provisional matrix	Reduction in collagen production on provisional matrix	(J. B. Pardes et al., 1995) Score: 3.83
PDGF spike decay	PDGF decays by a factor of 5 in 4 hours when bound to fibroblast.	(Heldin, H E Wasteson & Westermark8, 1982) Score 4.08

Table 2: List of behaviors, rules, sources, and scores for the rules defined in the aging/healing ABM

3. ABM Framework

The rules described above were used to formulate the framework for the ABM (Figure 5). The new model builds upon the aging only model chiefly by adding Injury at a variable age as an input. The addition of this input led to the expansion of the changes in ECM composition as well as the addition of decorin to the ECM composition. Further,

the processes of Inflammation and provisional matrix formation were necessary to inform the addition of a third output: collagen alignment.

The formation of provisional matrix is one of the first steps in tendon healing, and is crucial for directing the migration of fibroblasts, and the regulating macrophage phenotype (Doolittle, 2017). The precursor molecule, fibrinogen enters the tendon from the blood stream, and contributes to clot formation. Polymerization of fibrinogen to fibrin is partially mediated by IGF-I (Gligorijević et al., 2017). In lab experiments, it has been observed that macrophage activity depends on whether the cells are cultured on a fibrinogen- or fibrin-dominated matrix. Fibrinogen promotes inflammatory factors like the increased production of IL-1 β , while fibrin promotes anti-inflammatory activity represented in the ABM as the secretion of TGF- β (P. Hsieh & Chen, 1983). The presence of the provisional matrix also prevents collagen production (A. M. Pardes et al., n.d.), making the removal of this matrix critical to transitioning from inflammation to proliferation (Figure 6).

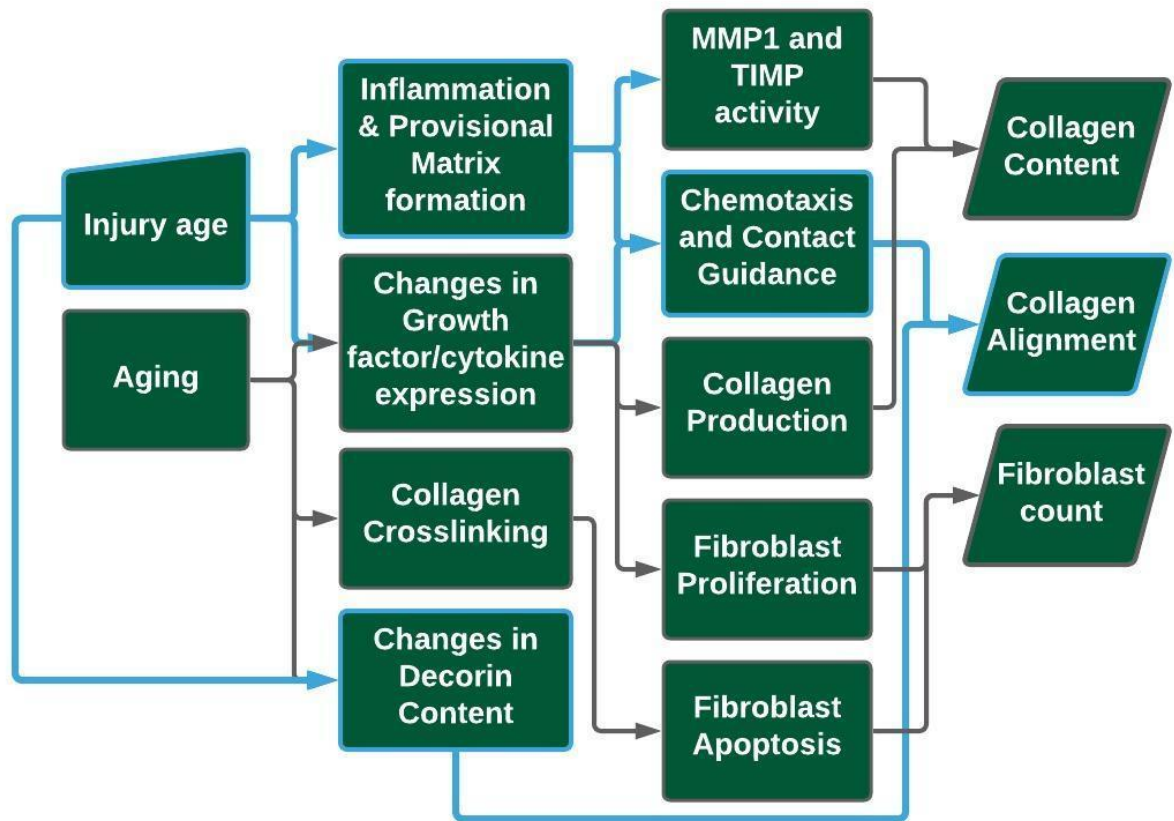


Figure 5: Flowchart illustrating the broad functions of the healing/aging ABM. Newly added processes and their direct affects are highlighted in blue. User can input whether an injury occurs, as well as the age of the mouse at the time of injury. These choices affect inflammation, molecular activity, and can trigger inflammation. The changes in growth factors cause chemotaxis. These processes lead to the final step of this framework: the output of Collagen Alignment.

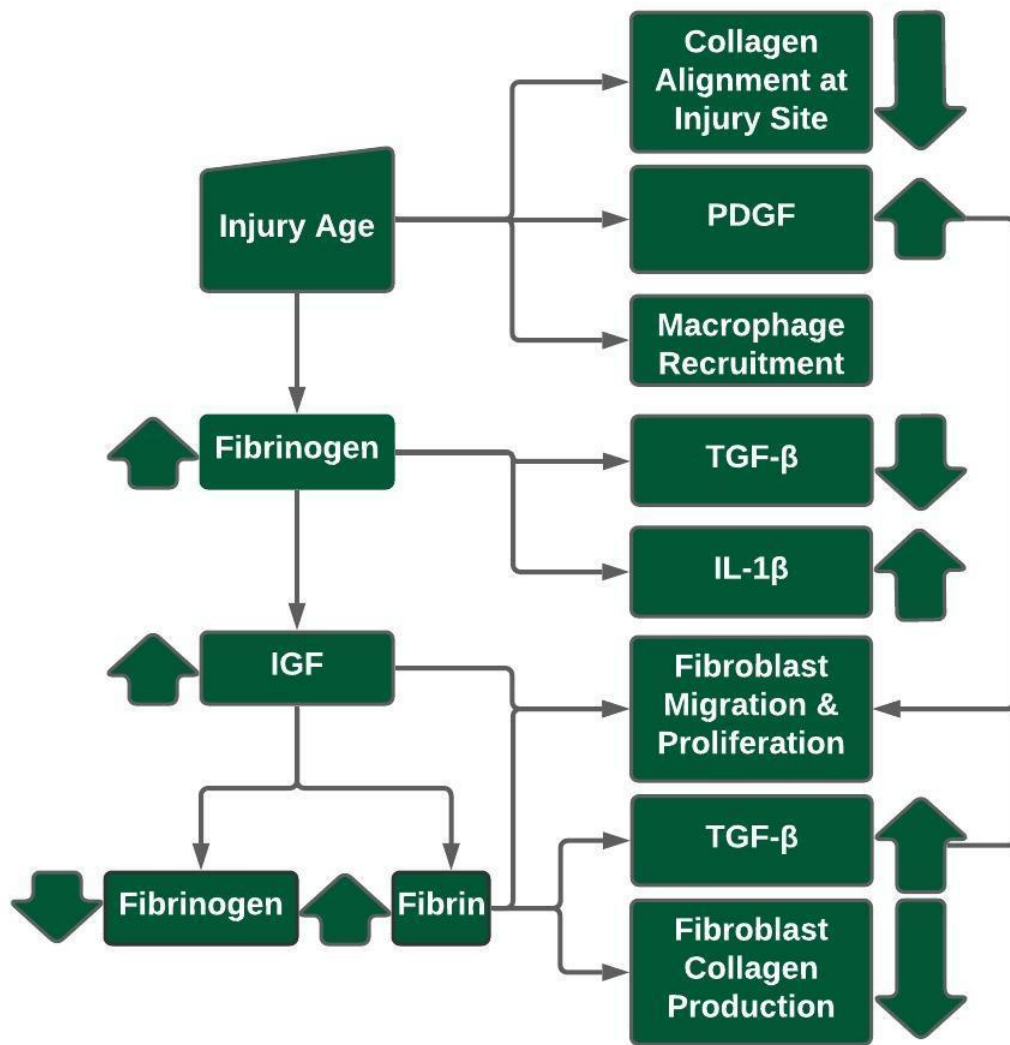


Figure 6: Flowchart showing the interactions between Provisional matrix proteins (Fibrinogen & Fibrin) and the various growth factors and cytokines released by macrophages and fibroblasts following an injury. Following the injury, and the direct consequences it has on the composition of tendon ECM, The effects of fibrinogen, IGF, and fibrin

The newly added output, collagen alignment was measured using a value known as alignment coefficient, or \bar{R} . Initial values of alignment were determined using data which quantified the Circular Standard Deviation (CSD) of wild type adult and geriatric murine patellar tendons. CSD is related to \bar{R} by the following equation (NCSS, 2010):

$$\bar{R} = e^{\frac{CSD^2}{-2}}$$

The calculated value of \bar{R} was used to define a circular probability density function, also known as a von Mises Distribution, defined as follows:

$$f(a, \theta, K) = \frac{1}{2\pi I_0(K)} * e^{K * \cos(a - \theta)}$$

Equation 6

$$I_0(x) = \sum_{r=1}^{\infty} \frac{1}{(r!)^2} * \left(\frac{x}{2}\right)^{2r}$$

Equation 7

Using this distribution, the probability of finding a collagen fiber is calculated every 5° at angles from -90° to 90°. The starting collagen for each patch agent is then divided into 100 discrete pieces, and each piece is randomly placed at an angle based on the probabilities calculated by the Von Mises distribution. This process results in a collagen matrix that is highly aligned in the axial direction and contains occasional deviations.

The ABM display shows fibroblasts as white stars and macrophages as black ovals. The ECM is represented as a colorimetric scale, that can be set to any ECM parameter. When viewed using this colorimetric scale for collagen content, an injury is represented as a red area enclosed by a circle in the center of the display. Alternatively, molecular gradients can be represented, which is useful for showing the localization of

molecular spikes. The graphical interface also contains charts plotting the values of various matrix properties with respect to time.

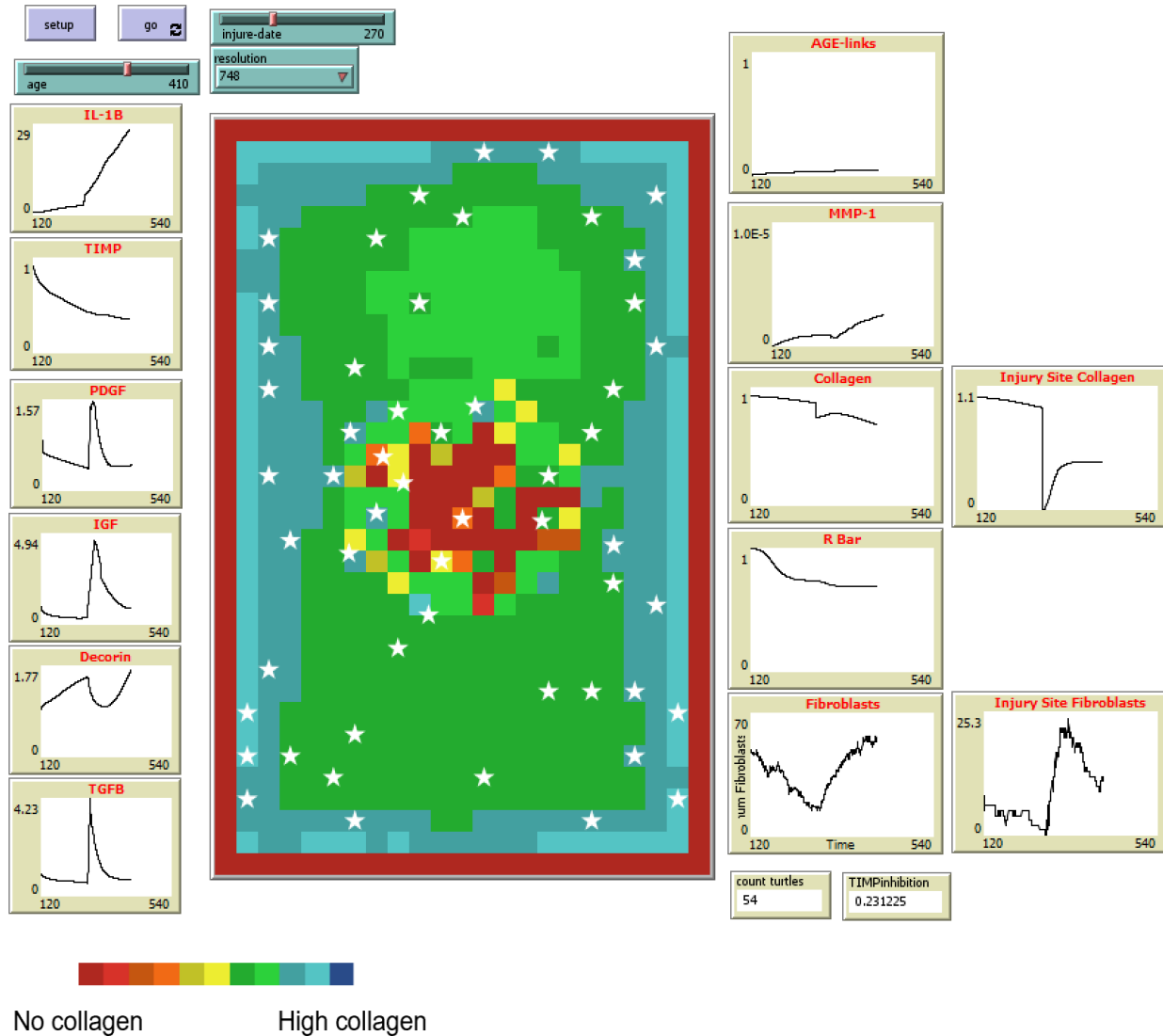


Figure 7: The graphical display of the ABM shows a number of fibroblast-like tenocytes on a multicolored background representing the ECM set to a colorimetric scale. In this image, the background represents collagen content where blue represents a relative value of 1, the amount of collagen present in a 120 day-old tendon, and red is a relative value of 0. The graphs on the left side of the image plot the relative values of matrix components that are expressed by and interact with tenocytes. The graphs on the right plot the values of matrix properties determined by interactions between cells and the matrix, namely the key outputs of collagen amount, collagen organization (R-Bar) and fibroblast count. In this image, an injury occurs at the age of 270 days old and has undergone 140 days of healing.

The age of the simulated tendon can be constantly monitored via the slider on the upper-left hand portion of the ABM display. An age for the injury can be selected using the second slider. A resolution of 748 or 2772 can be chosen using the dropdown menu. The higher resolution provides a more detailed representation of the model's outcomes, by dividing each patch by four. However, This added detail comes at the cost of greatly increased computing time.

IV. ABM Simulations

1. Introduction

Simulation of tendon healing using the previously determined framework allowed the model's outcomes to be quantified and compared to the literature from which they were derived. The key outcomes of cell counts, collagen amount, and collagen orientation are determined by the relative amounts of a variety of molecules present in the tendon's ECM. Additionally, fibroblast proliferation and apoptosis play a crucial role in determining the tendon's ability to regulate these outcomes.

The rules determined thus far are only a steppingstone towards the final model. They were translated to NetLogo in a largely qualitative manner based on the results of the numerous sources reviewed. While some rules, such as the spikes in TGF- β (Da Ré Guerra et al., 2016; Sciore et al., 1998), IL-1B (Berglund et al., 2007; Da Ré Guerra et al., 2016; Koshima et al., 2007), and IGF (Dunaiski & Belford, n.d.; Lee et al., 2010; Sciore et al., 1998) following injury are quantified in the studies they are derived from, the specific weights of these factors are not directly reflected in the outputs of the model. Other rules such as the interaction between macrophages, and the provisional

matrix are not quantified (J. Y. Hsieh et al., 2017; Perez et al., 1999; Smiley et al., 2001), requiring experiments to verify that the interactions observed in literature are supported by the ABM. Further, since the healing model is built atop the framework of an ABM of tendon aging, it is also necessary to verify that the trends observed in the previous model are upheld by the results of this model.

The equation for the spikes in TGF- β and IGF-I content reported previously is sufficient to recreate the overall shape of the change in TGF- β and IGF-I content in response to injury. However, initial simulations showed that these equations alone did not recreate the results reported in past investigations of relative TGF- β and IGF change following tendon injuries (Da Ré Guerra et al., 2016; Sciore et al., 1998). Thus, it was necessary to run experiments varying the weight given to this equation at various post-injury time ranges needed to recreate these results more closely.

The design of the ABM framework includes multiple areas of stochastic variability. The complex systems modeled by ABMs can be very hard to predict precisely due to the extreme complexity of the multitude of agents interacting within them. In biological research, much of the crosstalk between different cell types has only recently been understood, and there are many factors that remain unclear, affecting our ability to predict the behavior of such systems. Therefore, stochastic variability is a necessary feature of ABMs, especially those which model biological systems (Conte & Paolucci, 2014). To counteract this variability, it is necessary to run experiments many times to reliably conclude that the model recapitulated the results reported in literature.

The objectives of these experiments are two-fold. Firstly, they will define some of the parameters necessary to recapitulate the phenomena reported by the literature on

which the ABM is based. Secondly, they will evaluate the ability of the ABM to predict the salient outcomes of patellar tendon healing. The first of these goals will be accomplished by establishing bounds for unknown parameters and running multiple simulation runs at evenly spaced values between these two bounds. The second will be accomplished by running simulations for injuries occurring in 120-, 270-, and 540-day old mice, and comparing the results between injury groups, or with a non-injury control set of simulations. If successful, this ABM can serve as a platform for testing hypotheses about patellar tendon healing, and its outputs can be leveraged to inform a finite-element model of the patellar tendon under tension.

2. Methods

Parameterization of TGF- β

In an experiment measuring the overall TGF- β content in a healing rat Achilles tendon, it was observed that there was a 4-fold increase in TGF- β content at day-8 following the injury, and that by day-15 TGF- β decayed to about 2 times its previous value (Da Ré Guerra et al., 2016). In the first parametrization test for TGF- β , the change in TGF- β content was multiplied by constant: $K_{1,TGF-\beta}$, Transforming the piecewise function to:

$$TGF\beta = \begin{cases} K_{1,TGF-\beta} * \frac{1}{2}t + 1, & t \leq 8 \\ -K_{1,TGF-\beta} * 0.081t + 4.68, & 8 < t \leq 42 \end{cases}$$

Equation 8

Initial bounds for this constant were determined by observing the results of simulation runs. Values of five and fifteen were chosen for the respective lower and

upper bounds because it was observed that these values under- and over-estimated the desired spike in TGF-B. Thirty simulations were run for eleven equally spaced values between five and fifteen. The average and standard deviation of TGF- β amount at day-8 was plotted against the values of $K_{1,TGF-\beta}$. A linear equation was fit to the data using MATLAB's "fit" function.

This equation was used to determine the ideal value of $K_{1,TGF-\beta}$. Following this experiment, an observed was made that the relative amount of TGF- β reached an equilibrium higher than that of healthy tissue. Therefore, it was determined that a second constant, $K_{2,TGF-\beta}$ was needed to regulate the decay to normal TGF- β levels at later time points. The change in TGF- β was divided by this new constant as shown below:

$$TGF\beta = \begin{cases} K_{1,TGF-\beta} * \frac{1}{2}t + 1, & t \leq 8 \\ -\frac{K_{1,TGF-\beta}}{K_{2,TGF-\beta}} * 0.081t + 4.68, & 8 < t \leq 42 \end{cases}$$

Equation 9

Using a similar procedure to the one above lower and upper bounds of one and ten were determined. $K_{2,TGF-\beta}$ was varied at eleven equally spaced values between one and ten for thirty runs at each value. The average and standard deviation of TGF- β amount at day 15 was plotted against $K_{2,TGF-\beta}$. This time, an exponential equation was fit to the data using MATLAB's fit function. This equation was used to determine the ideal value for $K_{2,TGF-\beta}$.

Parametrization of IGF-I

The weight of the IGF-I spike was determined using a similar procedure to that of the TGF- β spike. According to published literature, the relative amount of IGF-I present in the tendon was 5 times greater than normal at day-21 post injury (Sciore et al., 1998). Thus, a weight, K_{IGF} is multiplied by the initial piecewise function to produce the following equation:

$$IGF = \begin{cases} K_{IGF} * 0.19 * t + 1 \\ K_{IGF} * -0.14 * t + 8 \\ K_{IGF} * -0.018 * t + 2.75 \end{cases}$$

Equation 10

When establishing bounds for this constant, it was observed that when total IGF-I surpassed a critical value of approximately five, the model began to produce too many fibroblasts, leading to a catastrophic failure of the model. This error is due to the equation defining the chance that a new fibroblast will be produced:

$$\frac{1}{P} = \left(5.6 * \frac{1}{PDGF} + \frac{100}{0.48} \right) - ((-0.00071 * t + 0.89)(IGF) * 10)$$

Equation 11

In this equation, $\frac{1}{P}$ is the probability that, at any given time, a fibroblast will undergo mitosis, producing a new fibroblast. PDGF and IGF represent the amount of respective growth factor at the same location as the fibroblast in question and t represents age. The probability of new fibroblast formation is directly proportional to IGF content, and the current number of fibroblasts, leading to a positive feedback loop when IGF concentration is too high. For the initial IGF parametrization experiment, ten equally

spaced values between four and five were used. Thirty simulations were run for each value, and the results were used to determine the optimal value of K_{IGF} .

Parametrization of PDGF

Because of the lack of published literature quantifying the change in PDGF content following injuries, Determination of the rule for changes in PDGF depended upon matching the magnitude of the PDGF spike with healing outcomes reported in literature. Injury site cellularity was chosen as the output to be paired with PDGF content because of PDGF's role as both a chemoattractant and a promoter of proliferation. ten evenly spaced values from five to fifty were chosen for PDGF produced by macrophages at each tick. 100 runs were completed for each value, and the percentage of fibroblasts was calculated for one-, three-, and nine-days post-injury. These timepoints correspond with the findings of Manning et. Al, who reported that fibroblasts become the dominant cell type in the injury site after nine days of healing (Manning et al., 2014).

Healing at Different ages

To investigate differences in patellar tendon healing with of age, simulations for injuries occurring in 120-, 270- and 540- day old mice were conducted. Fifty runs of each simulation were conducted and key outputs were measured, and reported for one, three, nine, fourteen, twenty-one, and forty-two days after the injury.

3. Results

Parameterization of TGF- β

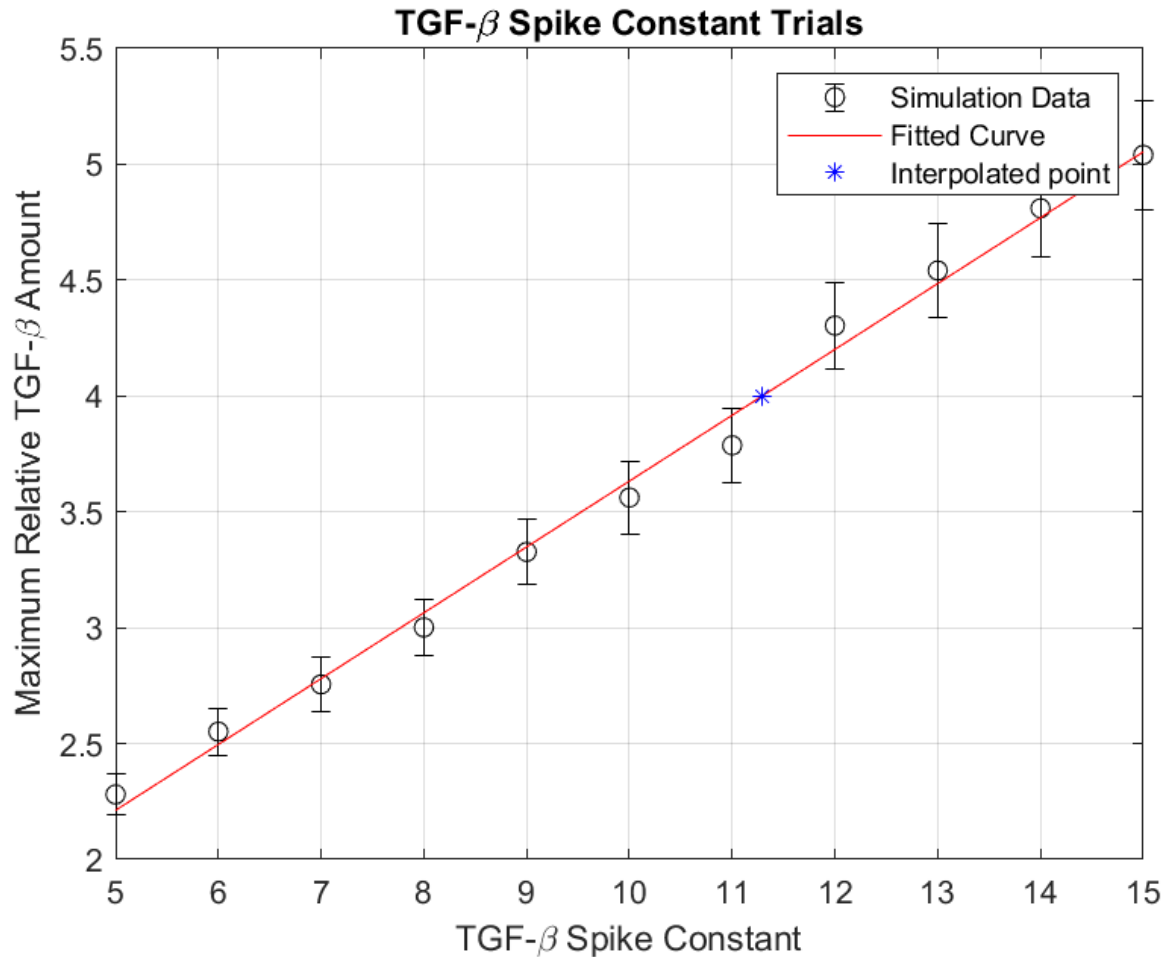


Figure 8: Average and confidence interval of maximum relative TGF- β plotted against evenly spaced $K_{(1,TGF-\beta)}$ values between 5 and 15 for 30 runs at each value (black). The fitted equation, determined by MATLAB's "fit" function (red), and the interpolated value corresponding to literature (blue). This experiment establishes the linear relationship between the $K_{(1,TGF-\beta)}$ spike constant and the maximum relative amount of TGF- β . The experimental data is then fit to a linear curve and the value of $K_{(1,TGF-\beta)}$ is determined using this linear equation.

The maximum values of relative TGF- β from the first parametrization experiment were plotted against the trial values of $K_{1,TGF-\beta}$ (Figure 8.). A linear equation of the following form was fit to this data:

$$TGF B_{max} = a * K_{1,TGF-\beta} + b$$

Equation 12

Where a and b are the coefficients determined by MATLAB's 'fit' function. $a = 0.3734 \pm 0.0133$, and $b = .8922 \pm 0.1421$. A value of 8.33 was interpolated for $K_{1,TGF-\beta}$ necessary to reach a maximum relative TGF- β of 4 reported in literature (Da Ré Guerra et al., 2016).

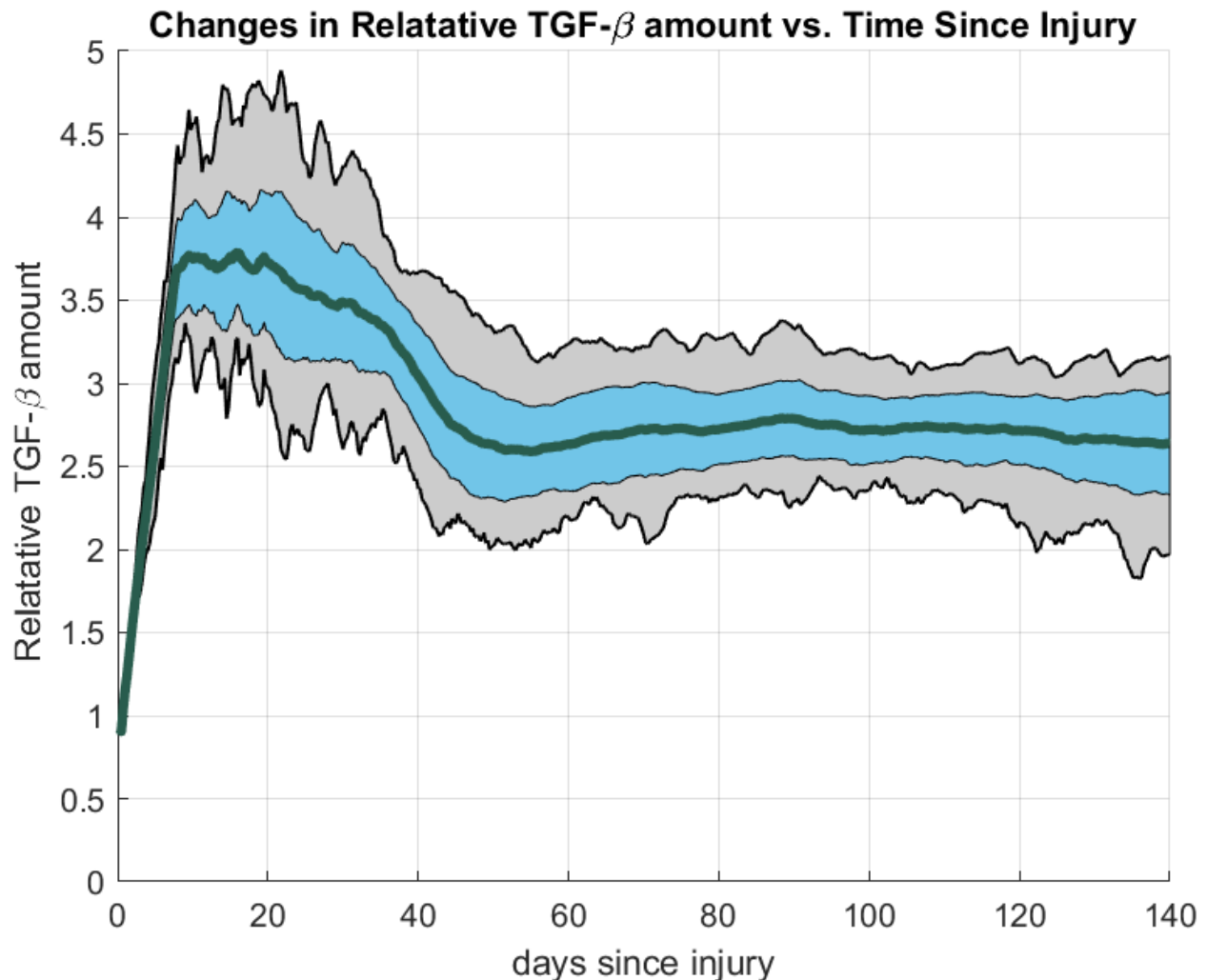


Figure 9: Plot of relative TGF- β content vs days since injury after applying only the first constant, $K_{(1,TGF-\beta)}$ using a value of 11 for 30 runs. Average relative TGF- β (Dark Green), standard deviation (light blue), and maximum/minimum (black). The shaded area represents the difference between the standard deviation and the maximum/minimum values. This graph makes it clear that further parametrization is needed to define the decay in TGF- β values.

It was determined that a second constant would be needed to properly constrain the relative TGF- β because TGF- β remained high long after the injury and appeared to reach an equilibrium near 2.5 times higher than the baseline value.

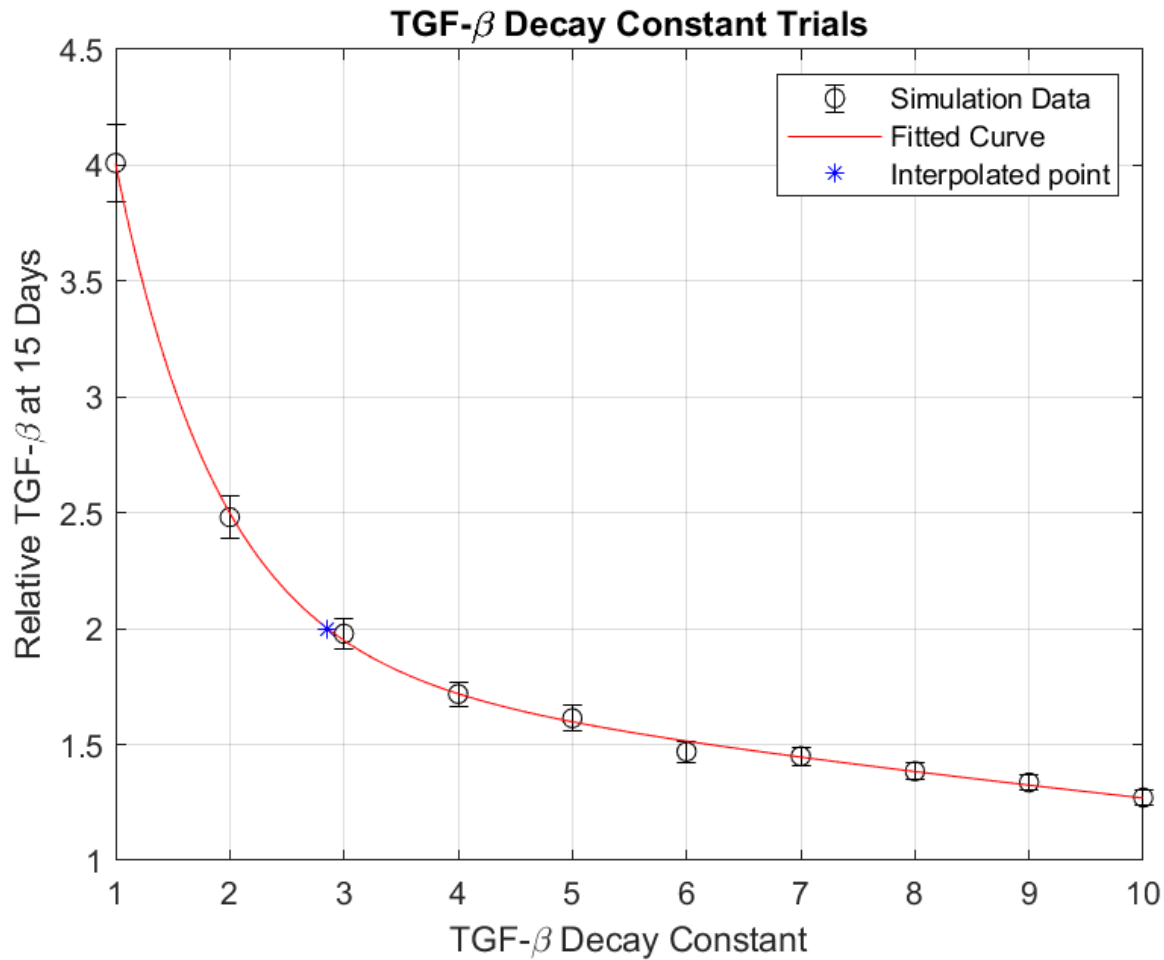


Figure 10: Plot of average and confidence interval of relative TGF-β amount 15 days after injury plotted against evenly spaced $K_{2,TGF-\beta}$ values between 5 and 15 for 30 runs at each value (black). The fitted equation, determined by MATLAB's "fit" function (red), and the interpolated value corresponding to literature (blue). This experiment establishes the exponential relationship between the $K_{2,TGF-\beta}$ spike constant and the relative amounts of TGF-β 15 days after injury. The exponential curve is used to determine the value of $K_{2,TGF-\beta}$.

The values of TGF-β 15 days after injury are plotted against the trial values of $K_{2,TGF-\beta}$ (figure 8). An exponential equation was fit to this data:

$$TGF\beta_{15} = ae^{bK_{2,TGF-\beta}} + ce^{dK_{2,TGF-\beta}}$$

Where a, b, c, and d are the coefficients determined by MATLAB's 'fit' function. $a = 2.92$, $b = -0.90$, $c = 1.53$, and $d = -0.22$. a value of $K_{2,TGF-\beta} = 1.89$ was interpolated to recapitulate the change in TGF-β observed 15 days after injury from experiments (Da Ré Guerra et al., 2016).

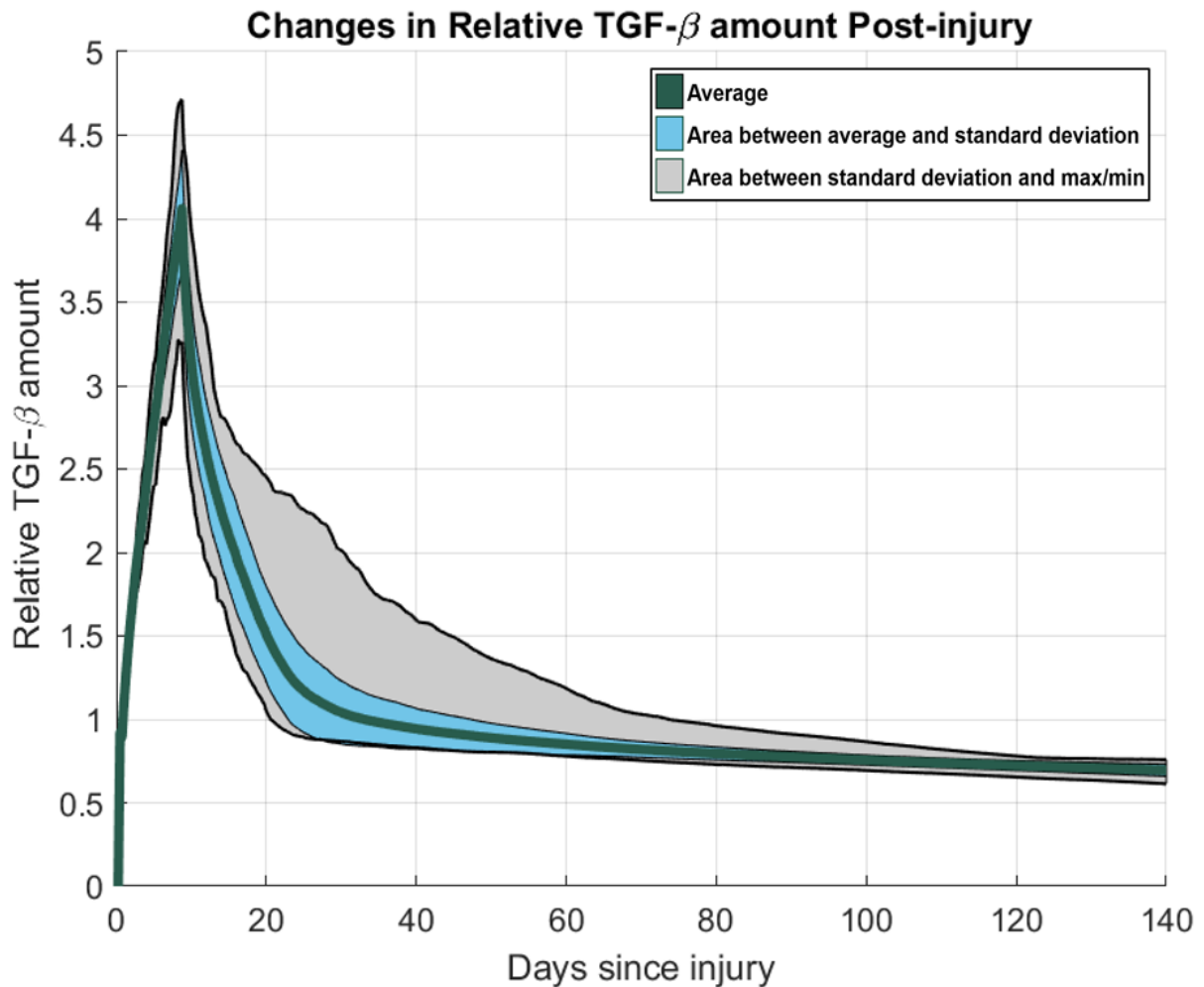


Figure 11: Plot of relative TGF- β content vs days since injury after applying both constants, $K_{(1,TGF-\beta)}$ and $K_{(2,TGF-\beta)}$ using a values of 8.33 and 1.89 respectively for 50 runs. Average relative TGF- β (Olive Green), standard deviation (light blue), and maximum/minimum (black). The shaded area represents the difference between the standard deviation and the maximum/minimum values. This graph demonstrates the spike in TGF- β content occurring during the inflammatory phase of healing, and the decay of this growth factor's concentration to normal soon after

Parametrization resulted in the ABM producing a spike in TGF- β within the first few days after an injury, and the concentration of this molecule quickly decreasing to normal levels by about 3 weeks after the injury is sustained (Figure 11). The decaying portion of the graph appears to show that decay in TGF- β content shows a high degree of variability, most likely due to the stochastic nature of the model. In simulations where more fibroblasts were produced, it is likely that TGF- β remained elevated for much longer than expected.

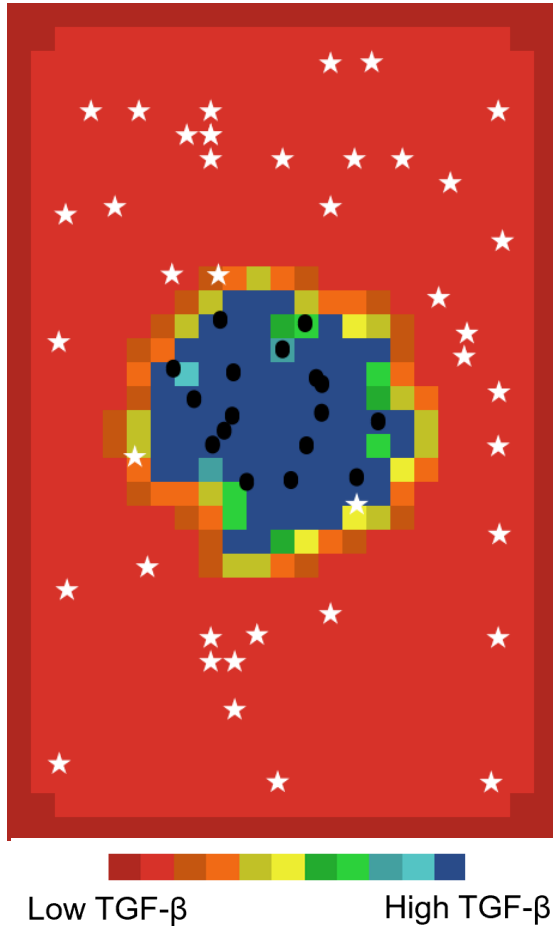


Figure 12: View of the ABM 3-days after an injury with the background set to represent the total TGF- β content. Blue represents high amount of TGF- β , and red is a low amount of collagen. This image illustrates the localization of the increased TGF- β values as reported in Natsu-ume et al.

For fibroblasts to perform key functions in the healing process, a localized spike in growth factor content is a necessity. Fibroblasts responding to an injury are stimulated to reproduce more often and to produce more collagen than fibroblasts in a homeostatic environment. Additionally, the increased growth factor concentration behaves as a chemotactic signal, directing the migration of fibroblasts to the site of injury (Guido & Tranquillo, 1993).

Past research has reported a significant increase in TGF- β content near the site of the injury during early healing time points (Natsu-

ume et al., 1997). This phenomenon was reflected in the ABM (Figure 12). It was

observed that at early healing timepoints, the

ABM produced a macrophage dominant injury site, and that a steep TGF- β gradient that was produced – as expected – by these cells.

Parametrization of IGF-I

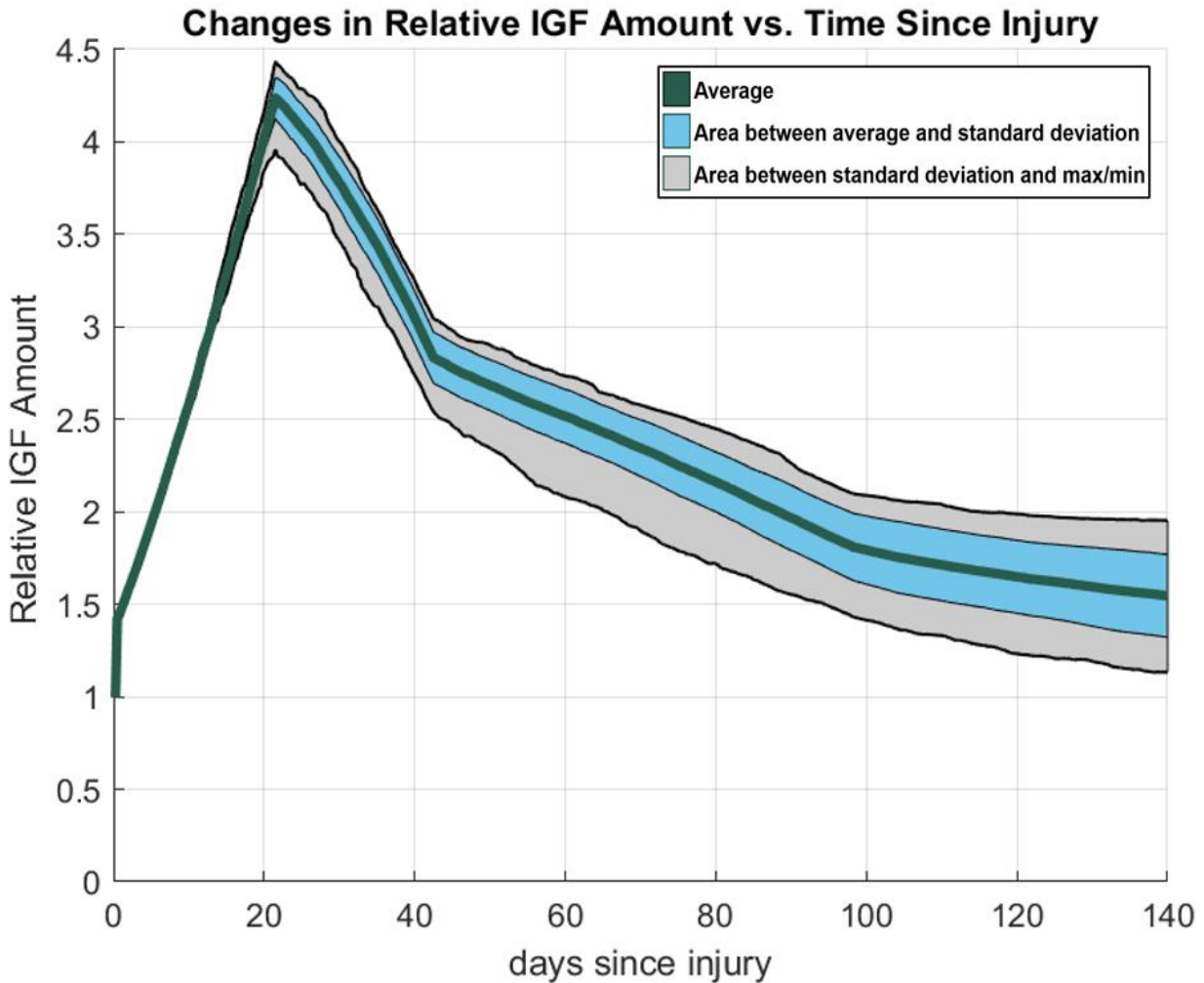


Figure 13: Plot of relative IGF content vs days since injury after applying the constant, $K_{1,IGF}$ using a value of 5 for 30 runs. Average relative IGF (Olive Green), standard deviation (light blue), and maximum/minimum (black). The shaded area represents the difference between the standard deviation and the maximum/minimum values. These data illustrate the spike in IGF content, which reaches a peak 21 days after injury as well as the slow decay of IGF content back to baseline levels as healing progresses beyond this peak.

While published literature states that IGF in murine ligament tissue increases 5-fold 21 days after injury, in trials to establish bounds for the IGF spike it was observed that when IGF increased to above five times its initial value, fibroblasts proliferated in an uncontrolled manner resulting in failure of the model. Because of this, a value of $K_{1,IGF} = 5$ was used. Using this value, $IGF = 4.52 \pm 0.12$ at day-21 post injury, $IGF = 2.97 \pm .18$ at day-42, $IGF = 1.71 \pm 0.23$ day-98, and 1.40 ± 0.25 at day-140. It was also

observed that once a weight was applied to the IGF spike, the ABM outputs appeared to show greater cellularity, and higher collagen production, due to the relationship between IGF, proliferation, and collagen production established in the previous aging only model.

Parametrization of PDGF

Because of literature showing that fibroblasts tend become the dominant injury site cell type. At day-9 of healing, fibroblast percentage data was collected and plotted against the trial values for PDGF production (figure 12). The value where fibroblast percentage is 50% +/- standard deviation was interpolated using the following exponential function fitted to the data:

$$\%F = ae^{b \cdot K_{PDGF}} - ce^{d \cdot K_{PDGF}}$$

Equation 13

Where a, b, c, and d are the coefficients determined by MATLAB's 'fit' function, K_{PDGF} is the interpolated value for PDGF production, and %F is the percentage of fibroblasts in the wound area. $a = 54.76$, $b = -2.57$, $c = 9.39$ and $d = -0.066$. the interpolated value of $K_{PDGF} = 10.72$.

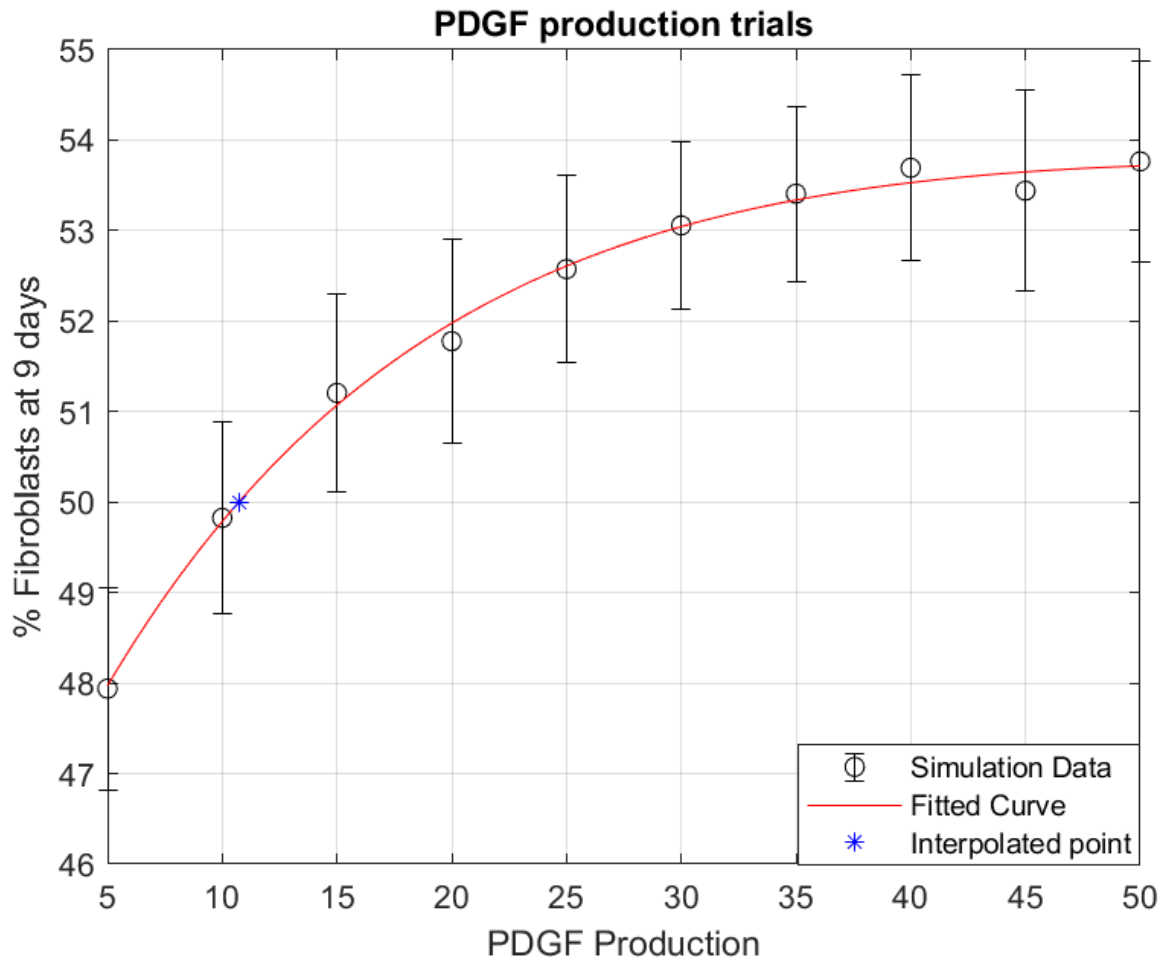


Figure 14: Plot of average and confidence interval of fibroblast percentage 9 days after injury plotted against evenly spaced PDGF Production values between five and fifty for 100 runs at each value (black). The fitted equation, determined by MATLAB's "fit" function (red), and the interpolated value corresponding to literature (blue). The results of this graph show that while there is a clear trend in the relationship between fibroblast percentage and PDGF production, the high amount of stochastic variability for this output means that the model is not very sensitive to PDGF production.

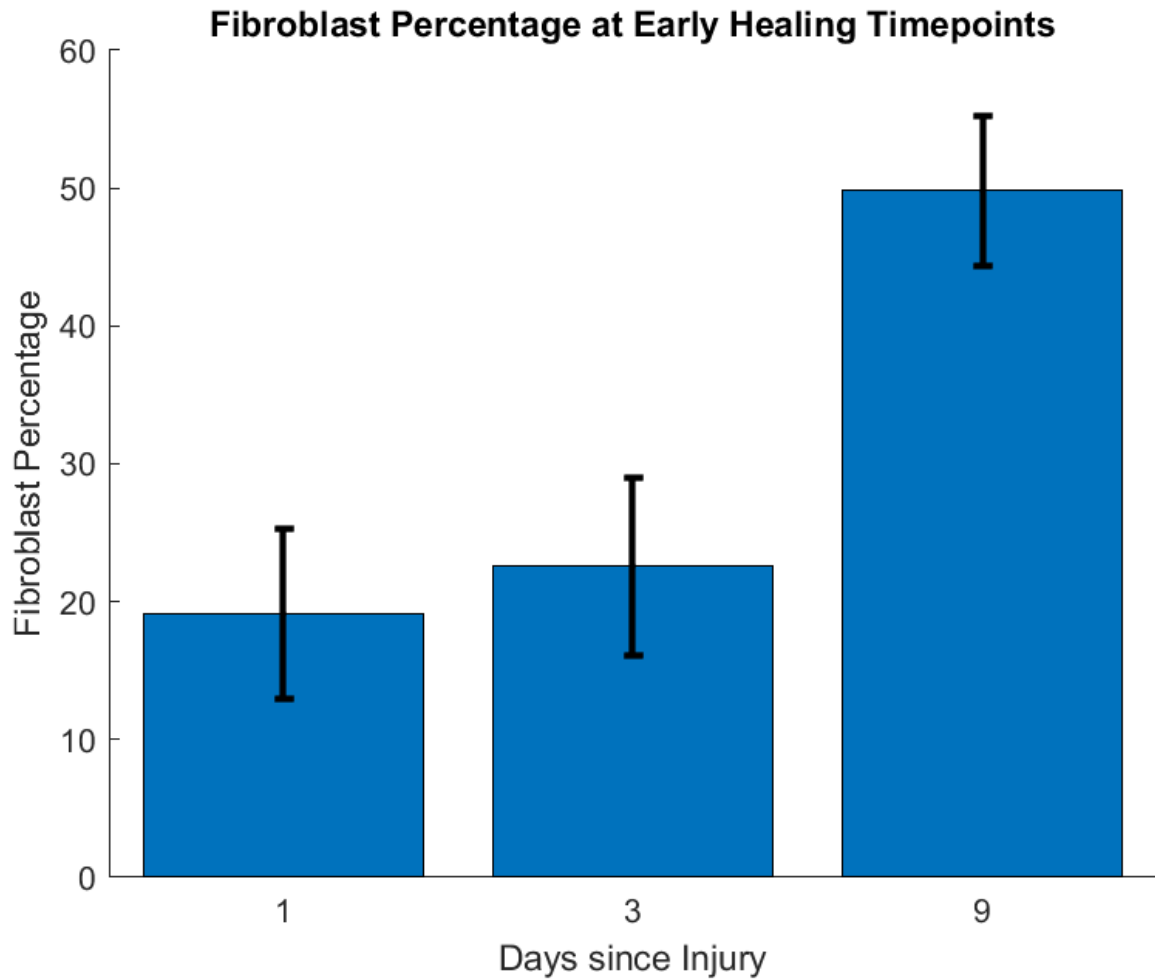


Figure 15: Average fibroblast percentage and confidence interval at one, three, and nine days after injury for 100 simulation runs, using the value of PDGF determined previously. This graph shows that fibroblast percentage remains low in the first few days following injury, but tends to dominate the wound area after about nine days of healing.

Trials evaluating the change in fibroblast percentage in the injury site as a function of time since injury show the transition between a macrophage dominated and fibroblast dominated injury site (Figure 15). Fibroblast percentage remains relatively stable in the first few days of injury, but with the steady decline in macrophage population and the combination of proliferative and chemotactic factor accumulation via PDGF, TGF- β , and IGF, fibroblast cellularity rapidly increases leading to the transition from the inflammatory phase of healing to the proliferative phase.

Healing at different ages

Because tendon function relies on the maintenance of a highly aligned, collagen dominated matrix (Kannus, 2000), ABM predictions of total collagen amounts at each of 6 frequently studied post-injury time-points is an indicator of overall tendon function (Figure 16). According to these experiments, Collagen content of healed tendons at all ages remained lower than that of their healthy counterparts of the same age.

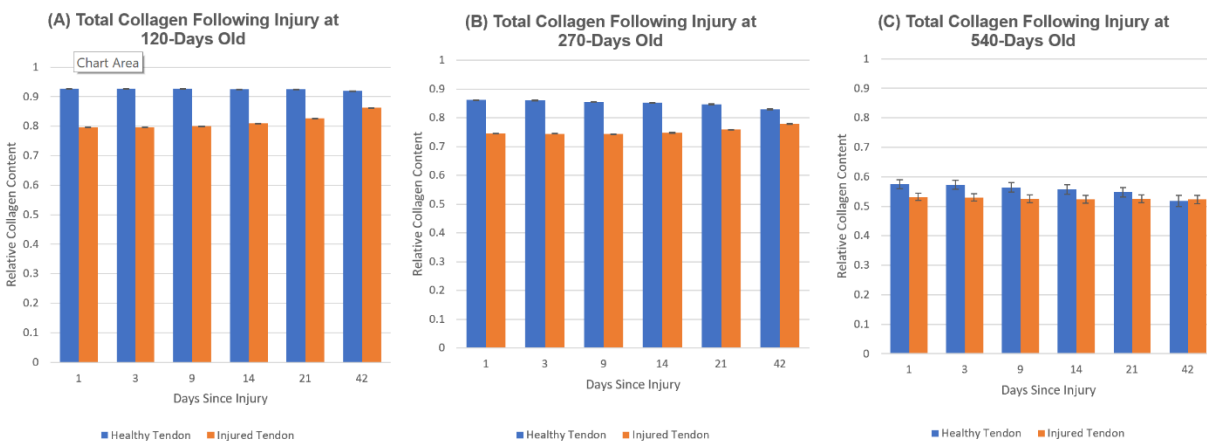


Figure 16: (A) Comparison of total relative collagen of (blue) healthy and (orange) healing 120-day old tendon simulations. (B) Comparison of total relative collagen of (blue) healthy and (orange) healing 270-day old tendon simulations. (C) Comparison of total relative collagen of (blue) healthy and (orange) healing 540-day old tendon simulations. ABM predicts that the healing tendon will not reach the level of collagen of its healthy counterpart by six weeks post-injury for 120-day old or 270-day old mice, but it does predict recapitulation of healthy collagen levels for a 540 day-old mouse. Error, reported by confidence interval is nearly negligible for the 120-day and 270-day age groups.

When comparing the difference between relative collagen of the entire simulated tendon and relative collagen of the injury site, the greatest difference is predicted during the inflammatory phase for the 120 day-old injury (Figure 17). This result was expected given that collagen content naturally degrades with age (Vanosdoll, 2017). After 42 days of healing, the difference in relative collagen content was nearly the same for all three injury ages, suggesting that while total collagen is still higher in younger specimens, the

ECM of healed tendons at increasing ages are much more similar to each other than those of healthy tendons at increasing ages.

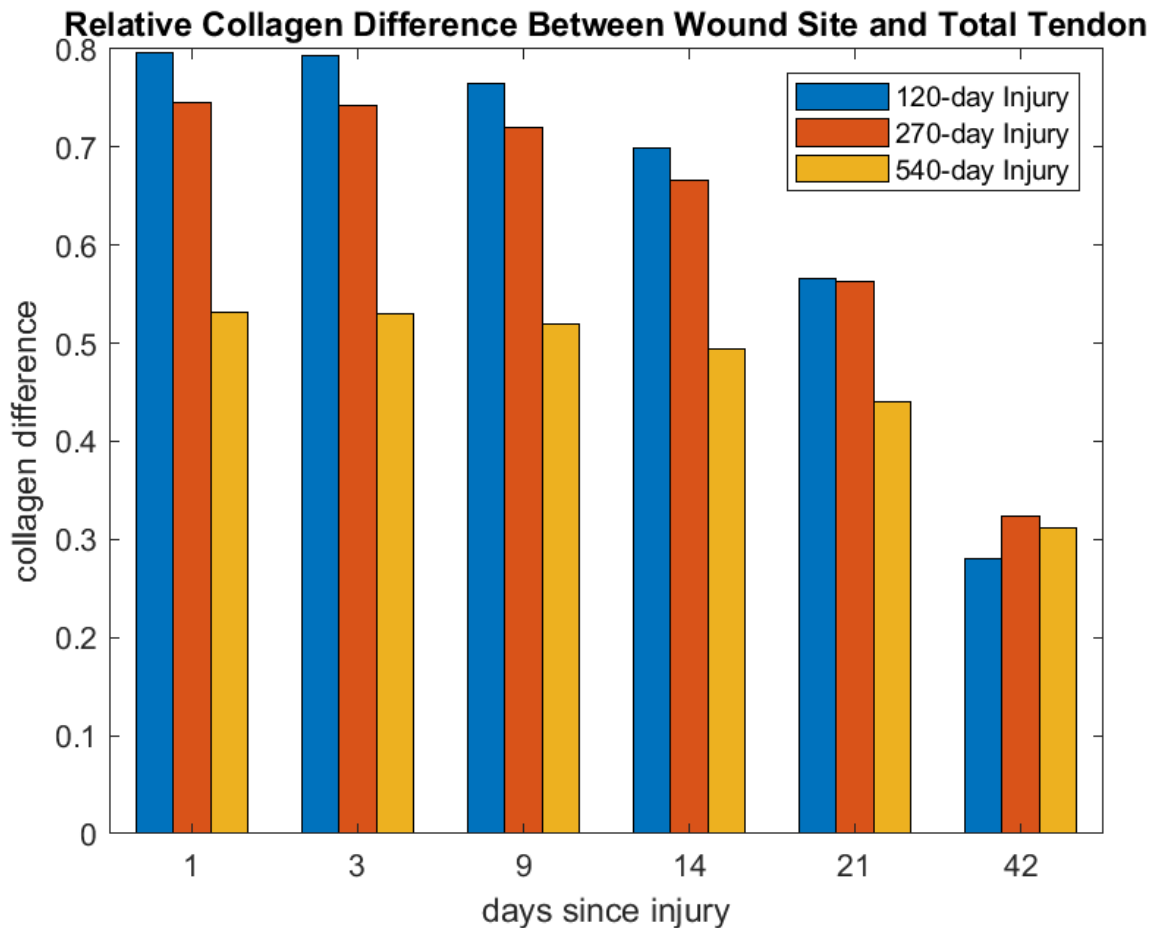


Figure 17: Prediction of the difference in Relative collagen of between the entire tendon and the wound site. Compared between mice injured at 120- 270- and 540-days old. This graph shows that the difference between the wound site and full tendon decreases over time, and that this difference is very comparable for all age groups after six weeks of healing.

Tendon function also depends on collagen alignment. Deviation from the standard, highly anisotropic structure of tendon tissue attenuates tendon’s ability to transmit force in one direction. Decrease in tendon organization is known to occur with both age and injury. However, surprisingly, the ABM appeared to only predict a difference in collagen alignment in tendons injured at 120 days old and not those injured at older ages (Figure 18). Additionally, the decrease in alignment appears to be

localized to the site of injury for injuries occurring at 120 days and 270 days, however it is much harder to distinguish disorganization caused by healing and that which is caused by aging in the geriatric 540 day-old tendons (Figure 19).

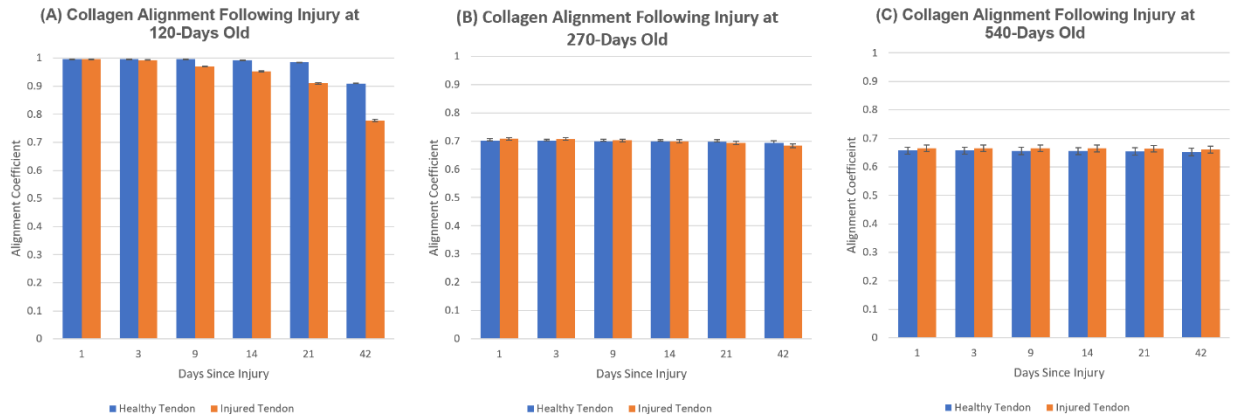


Figure 18: (A) Comparison of collagen alignment between (blue) healthy and (orange) healing 120-day old tendon simulations. (B) Comparison of collagen alignment between (blue) healthy and (orange) healing 270-day old tendon simulations. (C) Comparison of collagen alignment between (blue) healthy and (orange) healing 540-day old tendon simulations. ABM predicts that there is a difference in the collagen alignment between the healing and healthy tendons for mice injured at 120 days, but not for mice injured at 270 or 540 days. Error(confidence interval) is nearly negligible for all data reported.

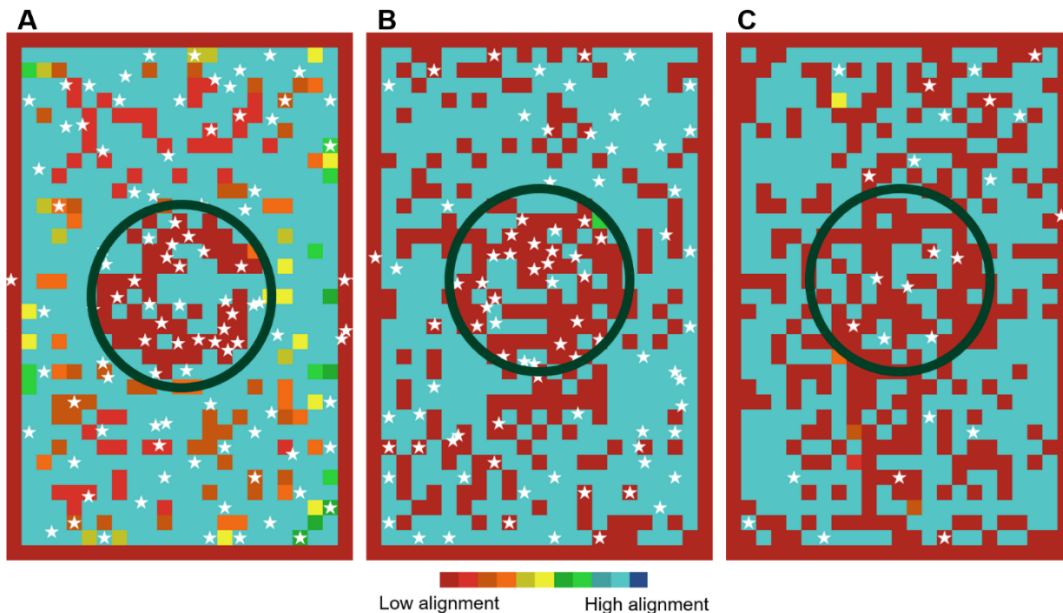


Figure 19: Predicted collagen alignment after six weeks of healing in the injury site of (A) a tendon injured at 120-days old (B) a tendon injured at 270-days old and (C) a tendon injured at 540-days old. The decrease in collagen alignment is much more noticeable in the younger two tendons, while the tendon injured at 540 days old appears to have a much more constant amount of alignment across all coordinates.

The speed of tendon recovery depends on how quickly fibroblasts can migrate to the site of injury. This is a crucial factor for avoiding further injuries because of the decreased time for which the tendon's structure is fully compromised (Sharma et al., 2006). While the ABM predicted that the injury site would become fibroblast dominant by day-9 post injury, as expected, the 270-day-old injured tendons took slightly longer to reach a fibroblast dominant state, and geriatric 540-day-old tendons did not reach fibroblast dominance until after 14 days of healing (figure 20). Further, the ABM predicted a drastic decrease in the number of fibroblasts to reach the wound site with increasing age (figure 21).

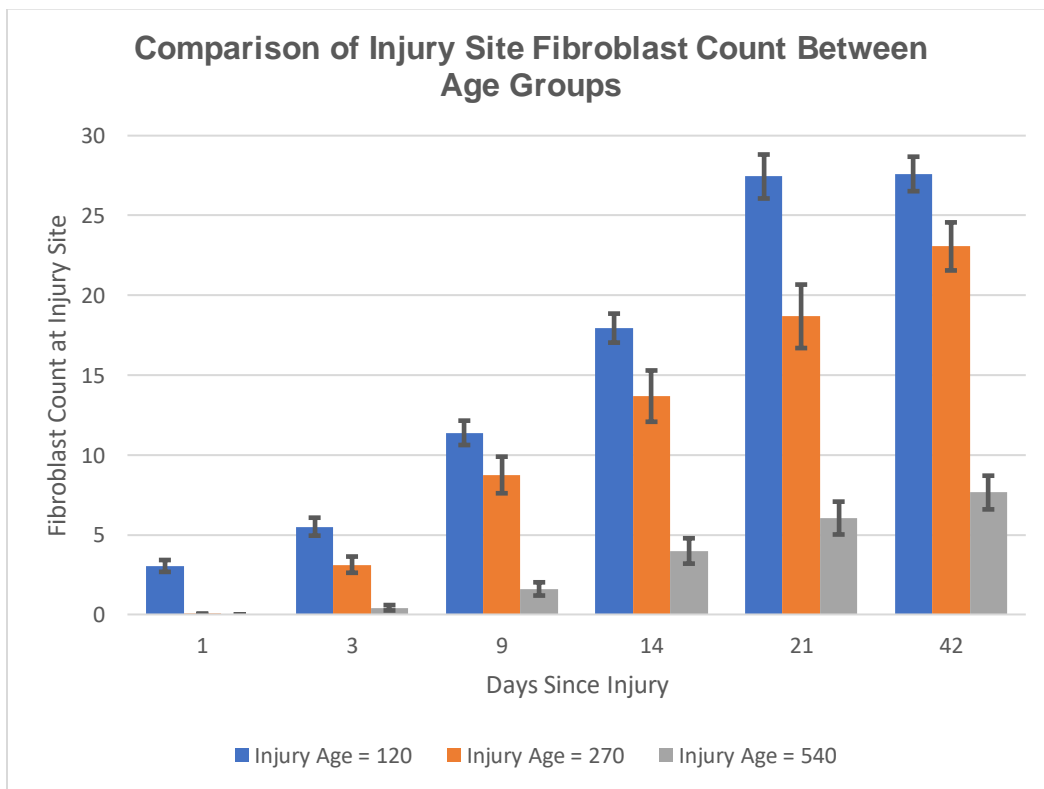


Figure 20: Predicted fibroblast percentage +/- confidence interval at key post-injury timepoints for (blue) mice injured at 120-days-old, (orange) mice injured at 270 days-old, and (yellow) mice injured at 540 days-old. ABM predicts a much longer time for older mice to reach fibroblast dominance at the wound site.

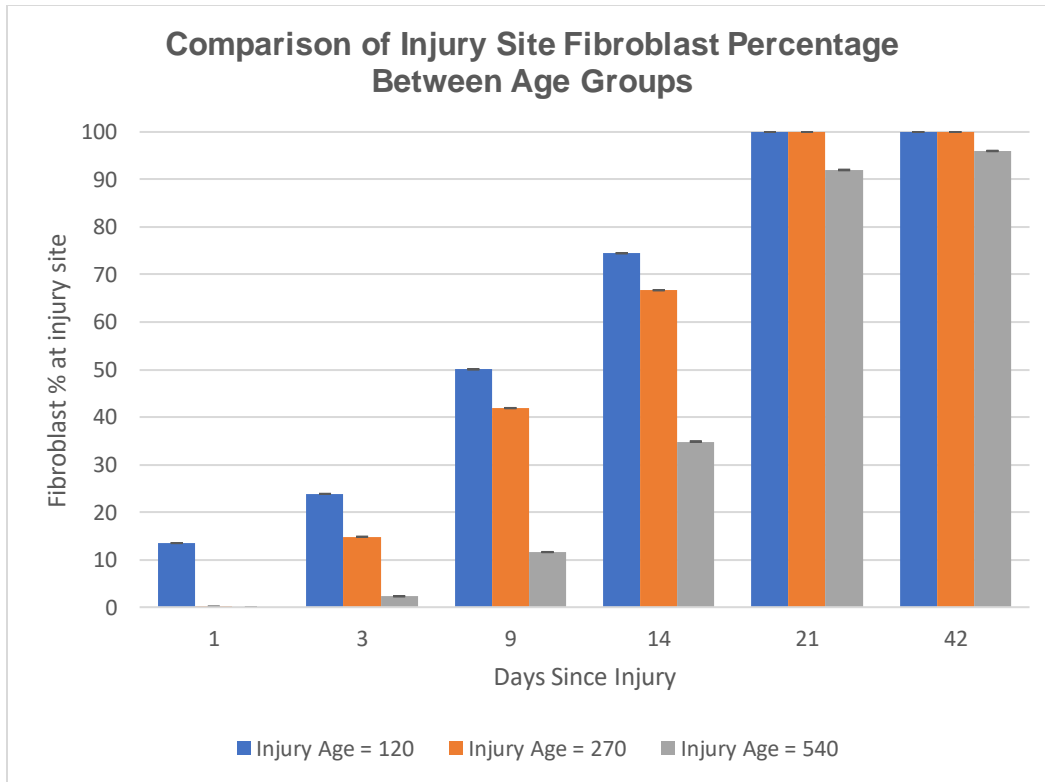


Figure 21: Predicted injury-site fibroblast count at key post-injury timepoints for (blue) mice injured at 120-days-pld, (orange) mice injured at 270 days-old, and (yellow) mice injured at 540 days-old. ABM predicts fewer fibroblasts reach the site of injury with increasing age. The Error (confidence interval) is nearly negligible for these data.

4. Discussion

ABM demonstrated the ability to recapitulate the inflammatory interactions observed during the initial stages of patellar tendon healing and predicted crucial outcomes as well as their dependence on age. This model predicted the inferiorities of the post-injury ECM, in terms of both collagen content and collagen orientation. Additionally, the focus on the inflammatory stage of healing resulted in the prediction of provisional matrix formation, fibroblast migration to the site of injury, and the clear demarcation between the inflammatory and proliferative phases of healing.

While information regarding the specific mechanisms is sparse, this research was useful in compiling the available information and using it to create a framework that

can predict the outcomes of patellar tendon healing. This framework in conjunction with the previous model of tendon aging create a powerful platform capable of testing hypotheses regarding age-related tendon healing and degeneration. Further, the formulation of a set of codified rules regulating the activity of the key actors involved in tendon healing allows us to gain insights into the inner workings of the healing tendon, deepening our understanding of an understudied field.

In the ABM TGF- β functions both as a signal promoting collagen production by fibroblasts, and as a chemotactic signal attracting cells to the injury site. The results of the initial trial runs of TGF- β were compared to literature that reported changes in TGF- β content in post-injury time-points to ensure that the ABM framework accurately recapitulated the physiological phenomena described by literature (Da Ré Guerra et al., 2016; Natsu-ume et al., 1997; Sciore et al., 1998). A set of two constants are determined by this parametric test, describing the spike and decay in TGF- β production by macrophages. The increased stochastic variability during the decay of TGF- β production shows that further investigation into the role of this growth factor in the proliferative and remodeling phases may be necessary.

IGF performs a similar function to TGF- β in that it promotes collagen production and fibroblast proliferation in the ABM. The intention was to vary IGF production in a similar manner to TGF- β production. However, when establishing upper and lower bounds for IGF production, it was observed that values greater than five appeared to trigger a positive feedback loop. Increase in IGF causes an increase in the chances that a fibroblast will undergo mitosis. Because the probability of proliferation is calculated for each fibroblast in the model, the probability of proliferation is increased further. This

feedback loop results in the infinite production of new fibroblasts, compromising ABM performance.

While it is known that changes in PDGF occur as a result of healing (Molloy et al., 2003), the lack of quantified data presented a challenge in determining the definition of a rule relating PDGF content to ABM outputs. The decay of PDGF was determined by a study that investigated the interaction between PDGF and human fibroblasts in culture (Heldin, H E Westeson & Westermark⁸, 1982). The rule generated assumes that during homeostasis PDGF decay is balanced by its production, so the decay equation was only applied when a cell's local environment contained a higher amount of PDGF than normal. PDGF spike was parametrized by varying growth factor production by macrophages and recording the resulting percentage of fibroblasts in the injury site. While an ideal value for growth factor production was determined by this experiment, the high degree of stochastic variability implies that PDGF may not be the most important factor in determining fibroblast migration during injury.

ABM predicted many key characteristics of healing at different ages. Predictions of the total collagen content and collagen content localized to the site of injury showed that the difference between collagen amounts in healthy tendons and healing tendons were not as great when age increased. This paradigm was true of both total collagen content and the collagen content of the injury site, and follows claims that healed tendons of any age are comparable to healthy geriatric tendons (Mienaltowski et al., 2016). Predictions of collagen alignment followed the same pattern, where the difference between healthy and healing tendon, as well as disorganization of the injury site was greater for younger mice. Since Collagen content and alignment are the two

main contributors to tendon function, it is reasonable to conclude that the ABM also predicted the functional deficit inherent to healing tendons (Mienaltowski et al., 2016). Lastly, Predictions of fibroblast count in the injury site offered possible clues to the mechanism behind the increased rates of chronic inflammatory conditions with age (Bell et al., 2018b; J.-F. Kaux et al., 2011; Sharma et al., 2006). ABM predicted that fewer fibroblasts reached the injury site with increasing age, and that it took longer to reach fibroblast dominance with increasing age. These results suggest that the inflammatory phase is longer for older specimens, possibly leading to a chronic condition.

V. Conclusions

ABM demonstrated the ability to recapitulate the salient features of early tendon healing, spikes in cytokines and growth factors, chemotaxis, and contact guidance. Further, it predicted healing outcomes such as the decrease in collagen content and alignment specifically when localized to the site of injury, as well as the decrease in cell migration to the site of injury with increasing age. Overall, the ABM predicted a trend whereby the key ECM features contributing to tendon function experienced a lesser deficit at higher ages.

Future Work

While the ABM was successful in accomplishing its two objectives, it represents only the beginning of what is possible with agent-based modelling of healing biological systems. There are still interactions within the model that can be refined to better recapitulate real life situations. Namely, the change in collagen alignment predicted by the ABM did not match that of published literature. While alignment did decrease with

age it decreased much more than expected. This is most likely due to the choice to discretize collagen fiber angles every 5°, or to break the initial collagen value into only 100 discrete pieces. Both choices were made for the sake of speed, as more exact approximations are likely to be more computationally expensive, and therefore take longer to obtain reliable predictions from simulations. In addition, the values of constants associated with fibroblast migration were not parametrized. In the future, these values should be more carefully refined, using an algorithm to identify the ideal value of multiple parameters simultaneously. Such parametrization would require an increase in prediction accuracy for collagen alignment because alignment is the main output related to fibroblast migration.

Through the literature search, there were many molecules that came up repeatedly in a healing context that were not previously defined in the aging ABM. Chief among these were: IL-6, IL-10, TNF- α , FGF and VEGF (Da Ré Guerra et al., 2016; Daley et al., 2010; J. Y. Hsieh et al., 2017; Molloy et al., 2003; Morita et al., 2017). The addition of these molecules to the ECM ground substance would likely increase the model's predictive accuracy a great deal with the likely cost of making the model more computationally expensive. The model can also be extended to predict mechanical outcomes by feeding its outputs into a finite element model and adding constant tension to predict failure properties, or cyclic tension to predict fatigue properties.

Because of the relative lack of studies investigating sex-based differences in tendon healing mechanics, sex was not considered in the formulation of this model. However, clinical data has shown that there are sex-related differences in tendon mechanics and healing (Garner et al., 2015; Magnusson et al., n.d.; Sarver et al., 2017;

Yu et al., 2001). The model's parameters can be adjusted, and the predicted results can be compared to clinical data to identify which factors most likely contribute to the current observations of healing in clinical settings. As a part of these efforts, it will be necessary to review the literature used to generate the model herein, and determine which sexes were used to obtain data.

Ultimately, this ABM is designed to be applied for drug discovery, or to be used in a clinical setting. For identifying therapeutics and healing strategies, parameters of the model should be varied to simulate the effects of prospective therapeutics. Simulation results will be used to identify experimental therapeutics to be used on an in-vivo system. In a clinical setting, it is hypothesized that a more refined version of this ABM can be used to recommend healing strategies for patients with tendonitis.

Bibliography

- Akintunde, A. R., & Miller, K. S. (2018). Evaluation of microstructurally motivated constitutive models to describe age-dependent tendon healing. *Biomechanics and Modeling in Mechanobiology*, 17(3), 793–814. <https://doi.org/10.1007/s10237-017-0993-4>
- Alexander, R. M. N. (2002). Tendon elasticity and muscle function. *Comparative Biochemistry and Physiology - A Molecular and Integrative Physiology*, 133(4), 1001–1011. [https://doi.org/10.1016/S1095-6433\(02\)00143-5](https://doi.org/10.1016/S1095-6433(02)00143-5)
- Ansorge, H. L., Adams, S., Jawad, A. F., Birk, D. E., Soslowky, L. J., & Soslowky, L. (2012). Mechanical Property Changes During Neonatal Development and Healing Using a Multiple Regression Model. *J Biomech*, 45(7), 1288–1292. <https://doi.org/10.1016/j.jbiomech.2012.01.030>
- Bailey, A. J., Paul, R. G., & Knott, L. (1998). Mechanisms of maturation and ageing of collagen. In *Mechanisms of Ageing and Development* (Vol. 106, Issues 1–2, pp. 1–56). [https://doi.org/10.1016/S0047-6374\(98\)00119-5](https://doi.org/10.1016/S0047-6374(98)00119-5)
- Bell, R., Robles-Harris, M. A., Anderson, M., Laudier, D., Schaffler, M. B., Flatow, E. L., & Andarawis-Puri, N. (2018a). Inhibition of apoptosis exacerbates fatigue-damage tendon injuries in an in vivo rat model. *European Cells & Materials*, 36, 44–56. <https://doi.org/10.22203/eCM.v036a04>
- Bell, R., Robles-Harris, M. A., Anderson, M., Laudier, D., Schaffler, M. B., Flatow, E. L., & Andarawis-Puri, N. (2018b). Inhibition of apoptosis exacerbates fatigue-damage tendon injuries in an in vivo rat model. *European Cells and Materials*, 36, 44–56. <https://doi.org/10.22203/eCM.v036a04>
- Berglund, M., Hart, D. A., & Wiig, M. (2007). The inflammatory response and hyaluronan synthases in the rabbit flexor tendon and tendon sheath following injury. *Journal of Hand Surgery: European Volume*, 32(5), 581–587. <https://doi.org/10.1016/j.jhse.2007.05.017>
- Byrne, M. D. (2013). How many times should a stochastic model be run? An approach based on confidence intervals. *Proceedings of the 12th International Conference on Cognitive Modeling*, 445–450.
- Chen, K., Hu, X., Blemker, S. S., & Holmes, J. W. (2018). Multiscale computational model of Achilles tendon wound healing: Untangling the effects of repair and loading. *PLoS Computational Biology*, 14(12), e1006652. <https://doi.org/10.1371/journal.pcbi.1006652>
- Conte, R., & Paolucci, M. (2014). On agent-based modeling and computational social science. *Frontiers in Psychology*, 5, 668. <https://doi.org/10.3389/fpsyg.2014.00668>
- Da Ré Guerra, F., Vieira, C. P., Oliveira, L. P., Marques, P. P., dos Santos Almeida, M., & Pimentel, E. R. (2016). Low-level laser therapy modulates pro-inflammatory cytokines after partial tenotomy. *Lasers in Medical Science*, 31(4), 759–766. <https://doi.org/10.1007/s10103-016-1918-7>
- Daley, J. M., Brancato, S. K., Thomay, A. A., Reichner, J. S., & Albina, J. E. (2010). The phenotype of murine wound macrophages. *J. Leukoc. Biol*, 87, 59–67. <https://doi.org/10.1189/jlb.0409236>
- Del Buono, A., Oliva, F., Osti, L., & Maffulli, N. (2013). Metalloproteases and tendinopathy. In *Muscles, Ligaments and Tendons Journal* (Vol. 3, Issue 1, pp. 51–57). <https://doi.org/10.11138/mltj/2013.3.1.051>

- Depalle, B., Qin, Z., Shefelbine, S. J., & Buehler, M. J. (2015). Influence of cross-link structure, density and mechanical properties in the mesoscale deformation mechanisms of collagen fibrils. *Journal of the Mechanical Behavior of Biomedical Materials*, 52, 1–13.
<https://doi.org/10.1016/J.JMBBM.2014.07.008>
- Doolittle, R. F. (2017). The conversion of fibrinogen to fibrin: A brief history of some key events. In *Matrix Biology* (Vols. 60–61, pp. 5–7). Elsevier B.V.
<https://doi.org/10.1016/j.matbio.2016.08.002>
- Dunaiski, V., & Belford, D. A. (n.d.). *Contribution of circulating IGF-I to wound repair in GH-treated rats*. [https://doi.org/10.1016/S1096-6374\(02\)00080-1](https://doi.org/10.1016/S1096-6374(02)00080-1)
- Dunkman, A. A., Buckley, M. R., Mienaltowski, M. J., Adams, S. M., Thomas, S. J., Kumar, A., Beason, D. P., Iozzo, R. V., Birk, D. E., & Soslowsky, L. J. (2014). The injury response of aged tendons in the absence of biglycan and decorin. *Matrix Biology*, 35, 232–238.
<https://doi.org/10.1016/j.matbio.2013.10.008>
- Dunkman, A. A., Buckley, M. R., Mienaltowski, M. J., Adams, S. M., Thomas, S. J., Satchell, L., Kumar, A., Pathmanathan, L., Beason, D. P., Iozzo, R. V., Birk, D. E., & Soslowsky, L. J. (2013). Decorin expression is important for age-related changes in tendon structure and mechanical properties. *Matrix Biology*, 32(1), 3–13.
<https://doi.org/10.1016/j.matbio.2012.11.005>
- Eekhoff, J. D., Fang, F., & Lake, S. P. (2018). *Connective Tissue Research Multiscale mechanical effects of native collagen cross-linking in tendon*.
<https://doi.org/10.1080/03008207.2018.1449837>
- enoch David John Leaper, stuart. (2008). *Basic science sURGeRY 26:2 31 Basic science of wound healing*. 26(2), 37–42. <https://doi.org/https://doi.org/10.1016/j.mpsur.2007.11.005>
- Flandry, F., & Hommel, G. (2011). Normal anatomy and biomechanics of the knee. In *Sports Medicine and Arthroscopy Review* (Vol. 19, Issue 2, pp. 82–92).
<https://doi.org/10.1097/JSA.0b013e318210c0aa>
- Fryhofer, G. W., Freedman, B. R., Hillin, C. D., Salka, N. S., Pardes, A. M., Weiss, S. N., Farber, D. C., & Soslowsky, L. J. (2016). Postinjury biomechanics of Achilles tendon vary by sex and hormone status. *Journal of Applied Physiology*, 121(5), 1106–1114.
<https://doi.org/10.1152/jappphysiol.00620.2016>
- Fu, S. C., Chan, B. P., Wang, W., Pau, H. M., Chan, K. M., & Rolf, C. G. (2002). Increased expression of matrix metalloproteinase 1 (MMP1) in 11 patients with patellar tendinosis. *Acta Orthopaedica Scandinavica*, 73(6), 658–662.
<https://doi.org/10.3109/17453670209178031>
- Garner, M. R., Gausden, E., Berkes, M. B., Nguyen, J. T., & Lorch, D. G. (2015). Extensor Mechanism Injuries of the Knee: Demographic Characteristics and Comorbidities from a Review of 726 Patient Records. *J Bone Joint Surg Am*, 97(19), 1592–1596.
<https://doi.org/10.2106/JBJS.O.00113>
- Gautieri, A., Redaelli, A., Buehler, M. J., & Vesentini, S. (2014). Age- and diabetes-related nonenzymatic crosslinks in collagen fibrils: Candidate amino acids involved in Advanced Glycation End-products. *Matrix Biology*, 34, 89–95.
<https://doi.org/10.1016/j.matbio.2013.09.004>
- Glorigijević, N., Penezić, A., & Nedić, O. (2017). Influence of glyco-oxidation on complexes

- between fibrin(ogen) and insulin-like growth factor-binding protein-1 in patients with diabetes mellitus type 2. *Free Radical Research*, 51(1), 64–72.
<https://doi.org/10.1080/10715762.2016.1268689>
- Guido, S., & Tranquillo, R. T. (1993). A methodology for the systematic and quantitative study of cell contact guidance in oriented collagen gels. Correlation of fibroblast orientation and gel birefringence. *Journal of Cell Science*, 105(2), 317–331.
- Heldin, H E Wasteson, C.-H., & Westermark, B. (1982). Interaction of platelet-derived growth factor with its fibroblast receptor. Demonstration of ligand degradation and receptor modulation. In *Journal of Biological Chemistry* (Vol. 257, Issue 8).
[https://doi.org/10.1016/S0021-9258\(18\)34708-2](https://doi.org/10.1016/S0021-9258(18)34708-2)
- Hsieh, J. Y., Smith, T. D., Meli, V. S., Tran, T. N., Botvinick, E. L., & Liu, W. F. (2017). Differential regulation of macrophage inflammatory activation by fibrin and fibrinogen. *Acta Biomaterialia*, 47, 14–24. <https://doi.org/10.1016/j.actbio.2016.09.024>
- Hsieh, P., & Chen, L. B. (1983). Behavior of cells seeded in isolated fibronectin matrices. *Journal of Cell Biology*, 96(5), 1208–1217. <https://doi.org/10.1083/jcb.96.5.1208>
- Id, K. C., Hu, X., Blemker, S. S., & Holmes Id, J. W. (2018). *Multiscale computational model of Achilles tendon wound healing: Untangling the effects of repair and loading*.
<https://doi.org/10.1371/journal.pcbi.1006652>
- Jones, G. C., Corps, A. N., Pennington, C. J., Clark, I. M., Edwards, D. R., Bradley, M. M., Hazleman, B. L., & Riley, G. P. (2006). Expression profiling of metalloproteinases and tissue inhibitors of metalloproteinases in normal and degenerate human achilles tendon. *Arthritis & Rheumatism*, 54(3), 832–842. <https://doi.org/10.1002/art.21672>
- Kannus, P. (2000). Structure of the tendon connective tissue. *J Med Sci Sports*, 10, 312–320.
- Karousou, E., Ronga, M., Vigetti, D., Passi, A., & Maffulli, N. (2008). Collagens, proteoglycans, MMP-2, MMP-9 and TIMPs in human achilles tendon rupture. *Clinical Orthopaedics and Related Research*, 466(7), 1577–1582. <https://doi.org/10.1007/s11999-008-0255-y>
- Kaux, J.-F., Forthomme, B., Le Goff, C., Crielaard, J.-M., & Croisier, J.-L. (2011). Current opinions on tendinopathy. In *Journal of Sports Science and Medicine* (Vol. 10).
<http://www.jssm.org>
- Kaux, J. F., Forthomme, B., le Goff, C., Crielaard, J. M., & Croisier, J. L. (2011). Current opinions on tendinopathy. In *Journal of Sports Science and Medicine* (Vol. 10, Issue 2, pp. 238–253).
- Kjær, M. (2004). Role of Extracellular Matrix in Adaptation of Tendon and Skeletal Muscle to Mechanical Loading. In *Physiological Reviews* (Vol. 84, Issue 2, pp. 649–698).
<https://doi.org/10.1152/physrev.00031.2003>
- Koshima, H., Kondo, S., Mishima, S., Choi, H.-R., Shimpo, H., Sakai, T., & Ishiguro, N. (2007). Expression of interleukin-1 β , cyclooxygenase-2, and prostaglandin E2 in a rotator cuff tear in rabbits. *Journal of Orthopaedic Research*, 25(1), 92–97.
<https://doi.org/10.1002/jor.20241>
- Kurtz, C. A., Loebig, T. G., Anderson, D. D., Demeo, P. J., Campbell, P. G., & Phd, §. (1999). *Insulin-Like Growth Factor I Accelerates Functional Recovery from Achilles Tendon Injury in a Rat Model**.

- Lee, S. W., Kim, S. H., Kim, J. Y., & Lee, Y. (2010). The effect of growth hormone on fibroblast proliferation and keratinocyte migration. *Journal of Plastic, Reconstructive & Aesthetic Surgery*, 63, 364–369. <https://doi.org/10.1016/j.bjps.2009.10.027>
- Lin, T. W., Cardenas, L., & Soslowsky, L. J. (2004). Biomechanics of tendon injury and repair. *Journal of Biomechanics*, 37, 865–877. <https://doi.org/10.1016/j.jbiomech.2003.11.005>
- Magnusson, S. P., Hansen, M., Langberg, H., Miller, B., Haraldsson, B., Westh, E. K., Koskinen, S., & Kjaer, M. (n.d.). *The adaptability of tendon to loading differs in men and women*. <https://doi.org/10.1111/j.1365-2613.2007.00551.x>
- Manning, C. N., Havlioglu, N., Knutsen, E., Sakiyama-Elbert, S. E., Silva, M. J., Thomopoulos, S., & Gelberman, R. H. (2014). The early inflammatory response after flexor tendon healing: A gene expression and histological analysis. *Journal of Orthopaedic Research*, 32(5), 645–652. <https://doi.org/10.1002/jor.22575>
- Marsolais, D., Côté, C. H., & Frenette, J. (2001). Neutrophils and macrophages accumulate sequentially following Achilles tendon injury. *Journal of Orthopaedic Research*, 19(6), 1203–1209. [https://doi.org/10.1016/S0736-0266\(01\)00031-6](https://doi.org/10.1016/S0736-0266(01)00031-6)
- Mcdougall, S., Dallon, J., Sherratt, J., & Maini, P. (2006). Fibroblast migration and collagen deposition during dermal wound healing: mathematical modelling and clinical implications. *Trans. R. Soc. A*, 364, 1385–1405. <https://doi.org/10.1098/rsta.2006.1773>
- Mehdizadeh, A., Gardiner, B. S., Lavagnino, M., & Smith, D. W. (2017). Predicting tenocyte expression profiles and average molecular concentrations in Achilles tendon ECM from tissue strain and fiber damage. *Biomechanics and Modeling in Mechanobiology*, 16(4), 1329–1348. <https://doi.org/10.1007/s10237-017-0890-x>
- Mienaltowski, M. J., Dunkman, A. A., Buckley, M. R., Beason, D. P., Adams, S. M., Birk, D. E., & Soslowsky, L. J. (2016). Injury response of geriatric mouse patellar tendons. *Journal of Orthopaedic Research*, 34(7), 1256–1263. <https://doi.org/10.1002/jor.23144>
- Molloy, T., Wang, Y., & Murrell, G. A. C. (2003). The roles of growth factors in tendon and ligament healing. In *Sports Medicine* (Vol. 33, Issue 5, pp. 381–394). <https://doi.org/10.2165/00007256-200333050-00004>
- Morita, W., Dakin, S. G., Snelling, S. J. B., & Carr, A. J. (2017). Cytokines in tendon disease: A systematic review. In *Bone and Joint Research* (Vol. 6, Issue 12, pp. 656–664). British Editorial Society of Bone and Joint Surgery. <https://doi.org/10.1302/2046-3758.612.BJR-2017-0112.R1>
- Natsu-ume, T., Nakamura, N., Shino, K., Toritsuka, Y., Horibe, S., & Ochi, T. (1997). Temporal and spatial expression of transforming growth factor- β in the healing patellar ligament of the rat. *Journal of Orthopaedic Research*, 15(6), 837–843. <https://doi.org/10.1002/jor.1100150608>
- NCSS. (2010). *Circular Data Analysis*. 1–28. <https://doi.org/10.1038/npp.2010.217>
- Pardes, A. M., Freedman, B. R., Fryhofer, G. W., Salka, N. S., Bhatt, P. R., & Soslowsky, L. J. (n.d.). *Males Have Inferior Achilles Tendon Material Properties Compared To Females in a Rodent Model*. <https://doi.org/10.1007/s10439-016-1635-1>
- Pardes, J. B., Takagi, H., Martin, T. A., Ochoa, M. S., & Falanga, V. (1995). Decreased levels of alpha 1(I) procollagen mRNA in dermal fibroblasts grown on fibrin gels and in response to fibrinopeptide B. *Journal of Cellular Physiology*, 162(1), 9–14.

<https://doi.org/10.1002/jcp.1041620103>

- Pearson, S. J., & Hussain, S. R. (2014). Region-specific tendon properties and patellar tendinopathy: A wider understanding. *Sports Medicine*, *44*(8), 1101–1112. <https://doi.org/10.1007/s40279-014-0201-y>
- Perez, R. L., Ritzenthaler, J. D., & Roman, J. (1999). Transcriptional regulation of the interleukin-1 β promoter via fibrinogen engagement of the CD18 integrin receptor. *American Journal of Respiratory Cell and Molecular Biology*, *20*(5), 1059–1066. <https://doi.org/10.1165/ajrcmb.20.5.3281>
- Rees, J. D., Wilson, A. M., & Wolman, R. L. (2006). Current concepts in the management of tendon disorders. *Rheumatology*, *45*, 508–521. <https://doi.org/10.1093/rheumatology/kel046>
- Sarver, D. C., Ashraf Kharaz, Y., Sugg, K. B., Gumucio, J. P., Comerford, E., & Mendias, C. L. (2017). Sex differences in tendon structure and function; Sex differences in tendon structure and function. *J Orthop Res*, *35*, 2117–2126. <https://doi.org/10.1002/jor.23516>
- Schneider, M., Angele, P., Järvinen, T. A. H., & Docheva, D. (2018). Rescue plan for Achilles: Therapeutics steering the fate and functions of stem cells in tendon wound healing. In *Advanced Drug Delivery Reviews* (Vol. 129, pp. 352–375). Elsevier B.V. <https://doi.org/10.1016/j.addr.2017.12.016>
- Sciore, P., Boykiw, R., & Hart, D. A. (1998). Semiquantitative reverse transcription-polymerase chain reaction analysis of mRNA for growth factors and growth factor receptors from normal and healing rabbit medial collateral ligament tissue. *Journal of Orthopaedic Research*, *16*(4), 429–437. <https://doi.org/10.1002/jor.1100160406>
- Sharma, P., Maffulli, N., & Maffulli, N. (2006). Tendon structure Biology of tendon injury: healing, modeling and remodeling. In *J Musculoskelet Neuronal Interact* (Vol. 6, Issue 2).
- Smiley, S. T., King, J. A., & Hancock, W. W. (2001). Fibrinogen Stimulates Macrophage Chemokine Secretion Through Toll-Like Receptor 4. *The Journal of Immunology*, *167*(5), 2887–2894. <https://doi.org/10.4049/jimmunol.167.5.2887>
- Sugg, K. B., Lubardic, J., Gumucio, J. P., & Mendias, C. L. (2014). Changes in macrophage phenotype and induction of epithelial-to-mesenchymal transition genes following acute Achilles tenotomy and repair. *Journal of Orthopaedic Research*, *32*(7), 944–951. <https://doi.org/10.1002/jor.22624>
- Theodossiou, S. K., & Schiele, N. R. (2019). Models of tendon development and injury. *BMC Biomedical Engineering*, *1*(1), 1–24. <https://doi.org/10.1186/s42490-019-0029-5>
- Thomopoulos, S., Parks, W. C., Rifkin, D. B., & Derwin, K. A. (2015). Mechanisms of tendon injury and repair. *Journal of Orthopaedic Research*, *33*(6), 832–839. <https://doi.org/10.1002/jor.22806>
- Thorne, B. C., Hayenga, H. N., Humphrey, J. D., & Peirce, S. M. (2011a). Toward a multi-scale computational model of arterial adaptation in hypertension: verification of a multi-cell agent based model. *Frontiers in Physiology*, *2*, 20. <https://doi.org/10.3389/fphys.2011.00020>
- Thorne, B. C., Hayenga, H. N., Humphrey, J. D., & Peirce, S. M. (2011b). Toward a multi-scale computational model of arterial adaptation in hypertension: verification of a multi-cell agent based model. *Frontiers in Physiology*, *2*, 20. <https://doi.org/10.3389/fphys.2011.00020>

- Thorpe, C. T., Birch, H. L., Clegg, P. D., & Screen, H. R. C. (2013). The role of the non-collagenous matrix in tendon function. In *International Journal of Experimental Pathology* (Vol. 94, Issue 4, pp. 248–259). <https://doi.org/10.1111/iep.12027>
- US Bone and Joint Initiative. (2014). *The Burden of Musculoskeletal Diseases in the United States*. www.boneandjointburden.org
- Vanosdoll, M. (2017). *DEVELOPMENT OF AN AGENT-BASED MODEL AND PATELLAR TENDON BIOPSY PUNCH INJURY PROCEDURE TO PREDICT THE SALIENT FEATURES OF AGE RELATED TENDON DEGENERATIO*. Tulane University.
- Yu, W. D., Panossian, V., Hatch, J. D., Liu, S. H., & Finerman, G. A. (2001). Combined effects of estrogen and progesterone on the anterior cruciate ligament. *Clin Orthop Relat Res*, 383, 268–281. <https://doi.org/10.1097/00003086-200102000-00031>

Biography

Appendix

ABM NetLogo code

```
extensions [array matrix]

globals [
  MMP-1
  TIMP
  collagen
  TGF-B
  PDGF
  IL-1B
  IGF
  Decorin
  totalIL-1B
  cells
  TIMPinhibition
  AGElinks
  healingmode
  healtime
  xedge
  yedge
  inj-radius
  max-migrate-dist
  migration-threshold
  Decorin-factor
  num-macrophages
  avg-radius
  numfibroblast
  difference
  sum-diff
  stdev-radius
  R-bar-sum
  csd
  weight-decay
  TGF-B-hf-weight
  IGF-hf-weight
  TGF-B-hf-weight-decay
  IGF-hf-weight-decay
  Discrete-const
  injury-site-fibroblasts
  total-cells
  PDGF-const
  injury-size
  injury-site-collagen
]
breed[fibroblasts fibroblast]
breed[macrophages macrophage]

macrophages-own [
  cellIL-1B
  cellPDGF
  cellTGF-B
  cellTGF-Bhealfactor
  tvec
```

]

```
fibroblasts-own [  
  chanceapoptosis  
  chanceproliferation  
  chanceproliferation1  
  cellMMP-1  
  cellTIMP  
  cellTGF-B  
  cellPDGF  
  cellIL-1B  
  cellIL-1Bhealfactor  
  cellDecorin  
  cellDecorinhealfactor  
  cellIGF  
  COL1A1  
  collagenproductionslope  
  num-fibroblasts  
  f  
  mag-f  
  fnorm  
  fdot  
  mag-fdot  
  fdot-delay  
  mag-fdot-delay  
  angle-fdot  
  fdot-recents-x  
  fdot-recents-y  
  u  
  v  
  rho  
  alpha  
  s  
  mag-u  
  mag-v  
  c  
  b  
  tau  
  which-angle  
  whichcollagen  
  whichfibrin  
  discrete-above  
  discrete-below  
  angle-new-collagen  
  col-fibers-here  
  fibrin-fibers-here  
  col-angles-here  
  col-angles-here-array  
  fibrin-angles-here  
  fibrin-angles-here-array  
  tvec  
  tempMMP1-2  
  radiusx  
  radiusy  
  radius  
]
```

]

```

patches-own[
  patchMMP-1
  patchcollagen
  patch-TIMP
  patch-TGF-B
  patch-PDGF
  patch-PDGFhealfactor
  patch-IL-1B
  patch-IGF
  patch-IGFhealfactor
  IGF-half-life
  patch-Decorin
  patch-fibrinogen
  patch-fibrin
  fibrin-angles
  fibrin-fibers
  fibrin-alignment
  patch-colors
  patch-vector-sum
  mag-patch-sum
  angle-patch-sum
  patch-CSD_deg
  patch-CSD_rad
  patch-variance
  patch-PDF
  patch-PDF-sum
  patch-pdf-sum-array
  patch-angles
  patch-mag-fdot
  patch-angle-fdot
  patch-c
  fiber-array
  angle-array
  alignment-matrix
  alignment-list-rad
  R-bar
  K
  I
  besse1
  n
  patchcollagen_degraded
  sum_patchcollagen_degraded
  angle-list
  fibrinogen-conversion-threshold
]

```

```

to setup
  clear-all
  reset-ticks
  ifelse resolution = 748
  [
    set xedge 11
    set yedge 17
    set inj-radius 5.5
    set max-migrate-dist 6
    set migration-threshold .1
  ]

```

```

[
  set xedge 21
  set yedge 33
  set inj-radius 10.5
  set max-migrate-dist 12
  set migration-threshold .00025
]
setup-patches
populate-cells
setup-cells
setHomeostasis
set healingmode false
set num-macrophages 20
end

to go
ask fibroblasts[agecells]
diffuse-GF
diffuse-MMPs
formAGElinks
healing-response
degradeCollagen
color-patches
plotdata
if age = injure-date[
  injure
]
set age age + (1 / 4) ;6hour timesteps
tick
; if healtime = 3 or healtime = 7 or healtime = 14 or healtime = 21 or
healtime = 42 [ stop ]
if age = 541 [ stop ]
end

to injure
if age = injure-date [
  create-macrophages num-macrophages [
    move-to one-of patches with [
      sqrt(pxcor ^ 2 + pycor ^ 2) <= inj-radius
    ]
  ]
  ask patches with [sqrt(pxcor ^ 2 + pycor ^ 2) <= inj-radius] [
    set patchcollagen 0
    let index 0
    let columns (item 1 (matrix:dimensions alignment-matrix))
    while [index < columns][
      matrix:set alignment-matrix 0 index 0
      set index index + 1
    ]
  ]
  ask fibroblasts with [sqrt(pxcor ^ 2 + pycor ^ 2) <= inj-radius][die]
  set healingmode true
]
ask turtles with [breed = macrophages] [
  set color black
  set shape "young"
]
]

```

```

end

to setup-patches
  set Discrete-const 5
  ask patches with [pxcor < xedge and pxcor > -1 * xedge and pycor < yedge
and pycor > -1 * yedge]
  [
    set pcolor 104
    set patchcollagen 1
    set patch-CSD_deg 5
    set patch-CSD_rad patch-CSD_deg * (pi / 180)
    set R-bar exp ((patch-CSD_rad ^ 2) / -2)
    set patch-variance 1 - R-bar
    set K 1 / patch-variance;
    set n 1
    set I 0
    let index 0
    set fibrinogen-conversion-threshold 0.95
    set patch-angles[]
    set patch-pdf[]
    set patch-pdf-sum[]
    set fibrin-angles []
    set fibrin-fibers []
    while[n <= 3] [
      ifelse n = 3 [
        set I I + (1 / 6 ^ 2) * (k / 2) ^ 2 * n
      ]
      [
        set I I + (1 / n ^ 2) * (k / 2) ^ 2 * n
      ]
      set n n + 1
    ]
    set bessel I
    let current-angle -90
    while[current-angle < 90][
      set patch-angles lput current-angle patch-angles
      set patch-pdf lput ((exp(K * cos(current-angle))) / (2 * pi * bessel))
patch-pdf
      set fibrin-angles lput current-angle fibrin-angles
      set fibrin-fibers lput 0 fibrin-fibers
      ifelse index > 0 [
        set patch-PDF-sum lput ( (item index patch-PDF) + (item (index - 1)
patch-PDF-sum ) ) patch-PDF-sum
      ]
      [
        set patch-PDF-sum lput (item index patch-PDF) patch-PDF-sum
      ]
      set patch-pdf-sum-array array:from-list patch-pdf-sum
      set current-angle current-angle + Discrete-const.
      set index index + 1
    ]
    let patch-pdf-array array:from-list patch-pdf
    let fiber-number 0
    let fiber-list []
    set angle-list []
    set index 0
    while [index < (180 / Discrete-const)][

```

```

    array:set patch-pdf-sum-array index ((array:item patch-PDF-sum-array
index))
    set fiber-list lput 0 fiber-list
    set angle-list lput 360 angle-list
    set index index + 1
]
set fiber-array array:from-list fiber-list
set angle-array array:from-list angle-list
while [fiber-number < 100][
    let fiber-angle random-float (array:item patch-PDF-sum-array ((180 /
Discrete-const) - 1))
    let angle-found false
    set index 0
    set current-angle -90
    while [angle-found = false] [
        if fiber-angle < array:item patch-pdf-sum-array index[
            array:set fiber-array index ((array:item fiber-array index) + .01)
            array:set fiber-array index (precision (array:item fiber-array
index) 2)
            array:set angle-array index (current-angle)
            set angle-found true
        ]
        set index index + 1
        set current-angle current-angle + Discrete-const
    ]
    set fiber-number fiber-number + 1
]

set fiber-list array:to-list fiber-array
set angle-list array:to-list angle-array
set index 0
while [index < length fiber-list][
ifelse item index fiber-list = 0
    [set fiber-list remove-item index fiber-list]
    [ set index index + 1]
]
set index 0
while [index < length angle-list][
ifelse item index angle-list = 360
    [set angle-list remove-item index angle-list]
    [set index index + 1]
]
set alignment-matrix (list fiber-list angle-list)
set alignment-matrix matrix:from-row-list alignment-matrix
set fibrin-alignment (list fibrin-fibers fibrin-angles)
set fibrin-alignment matrix:from-row-list fibrin-alignment
set index 0
set patch-vector-sum [0 0]
set patch-vector-sum array:from-list patch-vector-sum
while [index < (180 / Discrete-const)][
    array:set patch-vector-sum 0 ( (array:item patch-vector-sum 0) +
(array:item fiber-array index) * sin(item index patch-angles) )
    array:set patch-vector-sum 1 ( (array:item patch-vector-sum 1) +
(array:item fiber-array index) * cos(item index patch-angles) )
    set index index + 1
]
set mag-patch-sum sqrt( (array:item patch-vector-sum 0) ^ 2 + (array:item

```

```

patch-vector-sum 1) ^ 2)
  set angle-patch-sum (atan (array:item patch-vector-sum 0) (array:item
patch-vector-sum 1) )
]
ask patches with [pxcor = xedge or pxcor = -1 * xedge or pycor = yedge or
pycor = -1 * yedge]
[
  set pcolor 14
  set patchcollagen 0
  let fiber-list [1 1 1 1 1]
  set fiber-array array:from-list fiber-list
  set angle-list [270 305 0 45 90]
  set fibrin-angles []
  set fibrin-fibers []
  let current-angle -90
  let index 0
  while[current-angle < 90][
    set fibrin-angles lput current-angle fibrin-angles
    set fibrin-fibers lput 0 fibrin-fibers
    set current-angle current-angle + 5
    set index index + 1
  ]
  set fibrin-alignment (list fibrin-fibers fibrin-angles)
  set fibrin-alignment matrix:from-row-list fibrin-alignment
]
ask patches [set patch-pdgfhealfactor 0]
end

to populate-cells
  create-fibroblasts 48[
    move-to one-of patches with
      [
        patchcollagen = 1
      ]
  ]
  ;400cells/1mm^2 (Stanley et al.)
end

to setup-cells
  ask fibroblasts [
    set color white
    set shape "star"
    set f list (0) (0)
    set f array:from-list f
    set tau 0.00625 ; this is 0.15 hours as used in mcdougall et al
    let counter 0
    set fdot-recents-x []
    set fdot-recents-y []
    while [counter < 2][
      set fdot-recents-x lput 0 fdot-recents-x
      set fdot-recents-y lput 0 fdot-recents-y
      set counter counter + 1
    ]
    set fdot-recents-x array:from-list fdot-recents-x
    set fdot-recents-y array:from-list fdot-recents-y
    set fdot [0 0]
    set fdot array:from-list fdot
  ]

```

```

]
end

to healing-response
  if (remainder healtime 1) = ( 0 ) and (count macrophages) > 0 [ask one-of
macrophages [die]]
  set healtime age - injure-date
  if healtime >= 0 and healtime <= 1 [
ask patches with [sqrt(pxcor ^ 2 + pycor ^ 2) <= inj-radius][
  set patch-fibrinogen 1
]
]
set TGF-B-hf-weight-decay 1.89032
set IGF-hf-weight-decay 2
set TGF-B-hf-weight 8.32997
set IGF-hf-weight 5
set PDGF-const 10
ask macrophages [
  if healtime <= 8 and healtime >= 0 [
    set cellTGF-Bhealfactor TGF-B-hf-weight * (1 / 2 * healtime + 1)
    set cellpdgf PDGF-const
  ]
  if healtime <= 42 and healtime > 8 [
    set cellTGF-Bhealfactor (TGF-B-hf-weight / TGF-B-hf-weight-decay) *
(-.08088 * healtime + 4.647)
    set cellpdgf PDGF-const
  ]
  set cellTGF-B cellTGF-Bhealfactor
]
migrate-macrophages

ask patches [
if healtime >= 7 and patch-fibrin > 0.001[
  set patch-fibrin patch-fibrin / 2
]
]
ask fibroblasts [
  if healtime < 1 and healtime >= 0[
    set cellIL-1Bhealfactor 4 * healtime + 1
    let m1 -8 / 9
    set cellDecorinhealfactor m1 * healtime + 1
  ]
  if healtime < 3 and healtime >= 1 [
    set cellIL-1Bhealfactor -.5 * healtime + 5.5
  ]
  if healtime < 7 and healtime >= 3 [
    set cellIL-1Bhealfactor -.25 * healtime + 4.75
  ]
  if healtime < 21 and healtime >= 1 [
    let m2 3.2 / 1116
    set cellDecorinhealfactor m2 * healtime - (9 * m2 + 1) / 9
  ]
  if healtime < 21 and healtime >= 7 [
    set cellIL-1Bhealfactor -.07142 * healtime + 3.5
  ]
  if healtime < 42 and healtime >= 21 [

```

```

    set cellIL-1Bhealfactor .04762 + 3
  ]
  if healtime < 130 and healtime >= 21 [
    let m3 1 / 130.2
    set cellDecorinhealfactor m3 * healtime - (130.2 * m3 + 1) / 130.2
  ]
  if healtime = 140 [
    set healingmode false
  ]
  migrate-fibroblasts
]
ask patches with [patch-fibrinogen > 0 and patch-IGF > fibrinogen-
conversion-threshold]
[
  ifelse patch-fibrinogen >= .1 [
    set patch-fibrin patch-fibrin + .1
    set patch-fibrinogen patch-fibrinogen - .1
    let index 0
    while [index < 36] [
      matrix:set fibrin-alignment 0 index (patch-fibrin / 36)
      set index index + 1
    ]
  ]
  [
    set patch-fibrin patch-fibrin + patch-fibrinogen
    set patch-fibrinogen 0
  ]
]
ask patches with [sqrt(pxcor ^ 2 + pycor ^ 2) <= inj-radius]
[
  if healtime < 21 and healtime >= 0 [
    set patch-IGFhealfactor IGF-hf-weight * (0.19 * healtime + 1)
  ]
  if healtime < 42 and healtime >= 21 [
    set patch-IGFhealfactor IGF-hf-weight * (-0.1429 * healtime + 8)
  ]
  if healtime < 98 and healtime >= 42 [
    set patch-IGFhealfactor (IGF-hf-weight / IGF-hf-weight-decay) * (-
0.0179 * healtime + 2.75)
  ]
  set patch-IGF patch-IGFhealfactor
]
end

to migrate-macrophages
ask macrophages [
  let delta-x plus-or-minus
  let delta-y plus-or-minus
  let txcor pxcor + delta-x
  let tycor pycor + delta-y
  let collagen-target col-conc-at-patch txcor tycor
  let index 0
  while [collagen-target > 0.1 and index < 3] [
    set delta-x plus-or-minus
    set delta-y plus-or-minus
    set txcor pxcor + delta-x

```

```

    set tycor pycor + delta-y
    set collagen-target col-conc-at-patch txcor tycor
    set index index + 1
  ]
  let tcors list(txcor) (tycor)
  set tvec target-vector pxcor pycor tcors
  face patch (pxcor + (item 0 tvec)) (pycor + (item 1 tvec))
  if index != 3 [
    fd 1
  ]
]
end

to-report plus-or-minus
  let mag random 3
  set mag mag - 1
  report mag
end

to-report col-conc-at-patch [t-xcor t-ycor]
  let t patch t-xcor t-ycor
  ifelse t-ycor + 1 = yedge or t-ycor - 1 = -1 * yedge or t-xcor + 1 = xedge
or t-xcor - 1 = -1 * xedge[
  report -1
]
[
  report [patchcollagen] of t
]
end

to migrate-fibroblasts
  ; procedure migrates cells based on the principal of contact guidance,
  (Mcdougall et al. 2006)
  set col-fibers-here array:to-list [fiber-array] of patch-here
  set col-angles-here [angle-list] of patch-here
  set fibrin-fibers-here (matrix:get-row fibrin-alignment 0)
  set fibrin-angles-here (matrix:get-row fibrin-alignment 1)
  let tcors find-target
  let chemo-target gf-conc-at-patch (item 0 tcors)(item 1 tcors)
  let chemo-here gf-conc-at-patch pxcor pycor
  set tvec target-vector pxcor pycor tcors
  let t-angle atan (item 0 tvec) (item 1 tvec)
  set col-angles-here-array array:from-list col-angles-here
  set fibrin-angles-here-array array:from-list fibrin-angles-here
  set whichcollagen find-fiber col-angles-here-array t-angle tvec
  set whichfibrin t-angle
  define-vectors whichcollagen whichfibrin
  let k_m 0
  ifelse chemo-target - migration-threshold > chemo-here [
    while [ k_m < max-migrate-dist and chemo-here < chemo-target - migration-
threshold and (patchcollagen + patch-fibrin > collagen or (count fibroblasts-
here) > 1) ] [
      let move 0
      set col-angles-here-array array:from-list col-angles-here
      set fibrin-angles-here-array array:from-list fibrin-angles-here
      set whichcollagen find-fiber col-angles-here-array t-angle tvec
      set whichfibrin t-angle

```

```

define-vectors whichcollagen whichfibrin
if ((array:item f 0) != 0) and ((array:item f 1) != 0)
  [
    set heading atan (array:item f 0) (array:item f 1)
    set move 1
  ]
ifelse not any? turtles-on (patch (pxcor + (array:item fnorm 0)) (pycor +
(array:item fnorm 1))) [fd move]
  [
    set heading (heading + 180)
    fd move
    array:set f 0 -1 * (array:item f 0)
    array:set f 1 -1 * (array:item f 1)
  ]
set tcors find-target
  set chemo-target gf-conc-at-patch (item 0 tcors) (item 1 tcors)
  set chemo-here gf-conc-at-patch pxcor pycor
  set tvec target-vector pxcor pycor tcors
  set t-angle atan (item 0 tvec) (item 1 tvec)
produceCollagen
set k_m k_m + 1
]
ask fibroblasts [
  while [k_m < max-migrate-dist] [
    produceCollagen
    array:set f 0 0
    array:set f 1 0
    array:set fdot 0 0
    array:set fdot 1 0
    set k_m k_m + 1
  ]
]]
[
  ask fibroblasts [
    while [k_m < max-migrate-dist] [
      produceCollagen
      array:set f 0 0
      array:set f 1 0
      array:set fdot 0 0
      array:set fdot 1 0
      set k_m k_m + 1
    ]
  ]
]]
end

to-report find-nearest [t-angle angles-here]
  let indexplus 0
  let angle-search-plus t-angle
  while [(not member? angle-search-plus angles-here) and (indexplus <
length angles-here)][
    set angle-search-plus angle-search-plus + Discrete-const
    set indexplus indexplus + 1
  ]
  let indexminus 0
  let angle-search-minus t-angle
  while [(not member? angle-search-minus angles-here) and (indexminus <
length angles-here)][
    set angle-search-minus angle-search-minus - Discrete-const
    set indexminus indexminus + 1
  ]

```

```

]
(iffalse indexplus < indexminus[
  set which-angle angle-search-plus
]
indexminus < indexplus
[
  set which-angle angle-search-minus
]
indexminus = indexplus
[
  let randomangle random 2
  iffelse randomangle = 1 [
    set which-angle angle-search-plus
  ]
  [
    set which-angle angle-search-minus
  ]
]
)
report which-angle
end

to-report find-fiber [angles-here t-angle t-vec]
  let angles-here-L array:to-list angles-here
  iffelse t-angle = 0 or t-angle = 180
  [
    iffelse (member? t-angle angles-here-L) or (member? (t-angle - 180)
angles-here-L)
    [
      set which-angle t-angle
    ]
    [
      set which-angle (find-nearest t-angle angles-here-L)
    ]
  ]
  [
    iffelse item 0 t-vec > 0 ;right
    [
      let index 0
      while [index < array:length angles-here]
      [
        if (array:item angles-here index) < 0
        [array:set angles-here index ((array:item angles-here index) + 180)]
        set index index + 1
      ]
    ]
    ;left
    [
      let index 0
      while [index < array:length angles-here]
      [
        iffelse (array:item angles-here index) < 0
        [array:set angles-here index ((array:item angles-here index) + 360)]
        [array:set angles-here index ((array:item angles-here index) + 180)]
        set index index + 1
      ]
    ]
  ]
]

```

```

    ifelse member? t-angle angles-here-L
    [
      set which-angle t-angle
    ]
    [
      set which-angle (find-nearest t-angle angles-here-L)
    ]
  ]
  report which-angle
end

to define-vectors [which-collagen which-fibrin]
  set rho 0.5
  set s 15e-6
  set alpha 0.5
  ;optimal values of rho, s,and alpha should be determined by parametrization
  let fdotslope-x ((array:item fdot-recents-x 1) - (array:item fdot-recents-x
0)) / 0.25
  let fdotslope-y ((array:item fdot-recents-y 1) - (array:item fdot-recents-y
0)) / 0.25
  set fdot-delay list((array:item fdot-recents-x 1) - fdotslope-x * tau)
((array:item fdot-recents-y 1) - fdotslope-y * tau)
  set fdot-delay array:from-list fdot-delay
  set mag-fdot-delay sqrt( ((array:item fdot-delay 0) ^ 2) + ((array:item
fdot-delay 1) ^ 2) )
  set c [0 0]
  set c array:from-list c
  set b [0 0]
  set b array:from-list b
  set v [0 0]
  set v array:from-list v
  set fdot [0 0]
  set fdot array:from-list fdot
  set u [0 0]
  set u array:from-list u
  set fnorm [0 0]
  set fnorm array:from-list fnorm
  array:set c 0 patchcollagen * sin(which-collagen)
  array:set c 1 patchcollagen * cos(which-collagen)
  array:set b 0 patch-fibrin * sin(which-fibrin)
  array:set b 1 patch-fibrin * cos(which-fibrin)
  array:set u 0 (1 - alpha) * (array:item c 0) + alpha * (array:item b 0)
  array:set u 1 (1 - alpha) * (array:item c 1) + alpha * (array:item b 1)
  set mag-u sqrt( ((array:item u 0) ^ 2) + ((array:item u 1) ^ 2))
  (ifelse mag-fdot-delay = 0 and mag-u != 0
    [
      array:set v 0 (1 - rho) * ((array:item u 0)/(mag-u))
      array:set v 1 (1 - rho) * ((array:item u 1)/(mag-u))
    ]
    mag-fdot-delay != 0 and mag-u = 0
    [
      array:set v 0 rho * ((array:item fdot-delay 0) / (mag-fdot-delay))
      array:set v 1 rho * ((array:item fdot-delay 1) / (mag-fdot-delay))
    ]
    mag-fdot-delay != 0 and mag-u != 0
    [
      array:set v 0 (1 - rho) * ((array:item u 0)/(mag-u)) + rho *

```

```

((array:item fdot-delay 0) / (mag-fdot-delay))
  array:set v 1 (1 - rho) * ((array:item u 1)/(mag-u)) + rho *
((array:item fdot-delay 1) / (mag-fdot-delay))
  ])
  set mag-v sqrt( ((array:item v 0) ^ 2) + ((array:item v 1) ^ 2))
  ifelse mag-v = 0
  ;fdot is df/dt from McDougall et al.
  [
    array:set fdot 0 0
    array:set fdot 1 0
    set mag-fdot sqrt((array:item fdot 0) ^ 2 + (array:item fdot 1) ^
2)
  ]
  [
    array:set fdot 0 s * (array:item v 0) / mag-v
    array:set fdot 1 s * (array:item v 1) / mag-v
    set mag-fdot sqrt((array:item fdot 0) ^ 2 + (array:item fdot 1) ^
2)
  ]
  array:set f 0 (array:item f 0) + (array:item fdot 0)
  array:set f 1 (array:item f 1) + (array:item fdot 1)
  set mag-f sqrt((array:item f 0) ^ 2 + (array:item f 1) ^ 2)
  ]
array:set fdot-recents-x 0 (array:item fdot-recents-x 1)
array:set fdot-recents-y 0 (array:item fdot-recents-y 1)
array:set fdot-recents-x 1 (array:item fdot 0)
array:set fdot-recents-y 1 (array:item fdot 1)
if mag-f > 0 [ ;avoids divide by zero
  array:set fnorm 0 ((array:item f 0) / mag-f)
  array:set fnorm 1 ((array:item f 1) / mag-f)
]
end

to-report gf-conc-at-patch [p-xcor p-ycor]
  let p patch p-xcor p-ycor
  report [patch-PDGF + patch-TGF-B] of p
end

to-report find-target
  let target max-one-of neighbors [patch-pdgf]
  let txcor [pxcor] of target
  let tycor [pycor] of target
  report list txcor tycor
end

to-report target-vector [p-xcor p-ycor tcors]
  let txvec (item 0 tcors) - p-xcor
  let tyvec (item 1 tcors) - p-ycor
  report list txvec tyvec
end

to setHomeostasis
  ;all factors start at 1 indicating study of relative expression levels.
  Fibrinogen starts at 0 because there is none present preinjury.
  set age 120;assuming 1mg dry weight
  ask fibroblasts[
    set cellMMP-1 1 ;pg/cell
    set cellPDGF 1 ; mRNA expression for each cell

```

```

    set cellIL-1B 1
    set cellTIMP 1
    set cellPDGF 1
    set cellTGF-B 1
    set cellDecorin 1
    set chanceapoptosis 100 / .48 ] ;48 cells of 100 as the baseline
ask patches with [pcolor != 14] [
    set patchcollagen 1
    set patch-TIMP 1
    set patch-TGF-B 1
    set patch-PDGF 1
    set patch-IL-1B 1
    set patch-IGF 1
    set patch-Decorin 1
    set patch-fibrinogen 0
]
ask patches with [pxcor = -1 * xedge or pxcor = xedge][
    set patch-igf 1
]
end

to agecells
set cells count fibroblasts
proliferate
apoptosis
ageGF
ageMMP
; plotdata
end

to apoptosis
    if random chanceapoptosis < 0.4 + 0.00059 * AGElinks [
        ask one-of fibroblasts[
            die]];the equation comes from the fit of both Alikahani papers (line3 in
MATLAB code)
    end

to proliferate
let emptypatchlist patches with [
    pxcor < xedge and pxcor > -1 * xedge and pycor < yedge and pycor > -1 *
yedge and count turtles-here = 0 and not any? turtles-on neighbors;HIGH RES
CHANGE
]
ask fibroblasts[
    let PDGF-prolif patch-PDGF
    if PDGF-prolif = 0[
        set PDGF-prolif 0.01
    ]
    set chanceproliferation ((5.6 * (1 / PDGF-prolif) + (100 / .48)
));100/.48 to normalize cell# , from Lepisto
    set chanceproliferation1 chanceproliferation - ((- 0.00071 * age + 0.89)
* (patch-IGF) * 10)
]; decreased stimulation with age, this is weighted a little less because
of uncertainty in rule score and sensitivity to the parameter

    if random chanceproliferation1 < 1 [
        ifelse healtime > 8 and healtime < 28

```

```

    [let new-cell-location max-one-of emptypatchlist [PDGF]
      hatch 1 move-to new-cell-location
    ]
    [hatch 1 move-to one-of emptypatchlist]
  ]
end

to ageGF
  if healingmode = false [
    ask fibroblasts[
      set cellIL-1B (.045 * age - 4.4) ; IL-1B age changes from Xin ;
      set cellTIMP (-.0018 * age + 1.2) ;TIMP age changes from Yu data
      if age < 270 [
        set cellPDGF (( 8.4E-6 * age ^ 2) -(0.0055 * age) + 1.5)] ;Dragoo
PDGF aging: fit before middle age, constant after
      if age >= 270 [
        set cellPDGF cellPDGF]
      set cellTGF-B cellTGF-B; TGF no change with age
      set cellDecorin 1 / (1 + exp (-(age - 200) * .0229)) + 1
    ]
    ask patches with [pxcor = -1 * xedge or pxcor = xedge][
      set patch-igf (-0.00095 * age + 1.1) ;IGF changes from Neilson
    ]
  ]
  if healingmode = true [
    ask fibroblasts[
      set cellIL-1B (.045 * age - 4.4) * cellIL-1Bhealfactor ; IL-1B age
changes from Xin ;
      set cellTIMP (-.0018 * age + 1.2) ;TIMP age changes from Yu data
      if age < 270 [
        set cellPDGF (( 8.4E-6 * age ^ 2) -(0.0055 * age) + 1.5)] ;Dragoo
PDGF aging: fit before middle age, constant after
      if age >= 270 [
        set cellPDGF cellPDGF]
      set cellTGF-B cellTGF-B; TGF no change with age
      set cellDecorin (1 / (1 + exp (-(age - 200) * .0229)) + 1) *
cellDecorinhealfactor
      ; sum cell level GF to find total content
    ]
    ask patches with [pxcor = -1 * xedge or pxcor = xedge][
      set patch-igf (-0.00095 * age + 1.1)
    ]
  ]
  set patch-IL-1B cellIL-1B
  set patch-TIMP cellTIMP
  ifelse cellPDGF > patch-PDGF
    [set patch-PDGF cellPDGF]
    [set patch-PDGF patch-PDGF / 5]
  if celligf > patch-igf
    [set patch-igf celligf]
  set IGF-half-life 0.35
  let decay -1 * ln(2) / IGF-half-life
  ifelse resolution = 748 [
    set patch-igf patch-igf * exp(decay * .25)
  ]
  [
    ask neighbors4 [set patch-igf patch-igf * exp(decay * .25)] ;this is

```

equivalent, because the higher resolution has 4 times as many patches.

```
]
set patch-TGF-B cellTGF-B
set patch-Decorin cellDecorin
ask macrophages [
  set patch-PDGF cellPDGF
  set patch-TGF-B cellTGF-B
]
end

to ageMMP
ask fibroblasts[
  let tempMMP1-1 (-2.7 * (cellPDGF * 10 ^ -9) ^ 2 + 8.5 * (cellPDGF * 10 ^ -
9)) ; ug mmp
  ifelse patch-IL-1B > 0[
    set tempMMP1-2 tempMMP1-1 + (1.9E-6 * ln (patch-IL-1B));Tsusaki IL1B
MMP correlation
  ]
  [
    set tempMMP1-2 tempMMP1-1 + (1.9E-6 * ln (0.0001))
  ]
  let tempMMP1-3 tempMMP1-2 * 0.8 / cellTGF-B ; TGF-B decrease of MMP-1
expression
  set TIMPinhibition 0.5 * cellTIMP ; TIMP inhibition unclear relationship,
need more data
  set cellMMP-1 tempMMP1-3 - (tempMMP1-3 * TIMPinhibition )]
  set patchMMP-1 cellMMP-1 ; is this an acceptable format?
end

to diffuse-GF

diffuse patch-IL-1B .1
diffuse patch-TIMP .1
diffuse patch-PDGF .1
diffuse patch-TGF-B .1
diffuse patch-IGF .1
diffuse patch-Decorin .1
ask patches[
  if patchcollagen = 0 and ((pycor = yedge) or (pycor = -1 * yedge) or (pxcor
= -1 * xedge) or (pxcor = xedge)) [ ;HIGH RES CHANGE
    set patch-IL-1B 0
    set patch-TIMP 0
    set patch-PDGF 0
    set patch-TGF-B 0]]
  set IL-1B sum [patch-IL-1B / resolution] of patches ;divided by resolution
to normalize to multiple of 1 (divided by number of patches)
  set TIMP sum [ patch-TIMP / resolution] of patches
  set PDGF sum [patch-PDGF / resolution] of patches
  set TGF-B sum [patch-TGF-B / resolution] of patches
  set IGF sum [patch-IGF / resolution] of patches
  set Decorin sum [patch-Decorin / resolution] of patches
  set R-bar-sum sum [R-bar / (21 * 33)] of patches with [pycor != yedge and
pycor != -1 * yedge and pxcor != xedge and pxcor != -1 * xedge]
  let csd_rad sqrt(-2 * ln (R-bar-sum))
  set csd csd_rad * (180 / pi)
```

```

set-current-plot "IL-1B"
plotxy age IL-1B
set-current-plot "TIMP"
plotxy age TIMP
set-current-plot "PDGF"
plotxy age PDGF
set-current-plot "IGF"
plotxy age IGF
set-current-plot "TGFB"
plotxy age TGF-B
set-current-plot "Decorin"
plotxy age Decorin
set-current-plot "AGE-links"
plotxy age AGElinks
set-current-plot "MMP-1"
plotxy age MMP-1
set-current-plot "R Bar"
plotxy age R-bar-sum
end

to diffuse-MMPs
  diffuse patchMMP-1 1
  ask patches [
    if patchcollagen < .1 [
      set patchMMP-1 0]]
  set MMP-1 sum [patchMMP-1 / resolution] of patches
end

to produceCollagen
  set Decorin-factor 1
  let K-decorin patch-decorin * Decorin-factor
  if patch-PDGF > 0 and patch-TGF-B > 0[
    set collagenproductionslope (patch-TGF-B * 0.001 / (1.23 *
patchcollagen + 1)) * (1.3 * patch-igf) ; control 0.041% from Hansen, IGF
stimulation fromg
    set collagenproductionslope collagenproductionslope / max-migrate-dist
    ifelse patch-fibrin < 1
      [set collagenproductionslope collagenproductionslope * (1 - patch-
fibrin)]
      [set collagenproductionslope 0]
    set patchcollagen patchcollagen + collagenproductionslope
    let old-angle-patch-sum angle-patch-sum
    set angle-patch-sum angle-patch-sum + K-decorin * mag-fdot *
sin(heading - angle-patch-sum)
    ifelse angle-patch-sum = old-angle-patch-sum or collagenproductionslope
= 0
      [
        set angle-new-collagen angle-patch-sum
      ]
      [
        let bigterm (2 * (mag-patch-sum) * cos(old-angle-patch-sum) *
cos(angle-patch-sum) + 2 * (mag-patch-sum) * sin(old-angle-patch-sum) *
sin(angle-patch-sum))
        let smallterm mag-patch-sum ^ 2 - collagenproductionslope ^ 2
        let new-mag-patch-sum mag-patch-sum
        if ((bigterm ^ 2) - (4 * (smallterm))) >= 0
          [set new-mag-patch-sum (bigterm + sqrt((bigterm ^ 2) - (4 *

```

```

(smallterm))) / (2 * (smallterm))]
  ifelse abs (new-mag-patch-sum * (sin(angle-patch-sum - old-angle-patch-
sum)) / collagenproductionslope) < 1
    [set angle-new-collagen asin(new-mag-patch-sum * (sin(angle-patch-sum
- old-angle-patch-sum)) / collagenproductionslope)]
    [set angle-new-collagen heading]
  ]
  let index -90
  while [angle-new-collagen > index - Discrete-const][
    set discrete-above index
    set discrete-below (index - Discrete-const)
    set index index + Discrete-const
  ]
  let system-of-equations (list (list cos(discrete-below)
cos(discrete-above) (-1 * cos(angle-new-collagen)))
  (list sin(discrete-below) sin(discrete-above) (-1 * sin(angle-new-
collagen))) [1 1 0] )
  set system-of-equations (matrix:from-row-list system-of-equations)
  set system-of-equations (matrix:inverse system-of-equations)
  let column-matrix (list [0] [0] (list(collagenproductionslope)))
  set column-matrix matrix:from-row-list column-matrix
  let solution-matrix (matrix:times system-of-equations column-matrix)
  let matrix-results (matrix:get solution-matrix 0 0) + (matrix:get
solution-matrix 1 0)
  let temp-angles matrix:get-row alignment-matrix 1
  let old-angles temp-angles
  let new-angle []
  let which-discrete []
  if not member? discrete-below temp-angles
  [
    set temp-angles lput discrete-below temp-angles
    set new-angle lput discrete-below new-angle
    set which-discrete "below"
  ]
  if not member? discrete-above temp-angles
  [
    set temp-angles lput discrete-above temp-angles
    set new-angle lput discrete-above new-angle
    ifelse length(which-discrete) = 1[
      set which-discrete "both"
    ]
    [
      set which-discrete "above"
    ]
  ]
  set temp-angles sort-by < temp-angles
  ;create temporary list for the collagen fibers
  let temp-fibers-list matrix:get-row alignment-matrix 0
  let temp-fibers array:from-list temp-fibers-list

  (ifelse length(angle-list) = length(temp-angles)
  [
    let index-sort 0
    while [index-sort < length temp-angles] [
      if (item index-sort temp-angles) = discrete-below [
        array:set temp-fibers index-sort ((array:item temp-fibers index-

```

```

sort) + (matrix:get solution-matrix 0 0))]
  if (item index-sort temp-angles) = discrete-above [
    array:set temp-fibers index-sort ((array:item temp-fibers index-
sort) + (matrix:get solution-matrix 1 0))]
    set index-sort index-sort + 1
  ]
]

length(angle-list) + 1 = length(temp-angles) ;else
[
  ifelse (item 0 new-angle) = (item 0 temp-angles) or (item 0 new-angle)
= (item ((length temp-angles) - 1) temp-angles)[
  ifelse (item 0 angle-list) > (item 0 new-angle) ;
  [
    set temp-fibers-list fput (matrix:get solution-matrix 0 0) temp-
fibers-list
    set temp-fibers array:from-list temp-fibers-list
    array:set temp-fibers 1 ((array:item temp-fibers 1) + (matrix:get
solution-matrix 0 0))
  ]
  [
    set temp-fibers-list lput (matrix:get solution-matrix 1 0) temp-
fibers-list
    set temp-fibers array:from-list temp-fibers-list
    array:set temp-fibers ((length temp-angles) - 1) ((array:item
temp-fibers ((length temp-angles) - 1) ) + (matrix:get solution-matrix 1 0))
  ]
  set angle-list lput (item 0 new-angle) angle-list
  set angle-list sort-by < angle-list
]
[
  let index-find 0
  while [index-find < length(temp-fibers-list)][
    ifelse (item index-find temp-angles) = (item 0 new-angle)[
      ifelse which-discrete = "below"[
        set temp-fibers-list insert-item index-find temp-fibers-list
(matrix:get solution-matrix 0 0);
        set temp-fibers array:from-list temp-fibers-list
        array:set temp-fibers (index-find + 1) (matrix:get solution-
matrix 1 0)
      ]
      [
        set temp-fibers-list insert-item index-find temp-fibers-list
(matrix:get solution-matrix 1 0);
        set temp-fibers array:from-list temp-fibers-list
        array:set temp-fibers (index-find - 1) (matrix:get solution-
matrix 0 0)
      ]
    ]
    set index-find index-find + 1
  ]
  [
    set index-find index-find + 1
  ]
]
]
set temp-fibers-list array:to-list temp-fibers
set angle-list lput (item 0 new-angle) angle-list
set angle-list sort-by < angle-list

```

```

]
]

length(angle-list) + 2 = length(temp-angles) ;else
[
  ifelse (item 0 new-angle) = (item 0 temp-angles) or (item 1 new-angle)
= (item ((length temp-angles) - 1) temp-angles)[
  ifelse (item 0 angle-list) > (item 0 new-angle)
  [
    set temp-fibers-list fput (matrix:get solution-matrix 1 0) temp-
fibers-list
    set temp-fibers-list fput (matrix:get solution-matrix 0 0) temp-
fibers-list
    set temp-fibers array:from-list temp-fibers-list
  ]
  [
    set temp-fibers-list lput (matrix:get solution-matrix 0 0) temp-
fibers-list
    set temp-fibers-list lput (matrix:get solution-matrix 1 0) temp-
fibers-list
    set temp-fibers array:from-list temp-fibers-list
  ]
  set angle-list lput (item 0 new-angle) angle-list
  set angle-list lput (item 1 new-angle) angle-list
  set angle-list sort-by < angle-list
]
[
  let index-find 0
  while [index-find < length(temp-fibers-list)][
    ifelse (item index-find temp-angles) = (item 0 new-angle) [
      set temp-fibers-list insert-item index-find temp-fibers-list
(matrix:get solution-matrix 1 0)
      set temp-fibers-list insert-item index-find temp-fibers-list
(matrix:get solution-matrix 0 0)
      set index-find index-find + 1
    ]
    [set index-find index-find + 1]
  ]
  set angle-list lput (item 0 new-angle) angle-list
  set angle-list lput (item 1 new-angle) angle-list
  set angle-list sort-by < angle-list
]
]
[
  user-message ("ERROR! collagen production could not sort new collagen")
])
set alignment-matrix (list (temp-fibers-list) (angle-list) )
set alignment-matrix matrix:from-row-list alignment-matrix
]

end

to degradeCollagen
ask patches with [patchMMP-1 > 0][
  let prev-collagen patchcollagen ;I'll need this value for later
  set patchcollagen_degraded (150 * (patchMMP-1)); -150pgcollagen/pgMMP-1
  set patchcollagen_degraded precision patchcollagen_degraded 10

```

```

    set sum_patchcollagen_degraded sum_patchcollagen_degraded +
patchcollagen_degraded
    set patchcollagen patchcollagen - patchcollagen_degraded
    set collagen sum [patchcollagen / resolution] of patches
    set injury-size count patches with [sqrt(pxcor ^ 2 + pycor ^ 2) < inj-
radius]
    set injury-site-collagen sum [patchcollagen / injury-size] of patches
with [sqrt(pxcor ^ 2 + pycor ^ 2) < inj-radius]
    let index 0
    let columns (item 1 (matrix:dimensions alignment-matrix))
    while [index < columns][
        ifelse matrix:get alignment-matrix 0 index > 0
        [
            matrix:set alignment-matrix 0 index ( (matrix:get alignment-matrix
0 index) - (sum_patchcollagen_degraded * ((matrix:get alignment-matrix 0
index) / prev-collagen) ) )
            set index index + 1
        ]
        [
            set index index + 1
        ]
    ]
    set index 0
    set alignment-list-rad []
]
ask patches with [pxcor < xedge and pxcor > -1 * xedge and pycor < yedge
and pycor > -1 * yedge] [
let alignment-list matrix:get-row alignment-matrix 1
let alignment-sum sum alignment-list
if patchcollagen > .01 and alignment-sum > 0 [ ;this line is necessary to
avoid taking the square root of a negative number on a patch with very little
collagen, or the ln of 0 on a patch with no collagen
let index 0
let s-bar 0
let c-bar 0
let columns (item 1 (matrix:dimensions alignment-matrix))
while [index < columns][
set s-bar s-bar + (matrix:get alignment-matrix 0 index) * sin(item
index alignment-list)
set c-bar c-bar + (matrix:get alignment-matrix 0 index) * cos(item
index alignment-list)
set index index + 1
]
let vector-length sqrt( (s-bar) ^ 2 + (c-bar) ^ 2 )
let R-bar (vector-length / patchcollagen)
if R-bar < 1 and R-bar > 0 [
set patch-csd_rad sqrt(-2 * ln(R-bar)) ;ERROR! The square root of -0
is an imaginary number.
set patch-csd_deg patch-csd_rad * (180 / pi)
]
]
]
set-current-plot "Collagen"
plotxy age collagen
set-current-plot "Injury Site Collagen"
plotxy age injury-site-collagen
end

```

```

to color-patches
  ask patches [
    set patch-colors patchcollagen
  ]

  ask patches with [(pxcor < xedge and pxcor > -1 * xedge and pycor < yedge
and pycor > -1 * yedge) and patch-colors < .1] [
    set pcolor 14]
  ask patches with [(pxcor < xedge and pxcor > -1 * xedge and pycor < yedge
and pycor > -1 * yedge) and patch-colors < .2 and patch-colors >= .1] [
    set pcolor 15]
  ask patches with [(pxcor < xedge and pxcor > -1 * xedge and pycor < yedge
and pycor > -1 * yedge) and patch-colors < .3 and patch-colors >= .2] [
    set pcolor 24]
  ask patches with [(pxcor < xedge and pxcor > -1 * xedge and pycor < yedge
and pycor > -1 * yedge) and patch-colors < .4 and patch-colors >= .3] [
    set pcolor 25]
  ask patches with [(pxcor < xedge and pxcor > -1 * xedge and pycor < yedge
and pycor > -1 * yedge) and patch-colors < .5 and patch-colors >= .4] [
    set pcolor 44]
  ask patches with [(pxcor < xedge and pxcor > -1 * xedge and pycor < yedge
and pycor > -1 * yedge) and patch-colors < .6 and patch-colors >= .5] [
    set pcolor 45]
  ask patches with [(pxcor < xedge and pxcor > -1 * xedge and pycor < yedge
and pycor > -1 * yedge) and patch-colors < .7 and patch-colors >= .6] [
    set pcolor 65]
  ask patches with [(pxcor < xedge and pxcor > -1 * xedge and pycor < yedge
and pycor > -1 * yedge) and patch-colors < .8 and patch-colors >= .7] [
    set pcolor 64]
  ask patches with [(pxcor < xedge and pxcor > -1 * xedge and pycor < yedge
and pycor > -1 * yedge) and patch-colors < .9 and patch-colors >= .8] [
    set pcolor 84]
  ask patches with [(pxcor < xedge and pxcor > -1 * xedge and pycor < yedge
and pycor > -1 * yedge) and patch-colors < 1.0 and patch-colors >= .9] [
    set pcolor 85]
  ask patches with [(pxcor < xedge and pxcor > -1 * xedge and pycor < yedge
and pycor > -1 * yedge) and patch-colors >= 1] [
    set pcolor 104]
end

to formAGElinks
  set AGElinks (0.15 * age - 9.4) * (collagen / resolution)
end

to plotdata
  set injury-site-fibroblasts count fibroblasts with [sqrt(pxcor ^ 2 + pycor
^ 2) <= inj-radius]
  set-current-plot "Injury Site Fibroblasts"
  plotxy age injury-site-fibroblasts
  set total-cells injury-site-fibroblasts + (count macrophages)
  ask fibroblasts [
    set radiusx pxcor
    set radiusy pycor
    set radius sqrt((pxcor) ^ 2 + (pycor) ^ 2)
  ]
  set avg-radius sum [radius / (count fibroblasts)] of fibroblasts

```

```
set-current-plot "Fibroblasts"  
plotxy age (count fibroblasts)  
end
```